МАГНИТНЫЕ ИЗОТОПНЫЕ ЭФФЕКТЫ В МЕТАЛЛ-ЗАВИСИМОМ ФЕРМЕНТАТИВНОМ КАТАЛИЗЕ.

История вопроса, достижения и перспективы практического применения.

Кузнецов Д.А.

Кафедра медицинских нанобиотехнологий МБФ РНИМУ им. Н.И. Пирогова,

Отдел строения вещества Института химической физики им. Н.Н. Семёнова РАН.

www.rsmu.ru

2015

Mg and Ca Isotopes Natural Abundance

Nuclei	Abundance, %	Nuclear spin	Nuclear magnetic moment, μ
^{24}Mg	78,99	0	
^{25}Mg	10,00	+5/2	-0,85545
^{26}Mg	11,01	0	
^{40}Ca	96.94	0	
^{43}Ca	1.317	-7/2	+0,87515

Mg and Zn **Isotopes Natural Abundance**

Nuclei	Abundance, %	Nuclear spin	Nuclear magnetic moment, μ
^{24}Mg	78,99	0	
^{25}Mg	10,00	+5/2	-0,85545
^{26}Mg	11,01	0	
^{64}Zn	48,6	0	
^{66}Zn	27,9	0	
^{67}Zn	4,1	-5/2	+0,87515
^{68}Zn	18,8	0	
^{70}Zn	0,6	0	

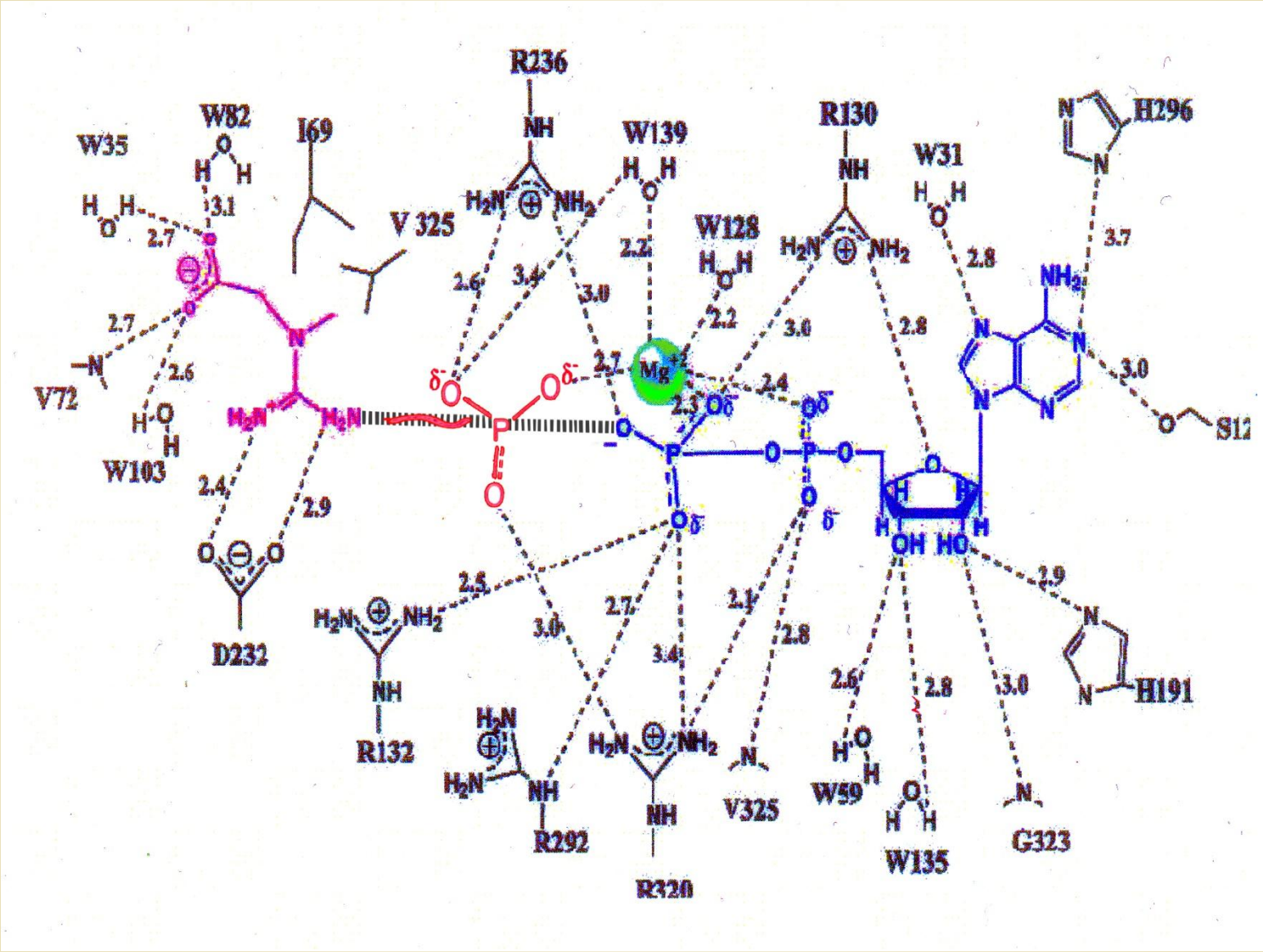

THE CREATINE KINASE ACTIVE SITE NANOTOPOLOGY

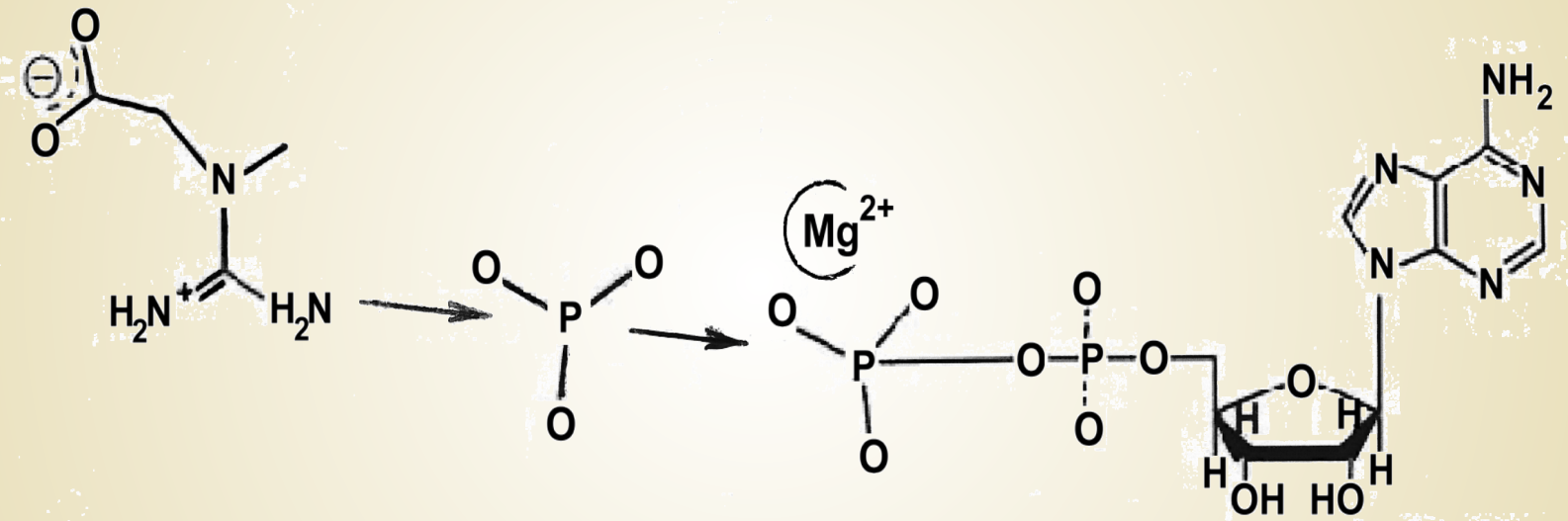
O
O
N
H2N+
H2N
O
O
P
O
Mg2+
O
O
P
O
O
P
O
O
O
O
O
H
H
H
OH
HO
H
NH2
N
N
N
N

The rate of ATP formation by mitochondria (A) and by creatine kinase (B) as a function of magnesium isotope

intact mitochondria

mitochondria subjected to a selective blockade of oxidative phosphorylation by 1-methylnicotine amide.

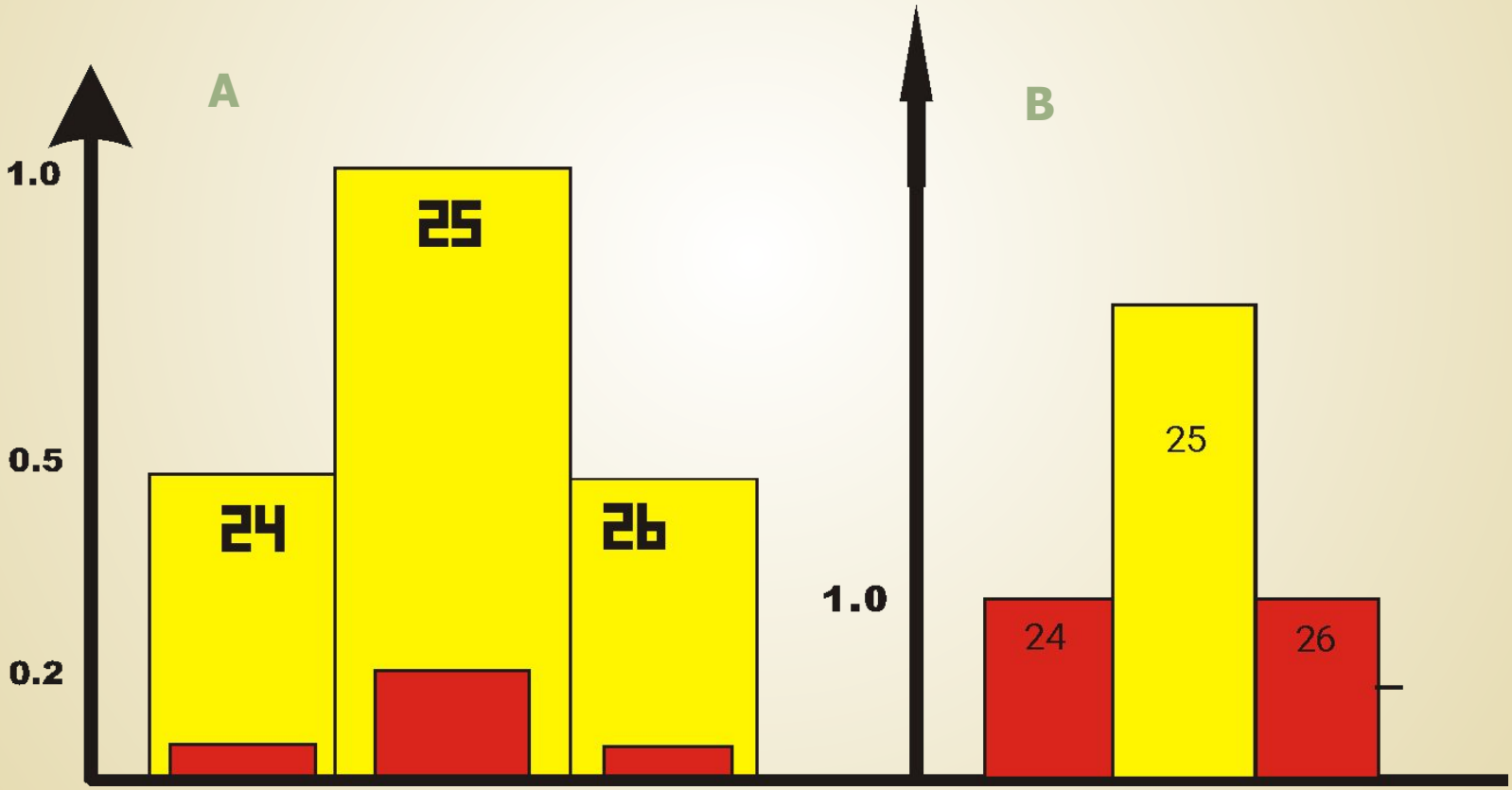

The yield of ATP is given in mmole/g total protein

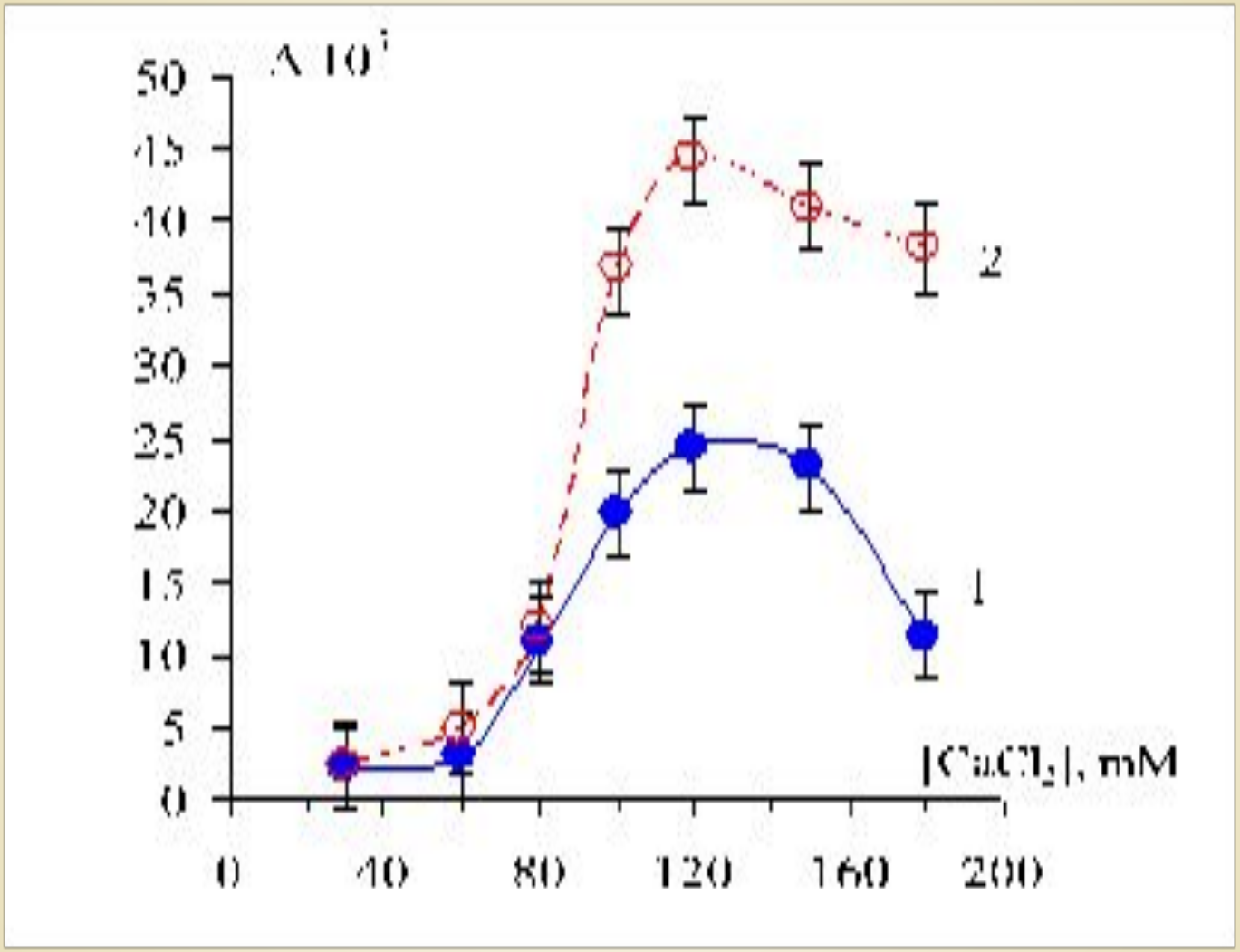

Figure 6: The rate of ATP synthesis by ^{40}Ca CK (1) and ^{43}Ca CK (2). A is the radioactivity of ^{32}P-ATP (in scintillations/min/mg CK)

ION – RADICAL PAIRS FORMATION

(SINGLET – TRIPLET PATH SHIFT)

MECHANISM

OF THE ^{25}Mg MAGNETIC ISOTOPE EFFECT

EXPRESSED

IN A BIOLOGICAL PHOSPHORYLATION PRECESSES

(Mt-CK)

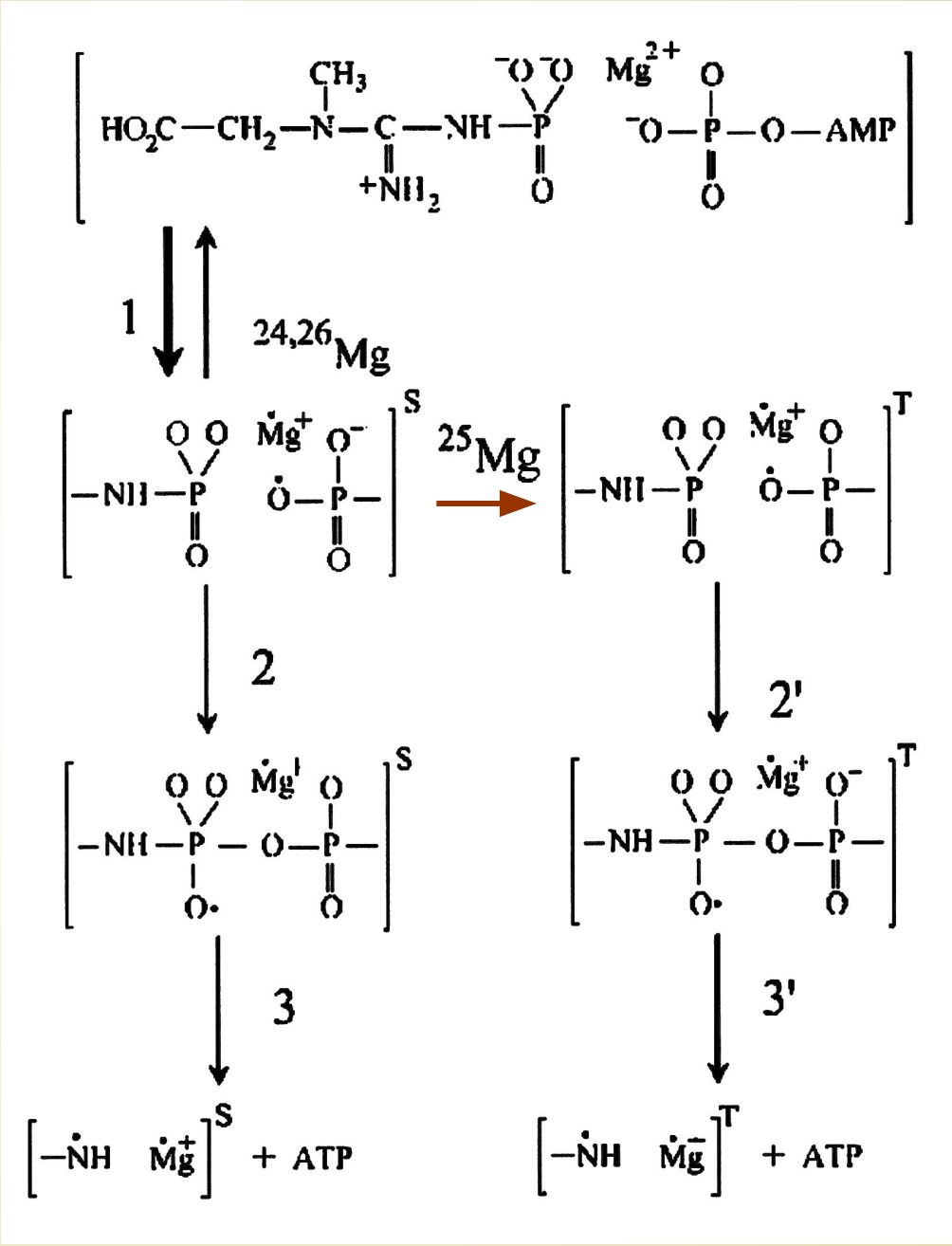

Phosphoglycerate kinase

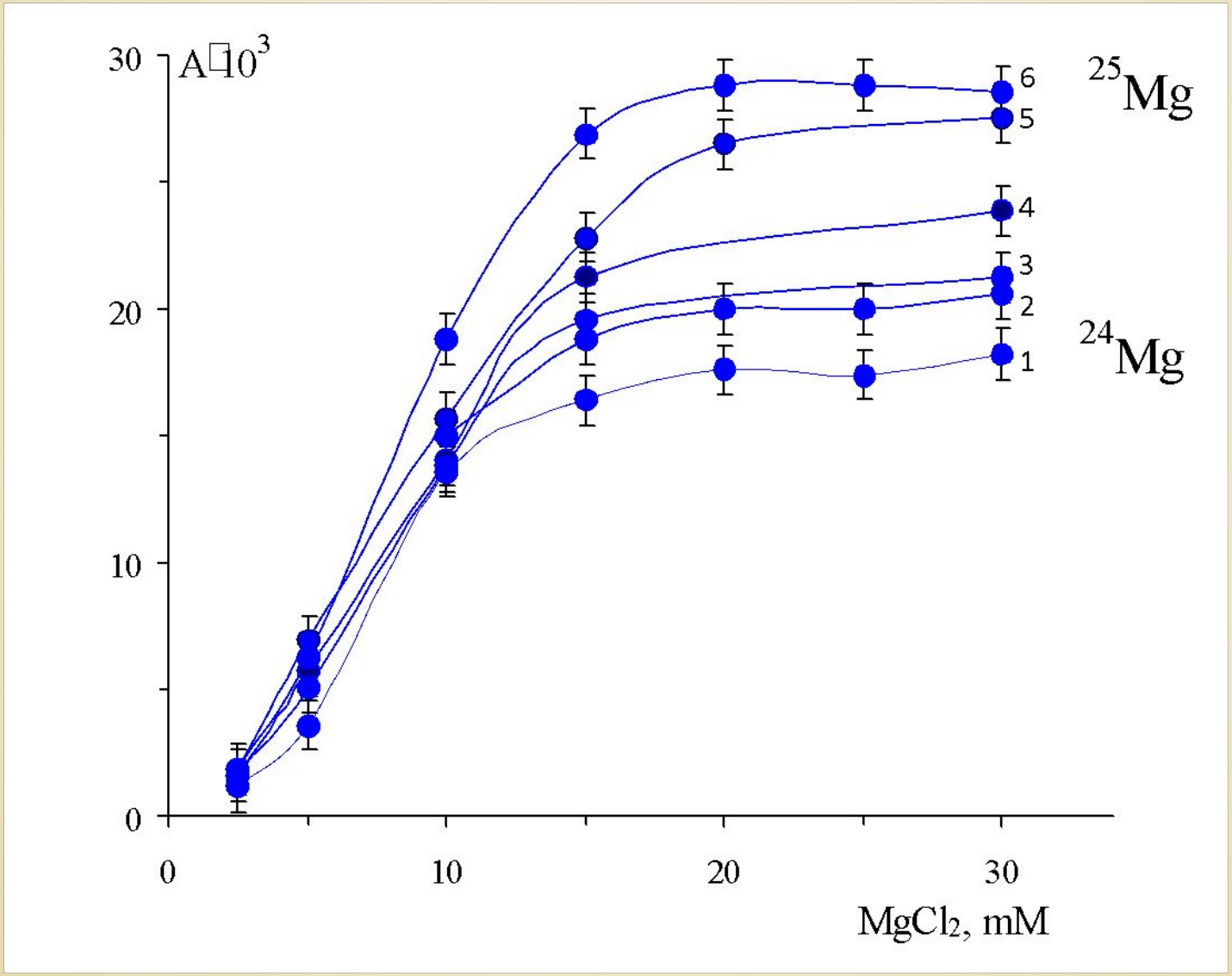

The GPK reaction ion-radical mechanism

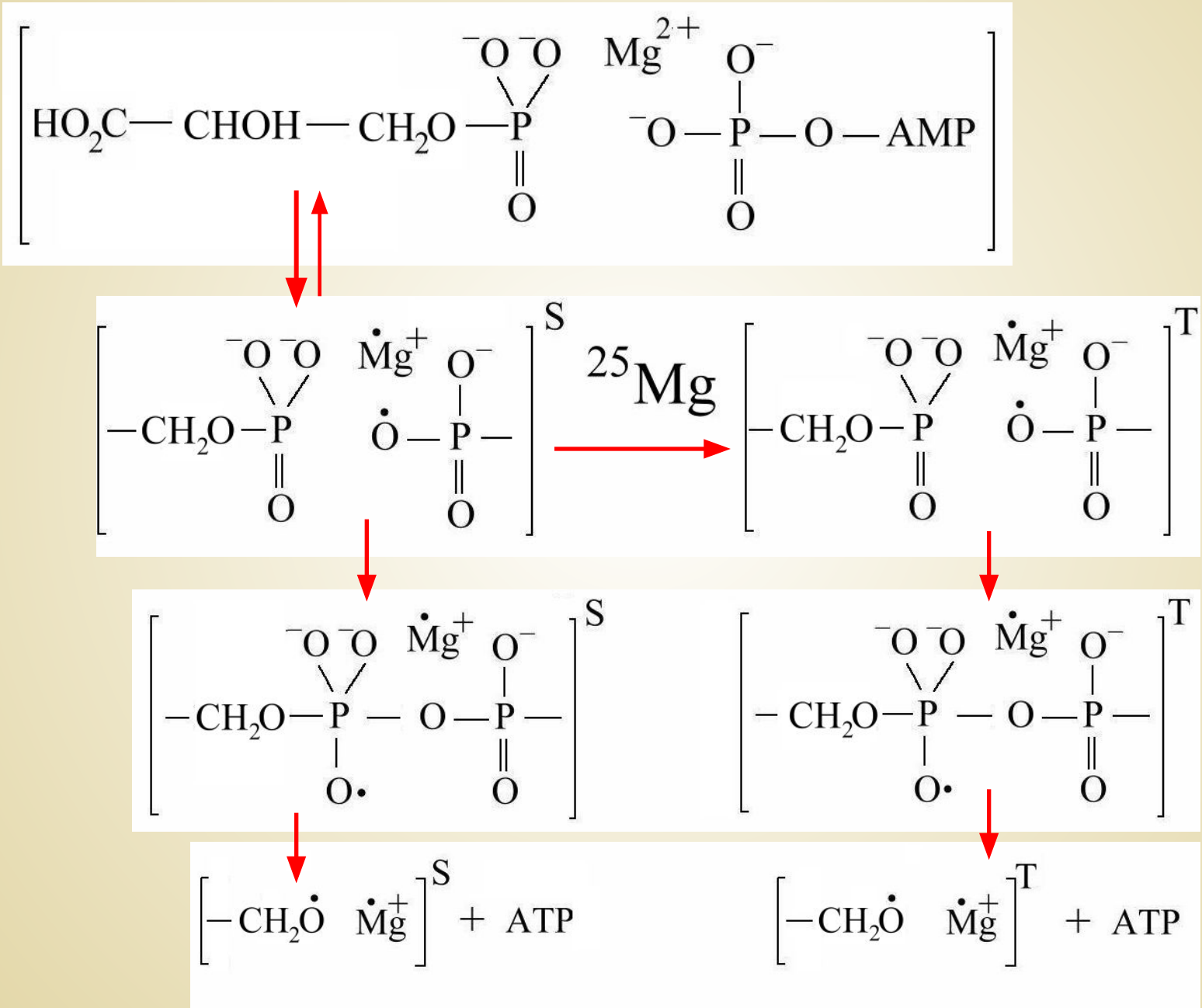

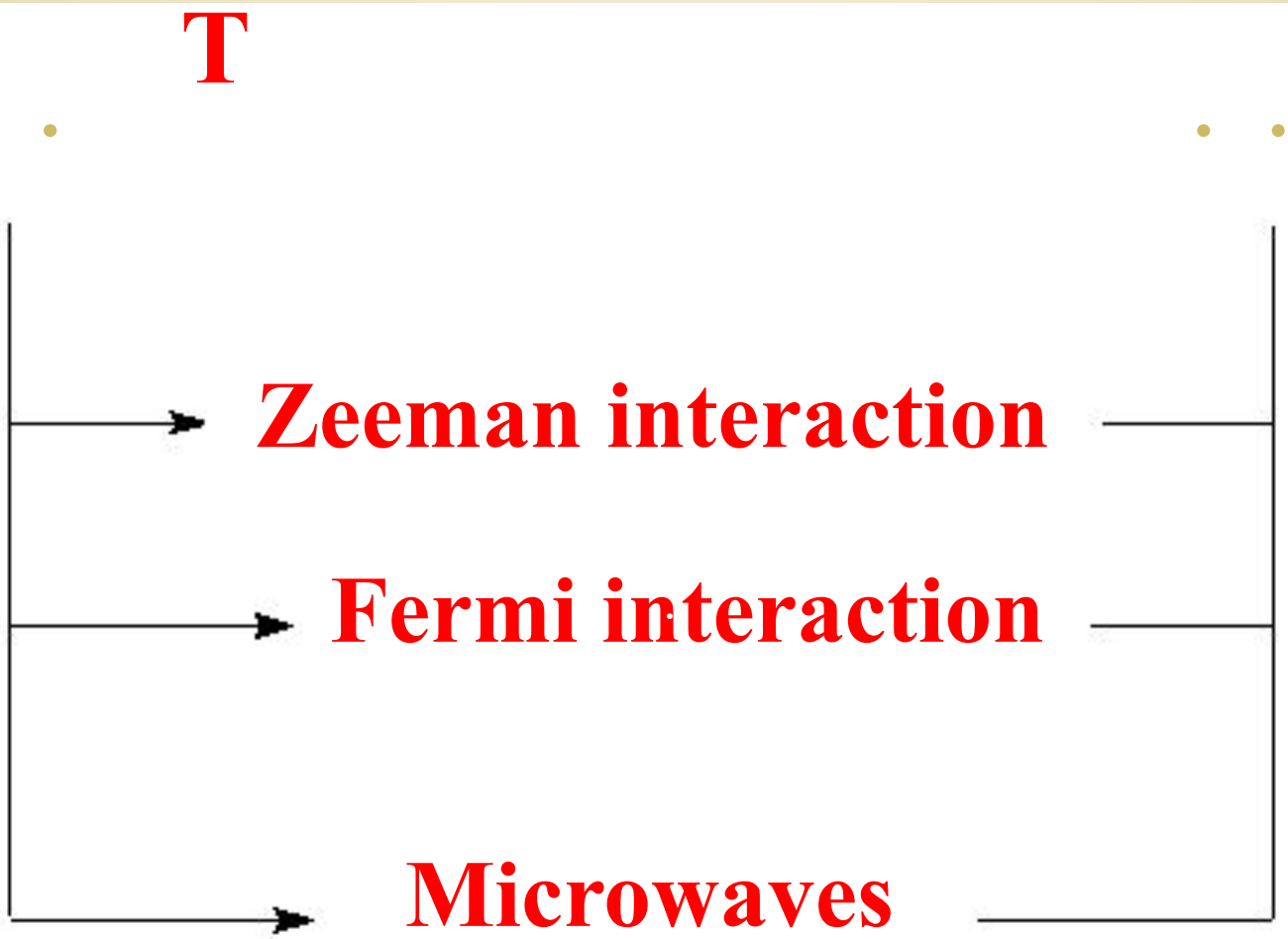
T
S
Zeeman interaction
Fermi interaction
Microwaves

PLENTY OF ROOM AT THE BOTTOM

Nanobiotechnology Ramps Up

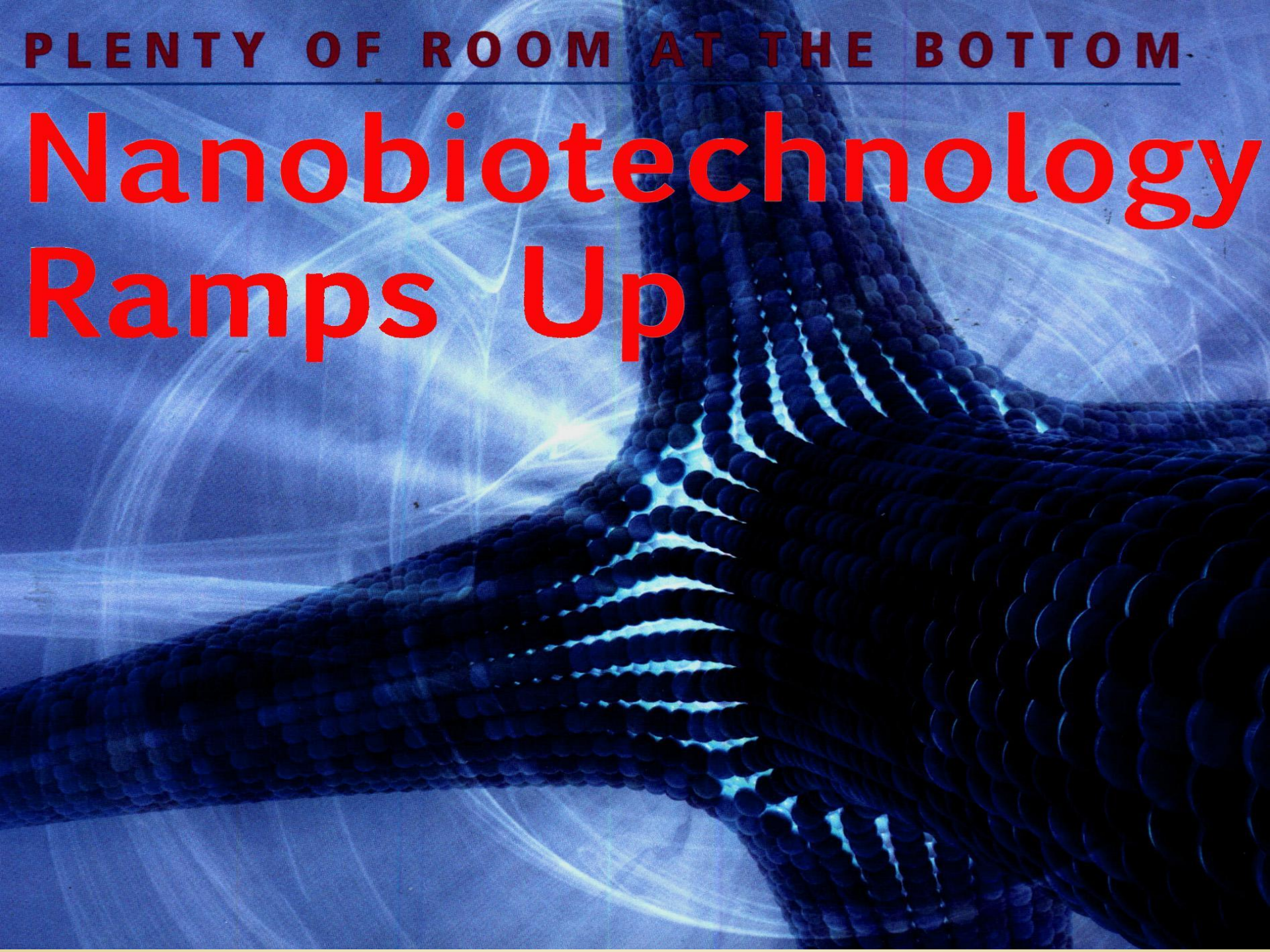

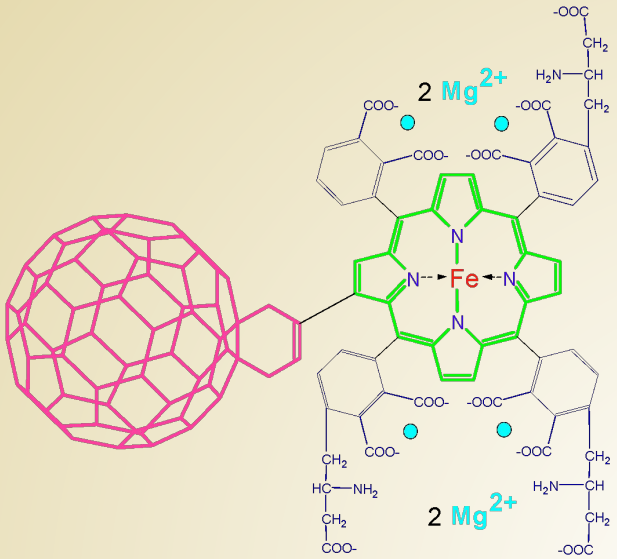
2 Mg2+
2 Mg2+

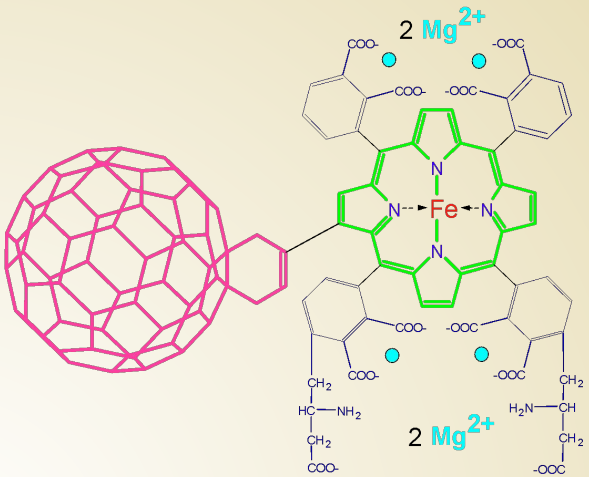
2 Mg2+
2 Mg2+

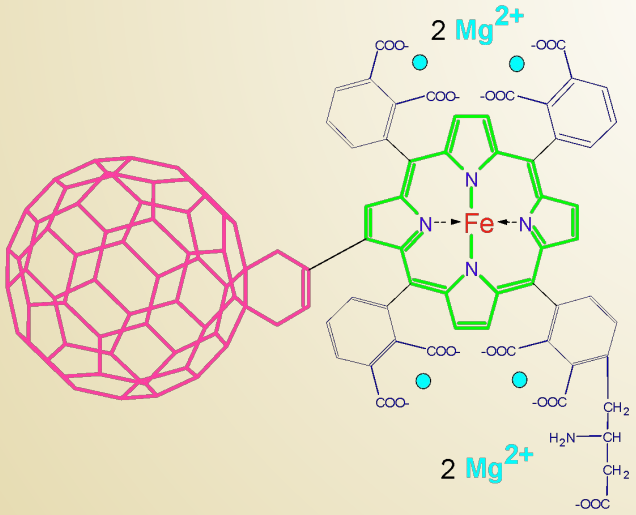
2 Mg2+
2 Mg2+

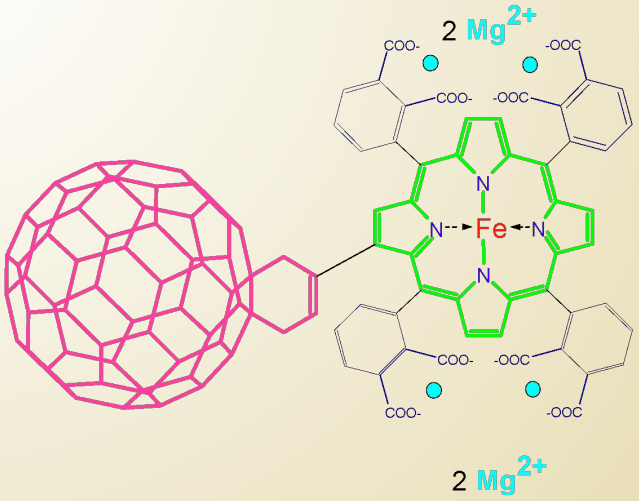
2 Mg2+
2 Mg2+

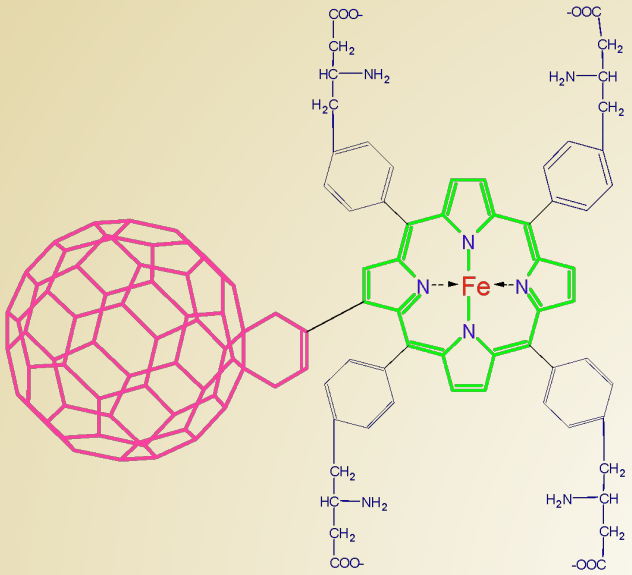
COO-
CH2
HC—NH2
H2C
-OOC
CH2
H2N—CH
CH2
N
N
Fe
N
N
CH2
HC—NH2
CH2
COO-
CH2
H2N—CH
CH2
-OOC

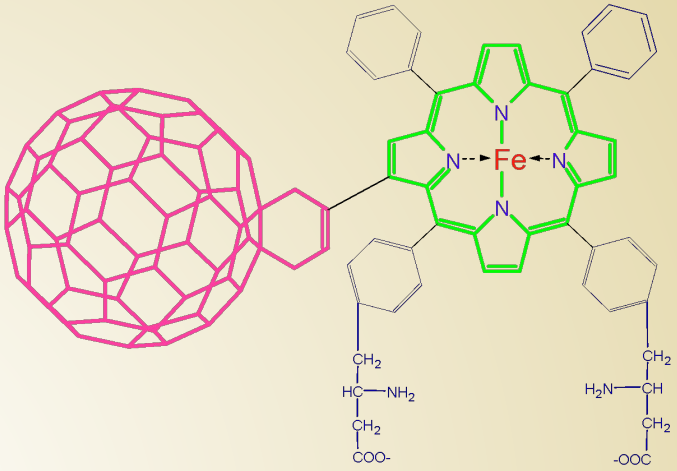
N
N
Fe
N
N
CH2
HC—NH2
CH2
COO-
CH2
H2N—CH
CH2
-OOC

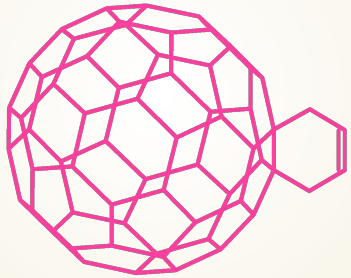

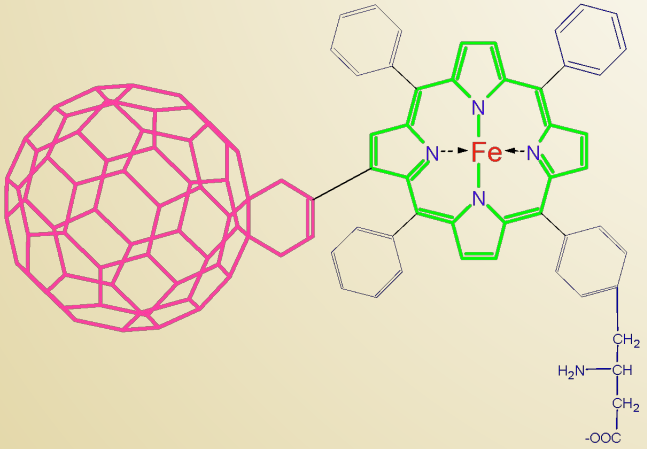
N
N
Fe
N
N
CH2
H2N—CH
CH2
-OOC

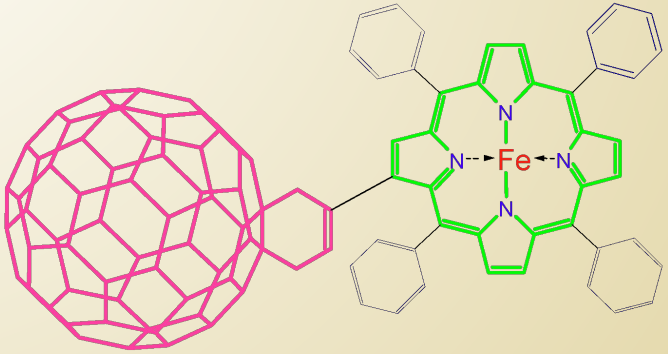
N
N
Fe
N
N

Buckminsterfullerene(C60)-2-(butadiene-1-yl)-
-tetra(o-γ-aminobutyryl-o-phtalyl)porphyrin
PORPHYLLERENE – MC16

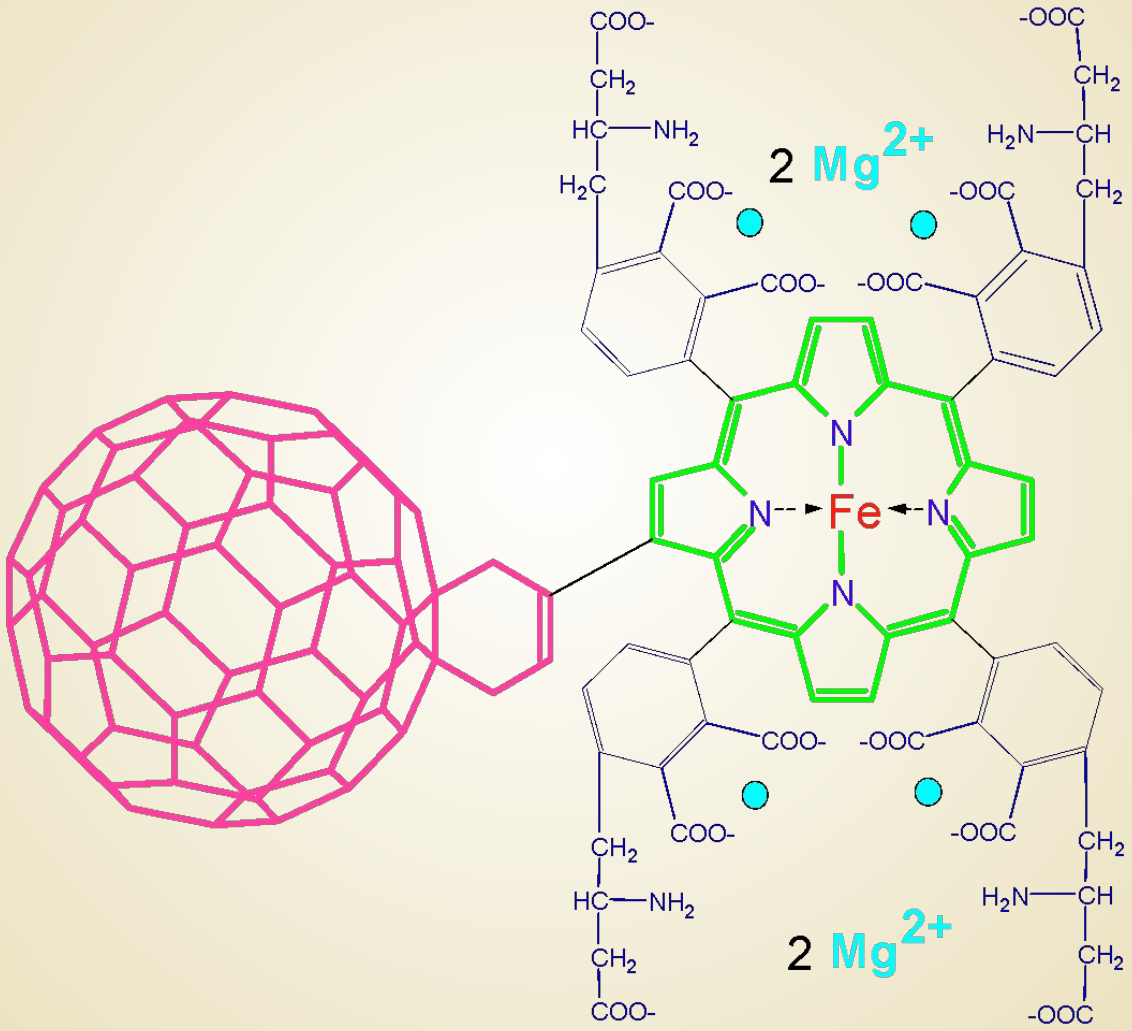


Heidolph

PMC16 CATIONITE PROPERTIES AND THE NANOCLUSTERS FORMATION AS A FUNCTION OF pH

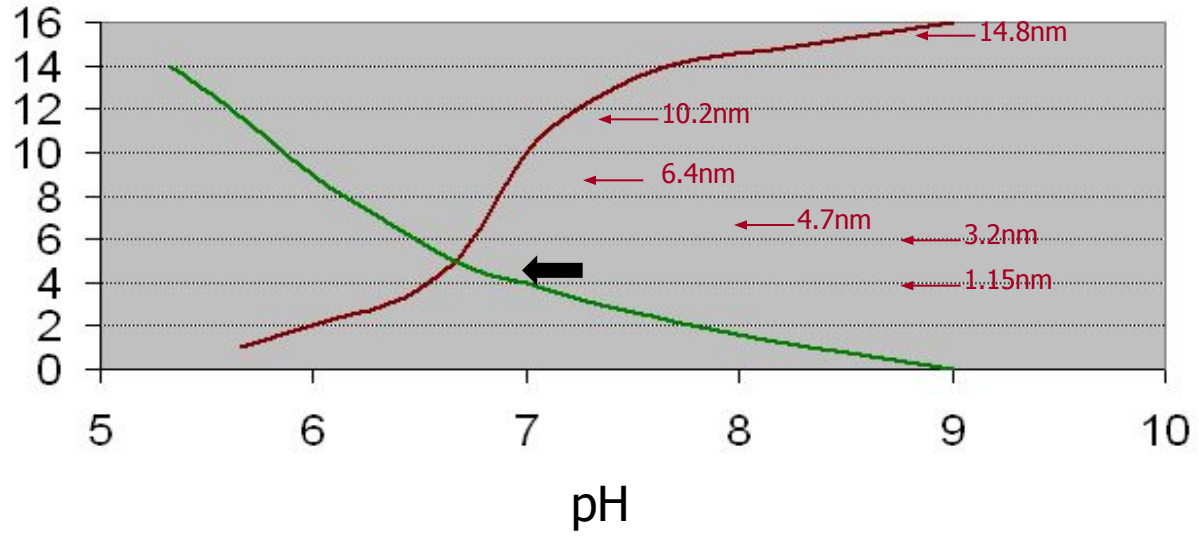

⬅ Blue arrow shows the iron-dextrane sphere exclusion limit

— NUMBER OF SUBUNITS
— 25Mg2+ RELEASE, *portion of the total PMC16 magnesium*

THE CELL COMPARTMENT RETAINING DISTRIBUTION OF [59Fe]PMC16 CAUSED BY A SINGLE i.v. ADMINISTRATION IN RATS (30 mg/kg, 470-520 Ci/kg).

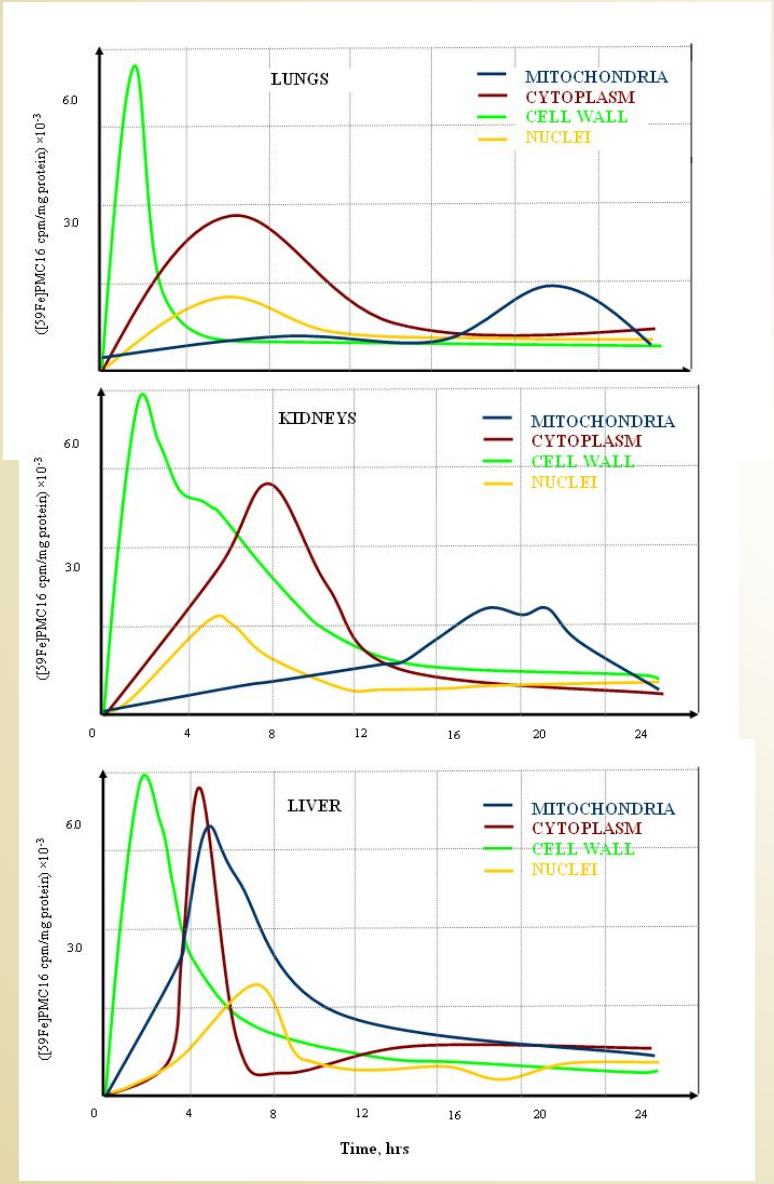

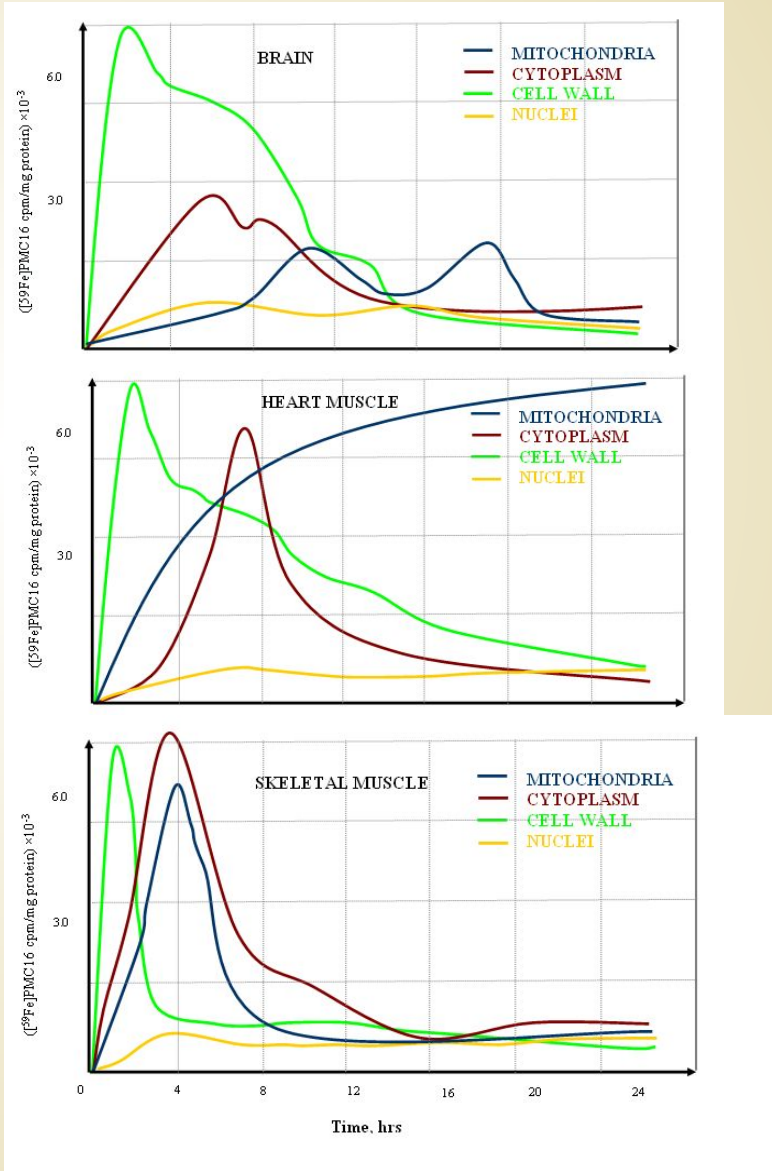

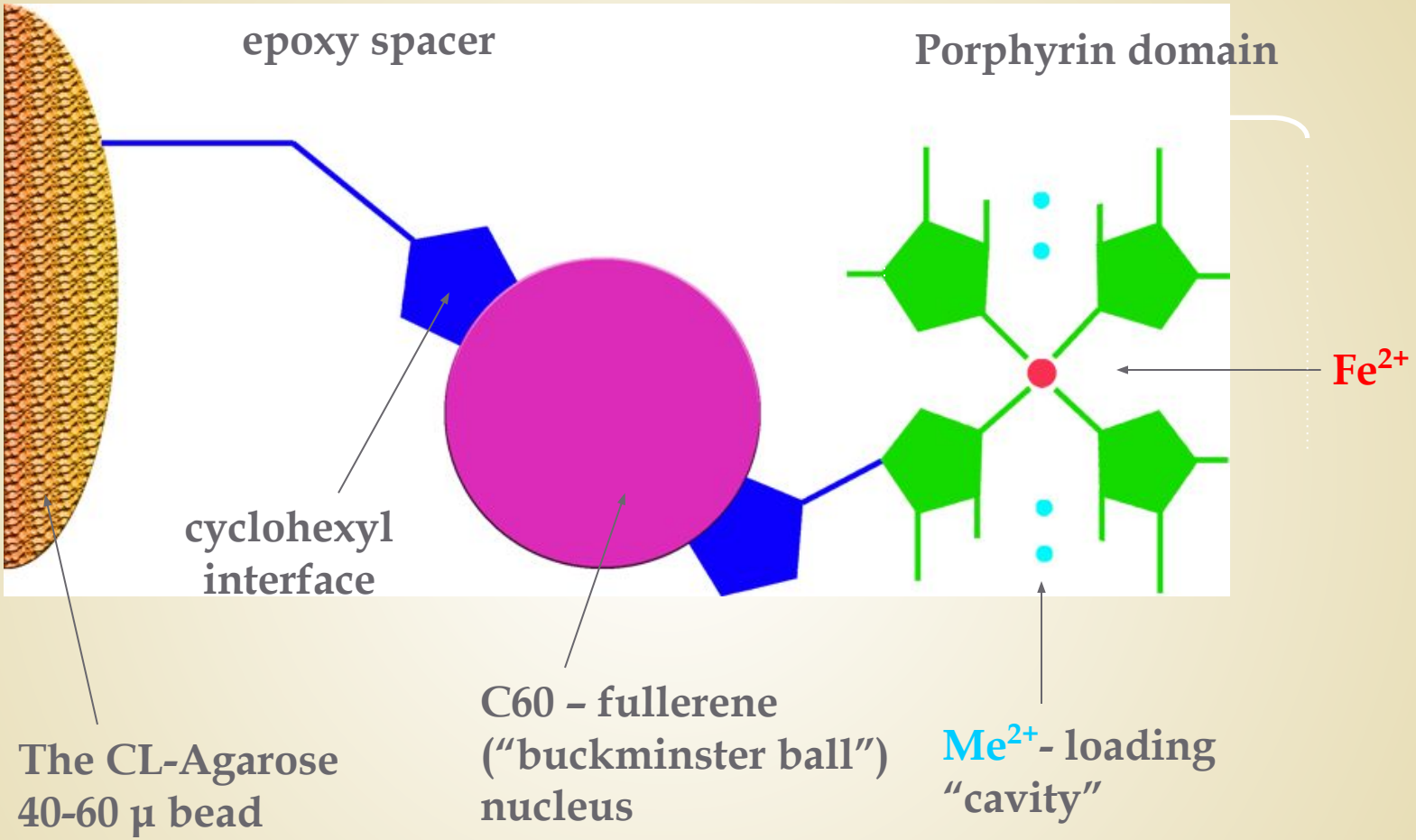
epoxy spacer
Porphyrin domain
Fe^{2+}
cyclohexyl interface
The CL-Agarose 40-60 µ bead
C60 – fullerene ("buckminster ball") nucleus
Me^{2+}- loading "cavity"

AN AFFINITY CHEROMATOGRAPHY OF THE HUMAN MYOCARDIAL MITOCHONDRIA MEMBRANE PROTEINS ON THE COLUMN WITH AGAROSE-6B-CL-[C_{17}]-PMC16

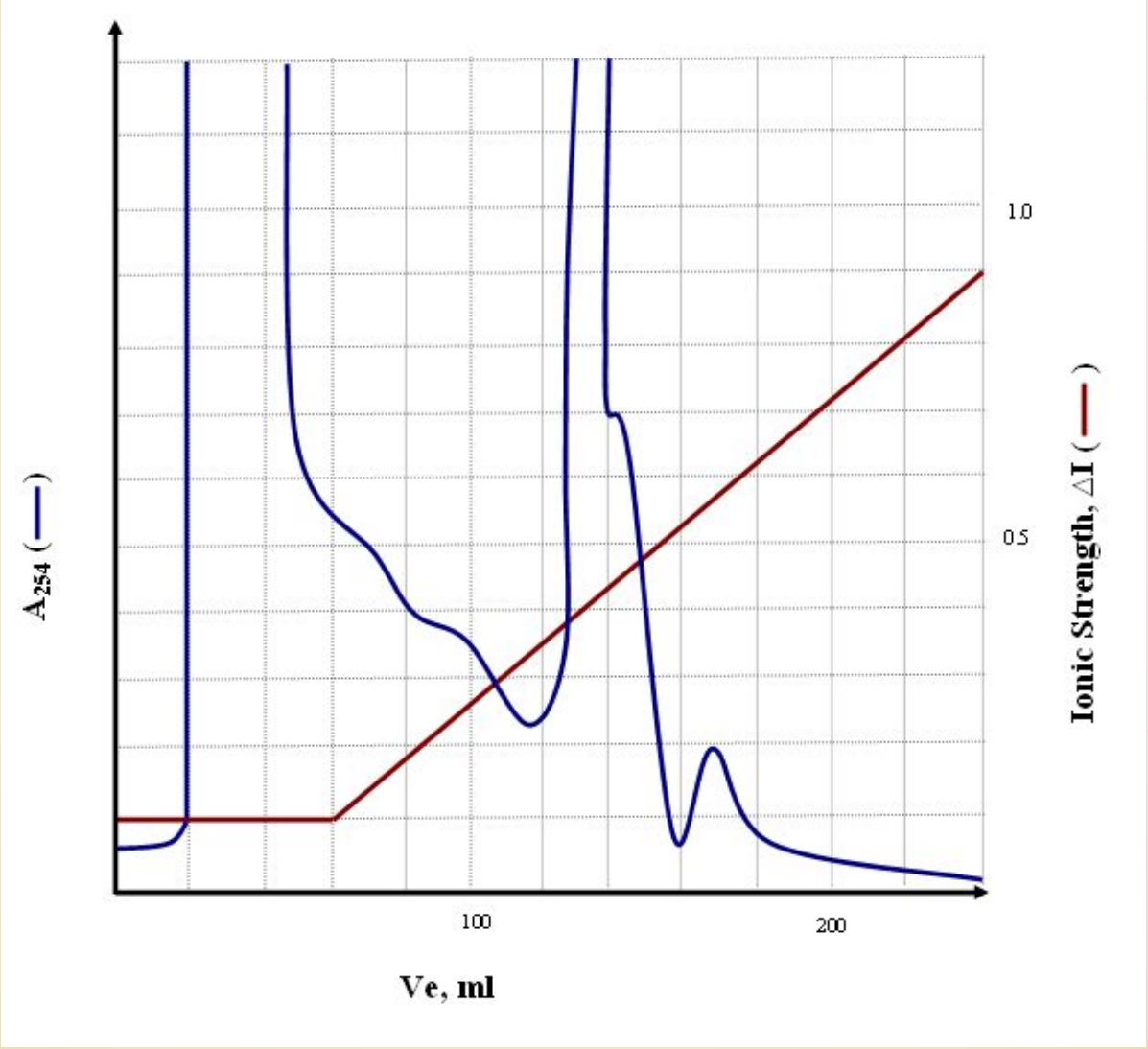

THE [Mg]PMC16 PHARMACOKINETICS IN RAT
Single 20mg/kg i.v. injection (M ± SEM, *n* = 6)
24 hrs monitoring presented

$T_{1/2} = 9.0$ hrs $T_{max} = 2.5$ hrs Cl = 32 ± 4 ml/min/kg $k = 0.685$	$C_0 = 62$ µg/ml $C_{max} = 260 \pm 83$ ng/ml $V_P = 16.2$ ml/kg $V_C = 12.4$ ml $V_1 = 0.08$ ml

Renal excretion:	28 ± 4.3%
Hepatic excretion: *(metabolization)*	16 ± 4.0%
Plasma proteins binding:	1.2 ± 0.3%
BLOOD CELLS UPTAKE	
Lymphocytes:	28.6 ± 5.5%
Erythrocytes:	8.0 ± 3.2%
TISSUE SPECIFIC ACCUMULATION	
Myocardium:	18.4 ± 3.40%
Brain:	0.6 ± 0.02%
URINE ELIMINATING PMC16 METABOLITES (258±4.0 µg/ml)	
Phthalate-depleted derivatives:	56.4 ± 8.7%
Alanyl derivatives:	27.0 ± 6.1%
Benzyl-C_{60}:	16.2 ± 3.3%
PMC16 urine content:	462 ± 11 µg/ml
C_{60} urine content:	2.9 ± 0.1 µg/ml

A MULTIEXPONENTIAL TWO-COMPAPTMENT DYNAMICS OF THE BLOOD SERUM [Mg]PMC16 CONCENTRATION AFTER A SINGLE 20 mg/kg i.v. INJECTION IN RATS

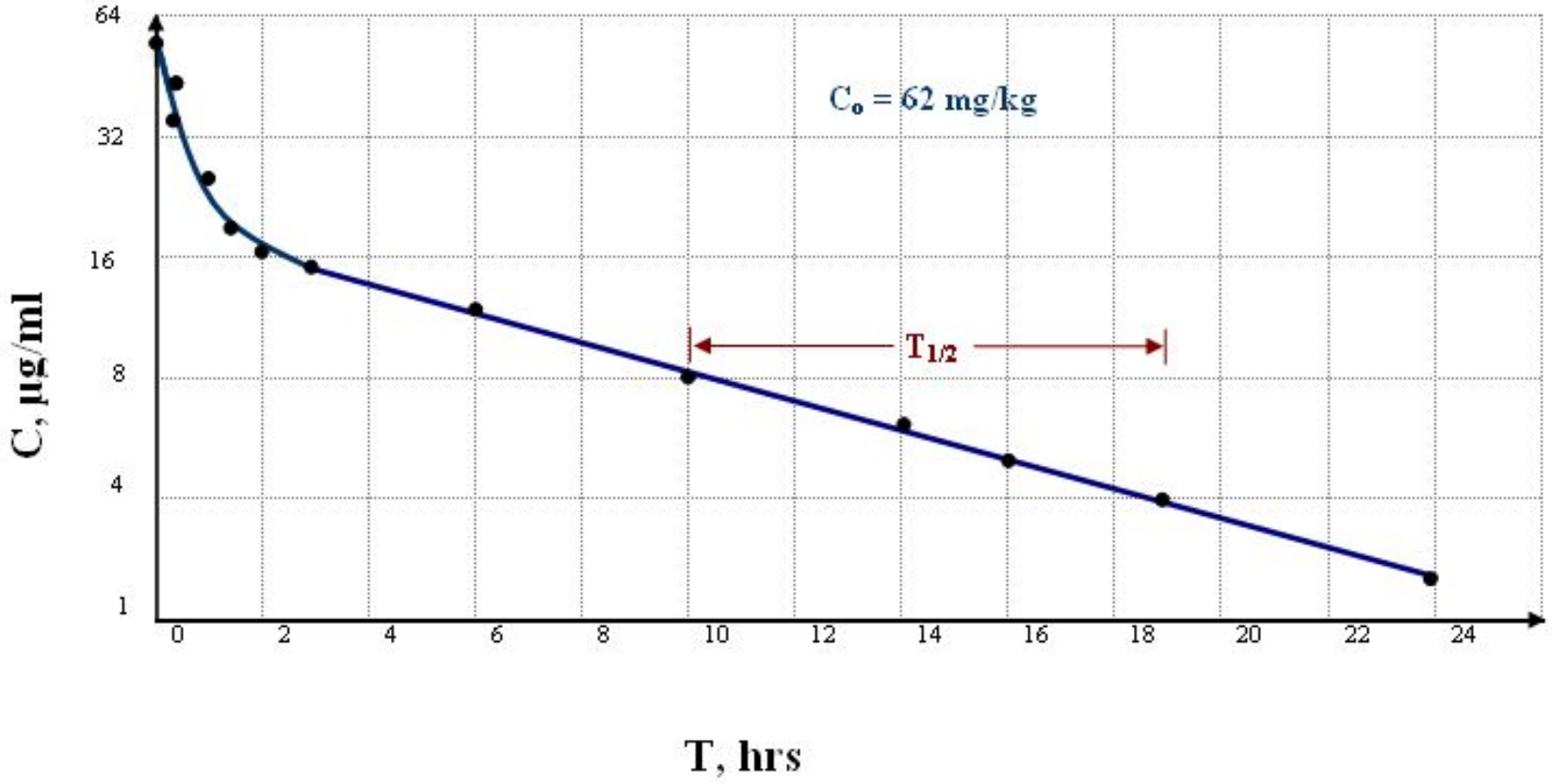

SYNERGISM OF THE MITOCHONDRIAL MATRIX CK ACTIVITY, MAGNESIUM CATIONS INFLUX AND THE FREE PROTONS EXCESS DEGREE

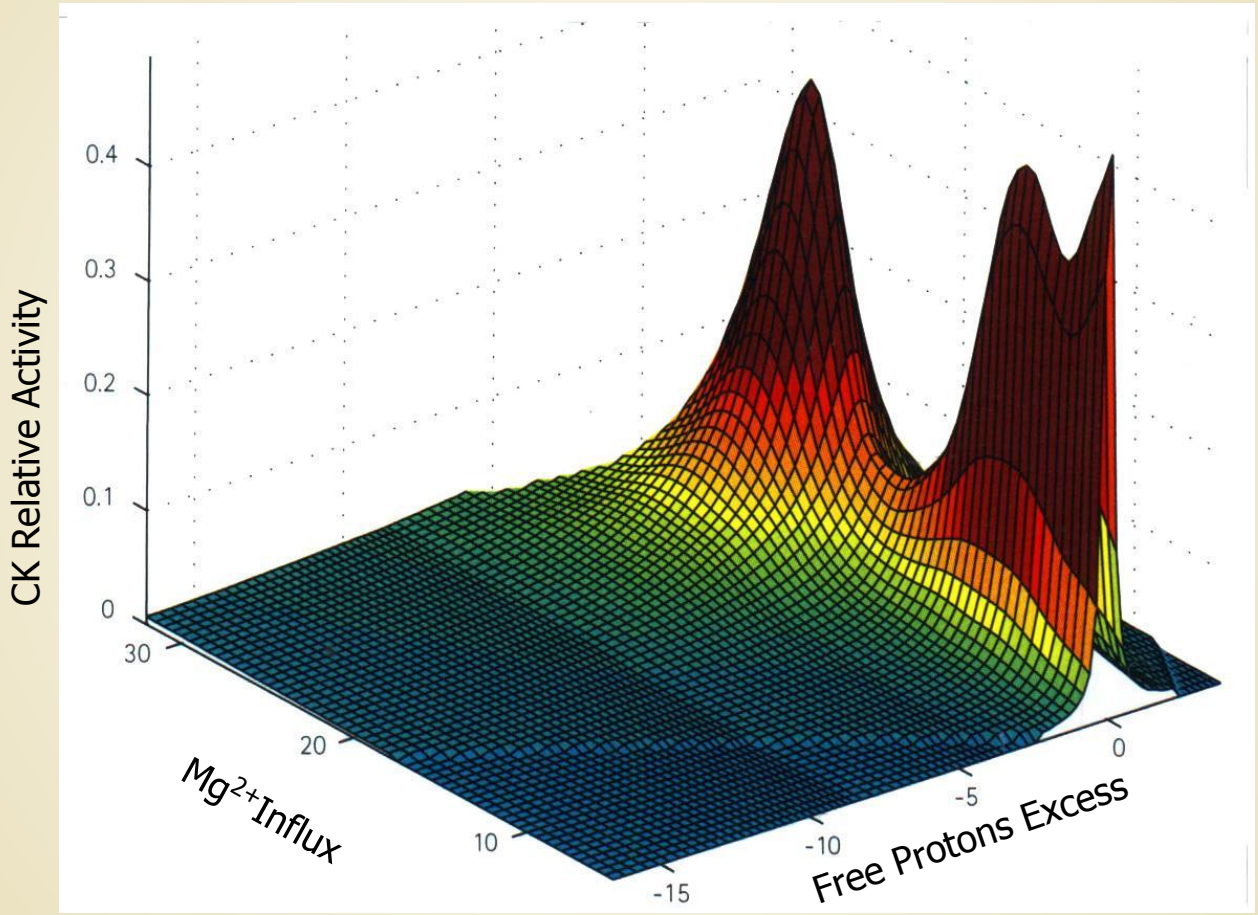

The isolated rat myocardium mitochondria tested.

Yellow / Red stands for the spinless / spin Mg isotopes ratio.

SYNERGISM OF THE ATP YIELD, OXYGEN CONSUMPTION AND THE Mg^{2+} INFLUX IN THE PERFUSED ISOLATED RABBIT HEART MUSCLE TISSUE

A

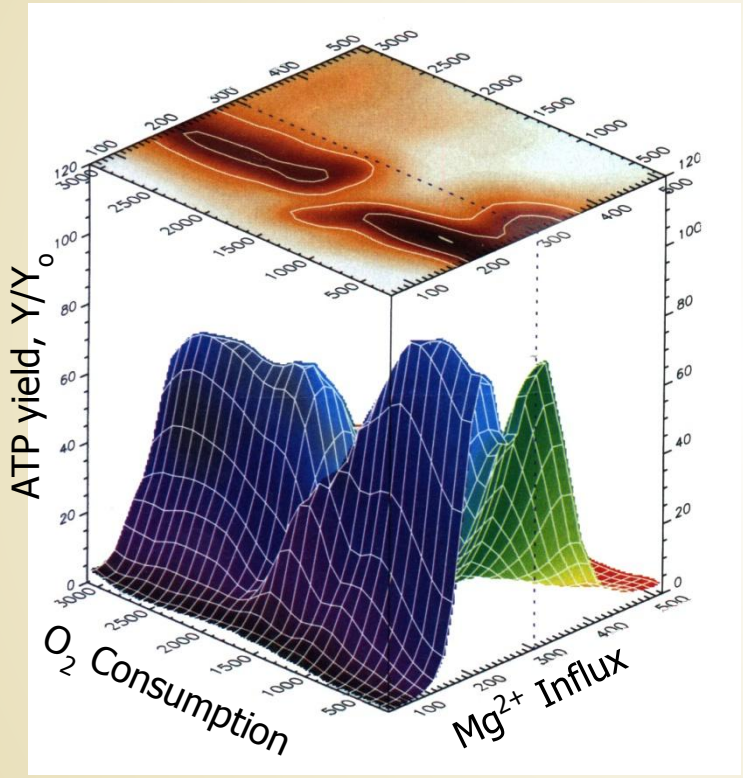

B

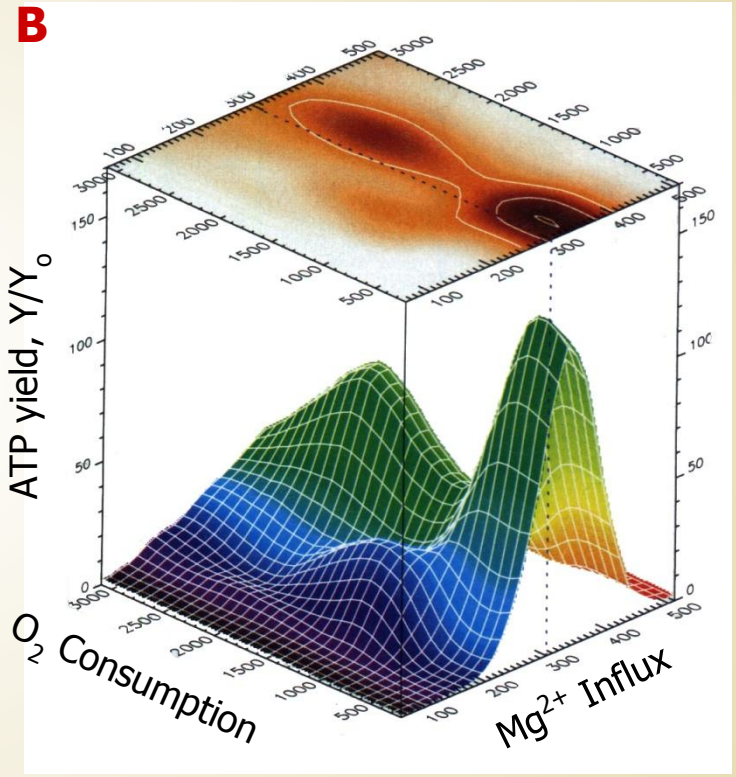

A – Zero spin magnesium test

B – Magnetic magnesium test


Lenovo
PerkinElmer
Lenovo

ELECTRON TRANSMITTING MICROPHOTOGRAMS OF THE RAT MYOCARDIOCYTIC PERINUCLEAR AREAS

A

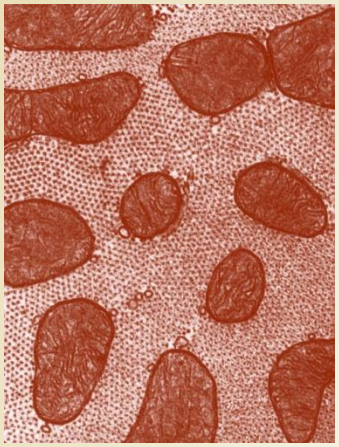

B

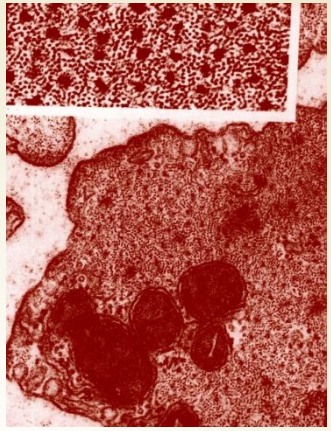

C

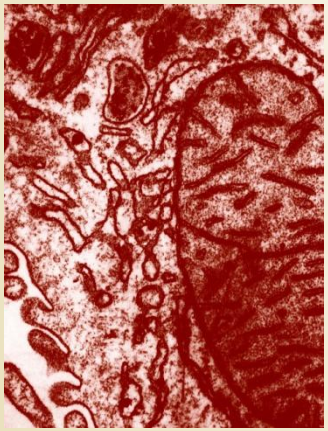

D

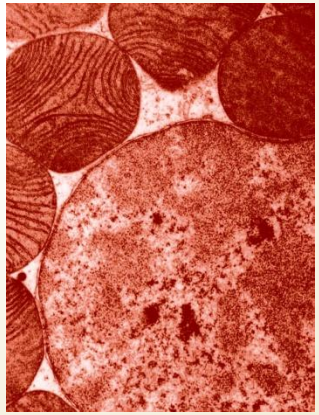

A, C – PMC16 related hypoxia preventing effect

B – Inhalation oxygen deficiency hypoxia model

D – Intact myocardium

DXR – INDUCED MITOCHONDRIAL DISPLASIA IN RABBIT MYOCARDIOCYTES

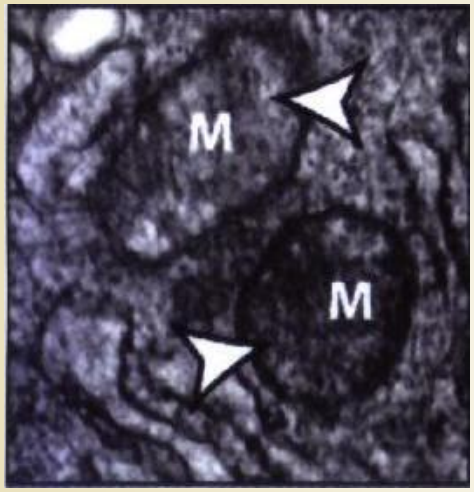

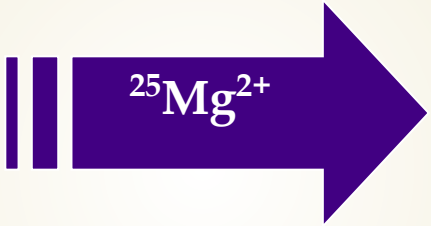

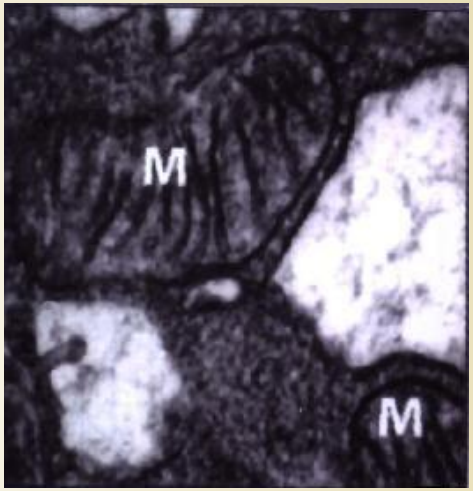

A

B

(A) Mitochondria (M): 0.5 DL50 DXR, 12 hrs

(B) Mitochondria (M): 0.2 DL_{50} PMC16, 6 hrs → 0.5 DL_{50} DXR, 12 hrs.

Arrow sign points to a matrix granular destruction

DXR – INDUCED NUCLEAR DISPLASIA IN RABBIT MYOCARDIOCYTES

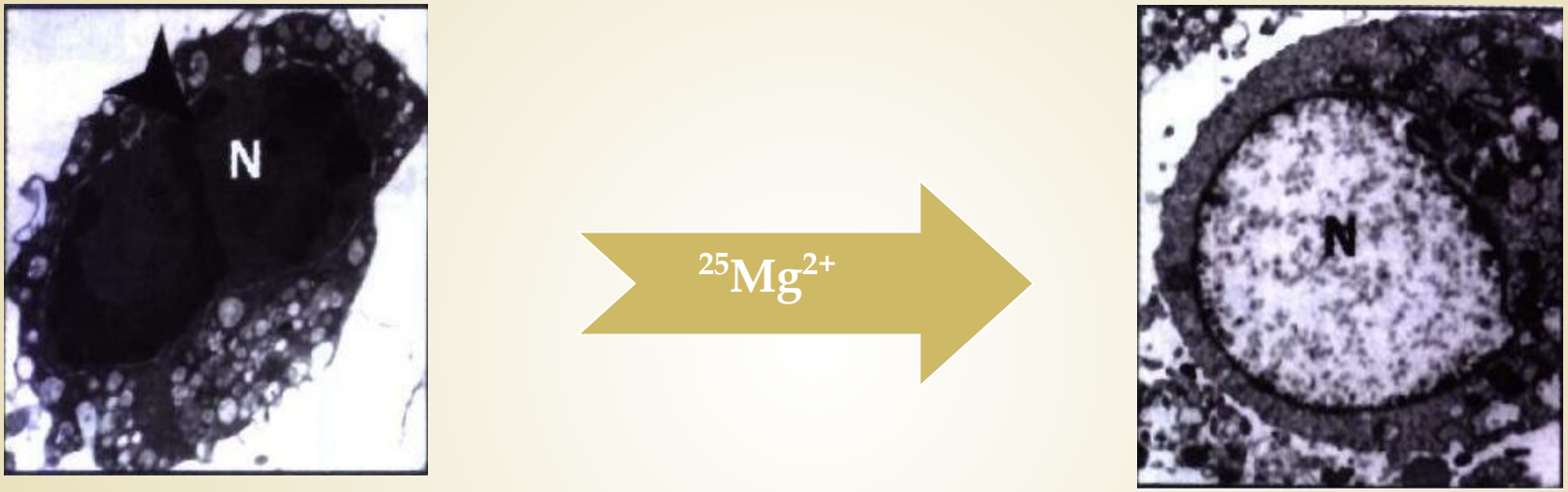

A B

(A) Nucleus (N):0.5 DL50 DXR, 12 hrs.

(B) Nucleus (N): 0.2 DL50 PMC16, 6 hrs → 0.5 DL50 DXR, 12 hrs.

Arrow sign points to a matrix granular destruction

FRAGMENTATION OF THE RABBIT MYOCARDIOCYTES MITOCHONDRIA IN THE DXR-INDUCED ACUTE HYPOXIA

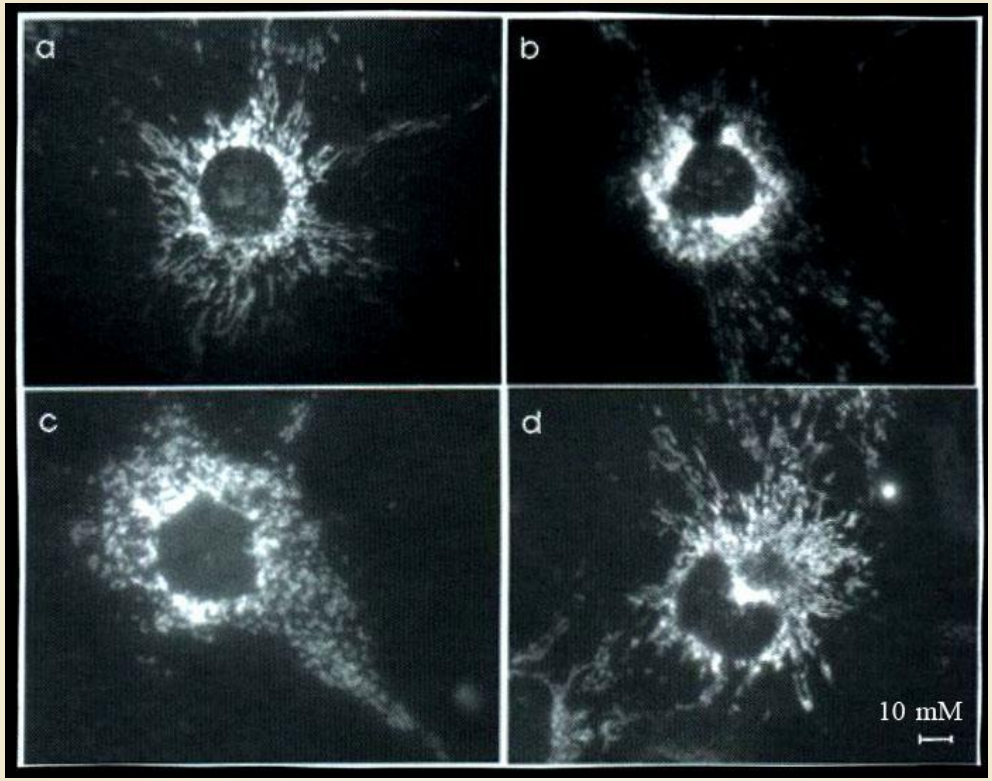

(a) 0.8 DL_{50} DXR, 20 min (i.v.)
(b) 0.8 DL_{50} DXR, 4 hrs (i.v.)
(c) 0.8 DL_{50} DXR, 12 hrs (i.v.)
(d) 0.2 DL_{50} PMC16, 10 hrs (i.v.)→ DL_{50} DXR, 12 hrs (i.v.)

FRAGMENTATION OF THE RABBIT MYOCARDIOCYTES MITOCHONDRIA IN THE 1-METHYLNICOTINE AMIDE (MNA) – INDUCED ACUTE HYPOXIA

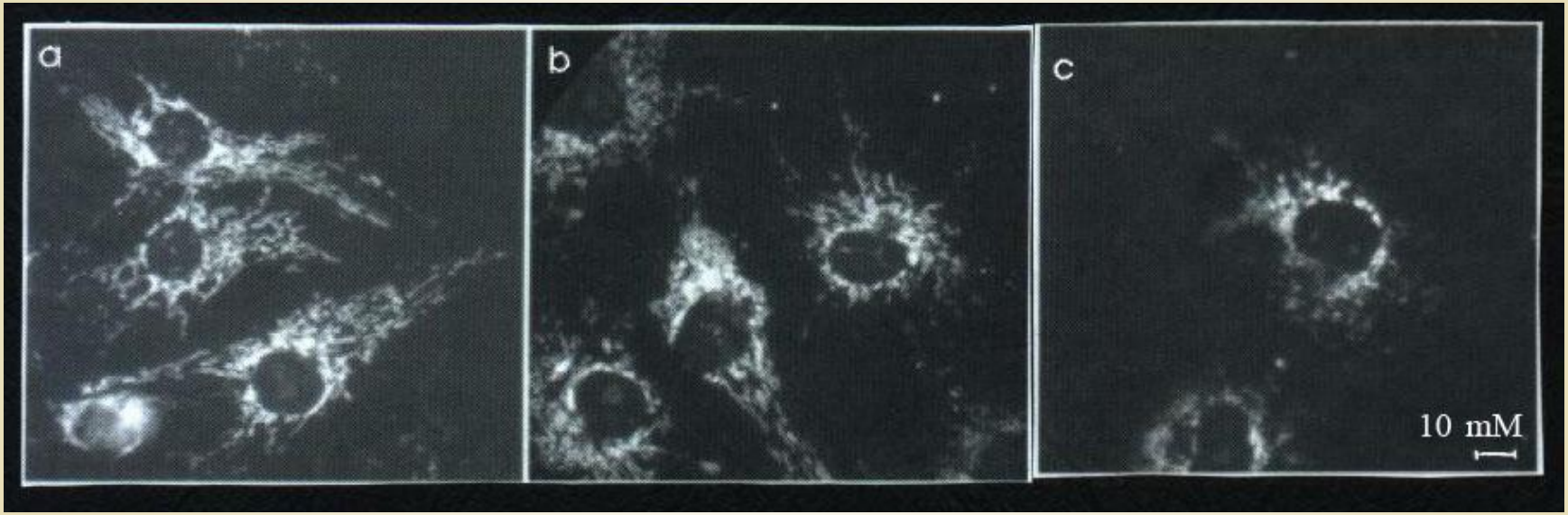

(a) 1.0 DL_{50} MNA, 6 HRS (i.v.)
(b) 1.0 DL_{50} MNA, 12 hrs (i.v.)
(c) 1.0 DL_{50} MNA, 24 hrs (i.v.)


BECKMAN COULTER
Avanti J-HC
21013400000279
BECKMAN COULTER
Optima L-90K Ultracentrifuge
21013400000280

THE EFFECT OF A PMC16 – TARGETED DELIVERY OF Mg^{2+} ON THE DOXORUBICIN (DXR) PRE – SUPPRESSED ATP PRODUCTION IN RAT MYOCARDIUM

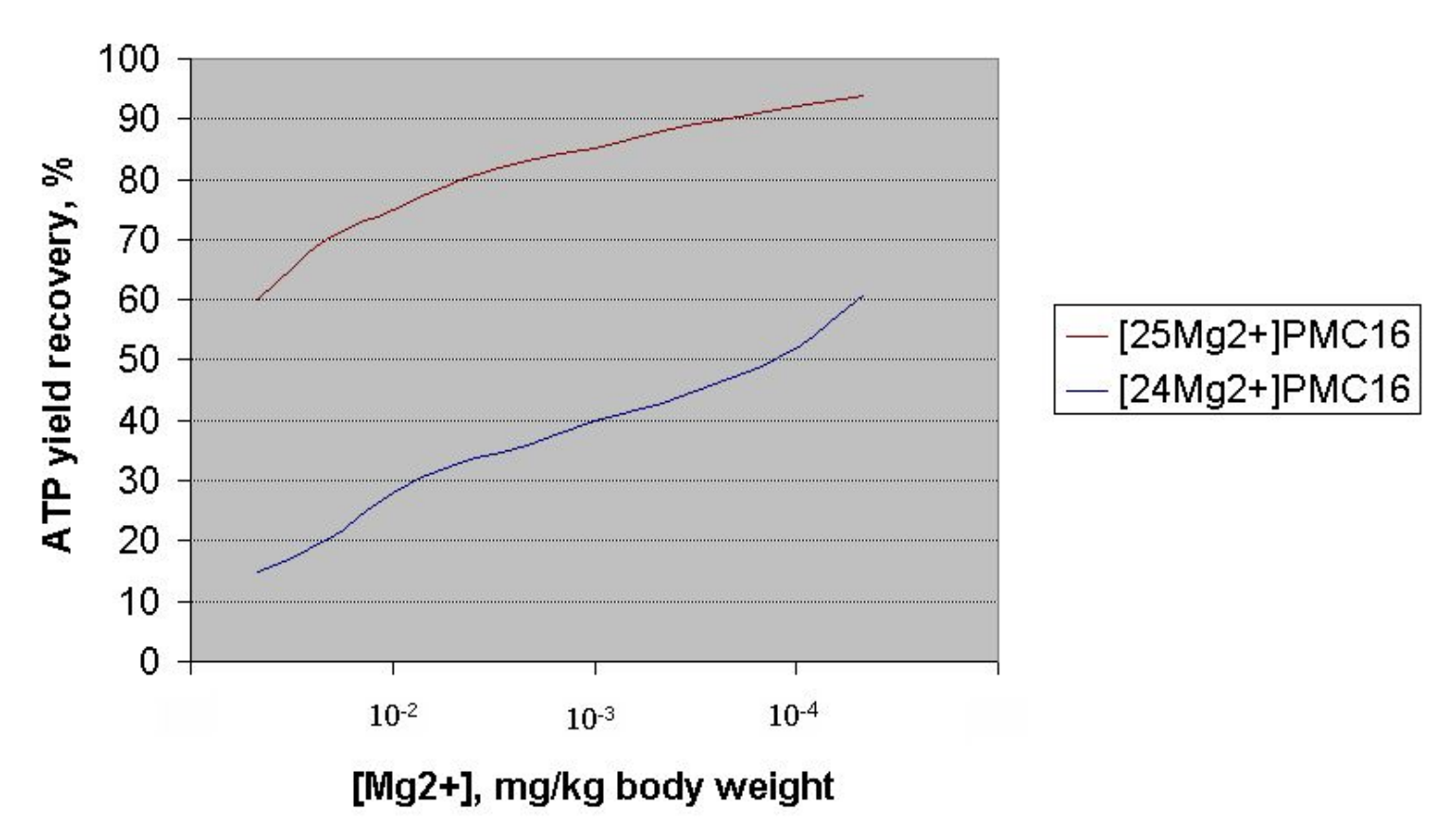

0.8 DL_{50} DXR, i.v., 6 hrs → PMC16, i.v., 6 hrs

THE PORPHYLLEREN – MC16 (PMC16)
PRE – CLINICAL TRIAL

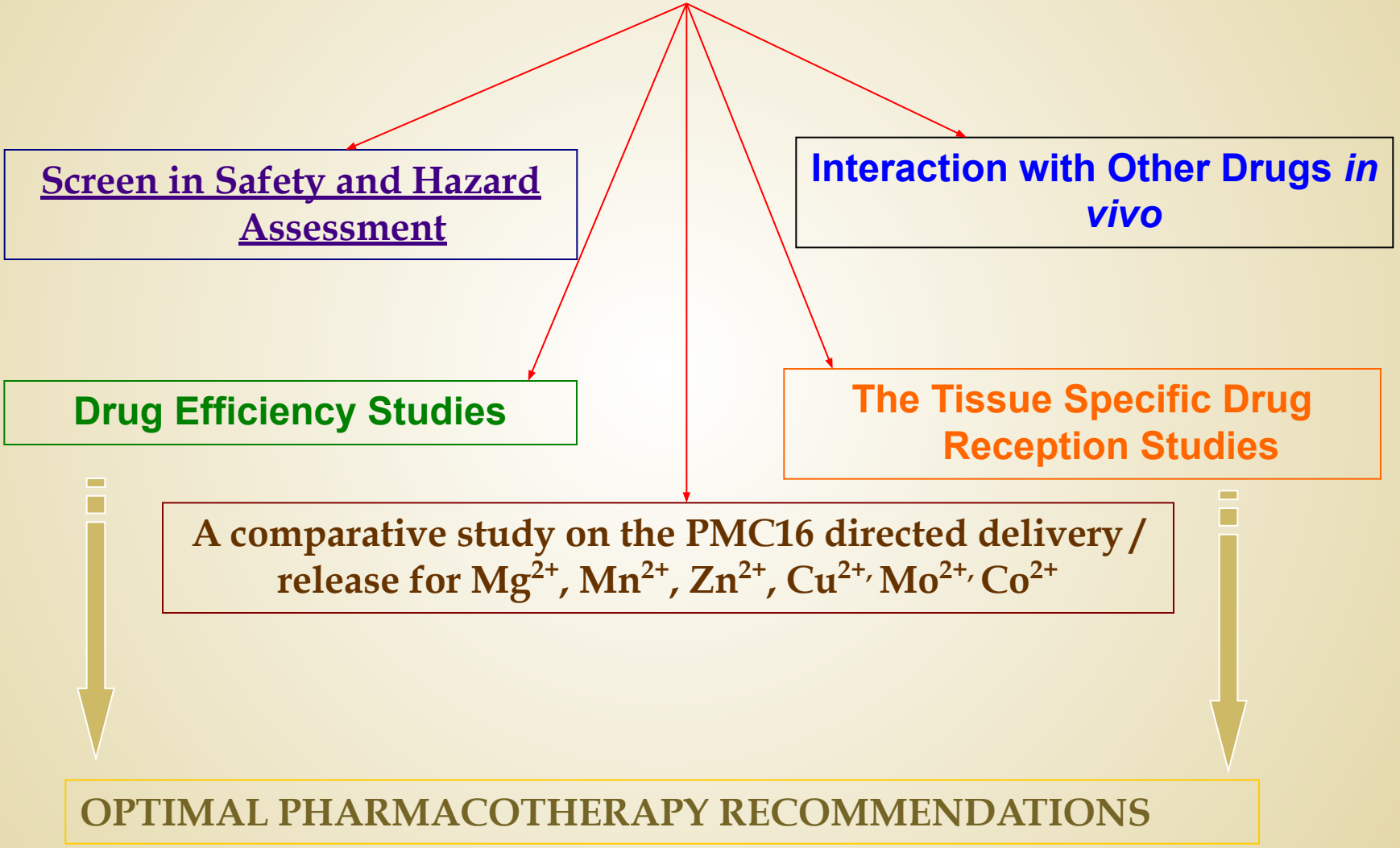

PMC16 CLUSTER POSITIONING INSIDE THE RAT MYOCARDIOCYTIC MITOCHONDRIAL MEMBRANE IN METABOLIC ACIDOSIS (a, c) AND IN NORMAL CONDITIONS (b, d)

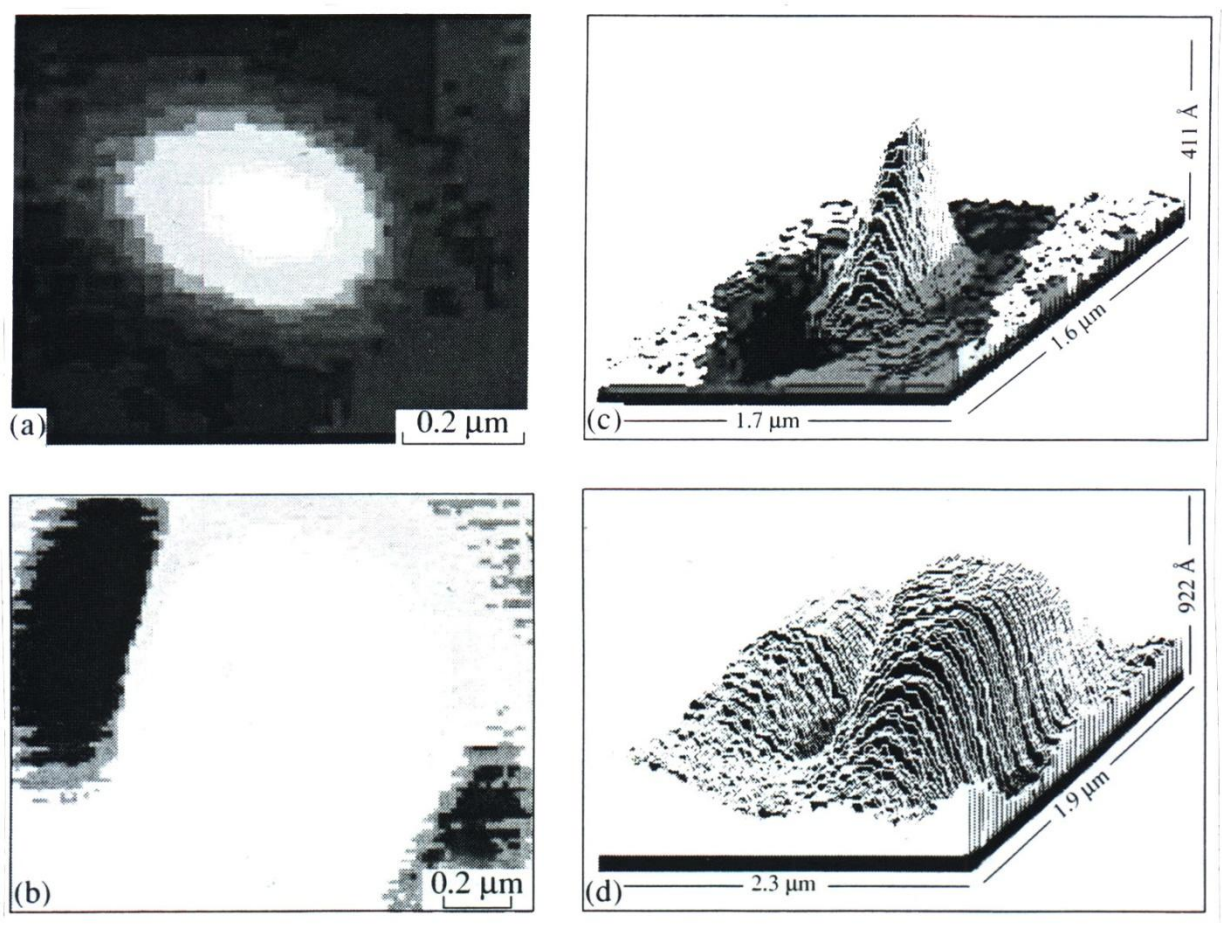

a, b – Laser contrast (Nanofinder-S-6A) images

C, d – Confocal scanning microscopy

THE PMC16 BLOOD CELLS UPTAKE IN RATS.

Single i.v. injection, 30 mg/kg [^{59}Fe]PMC16, 470-520 Ci/kg

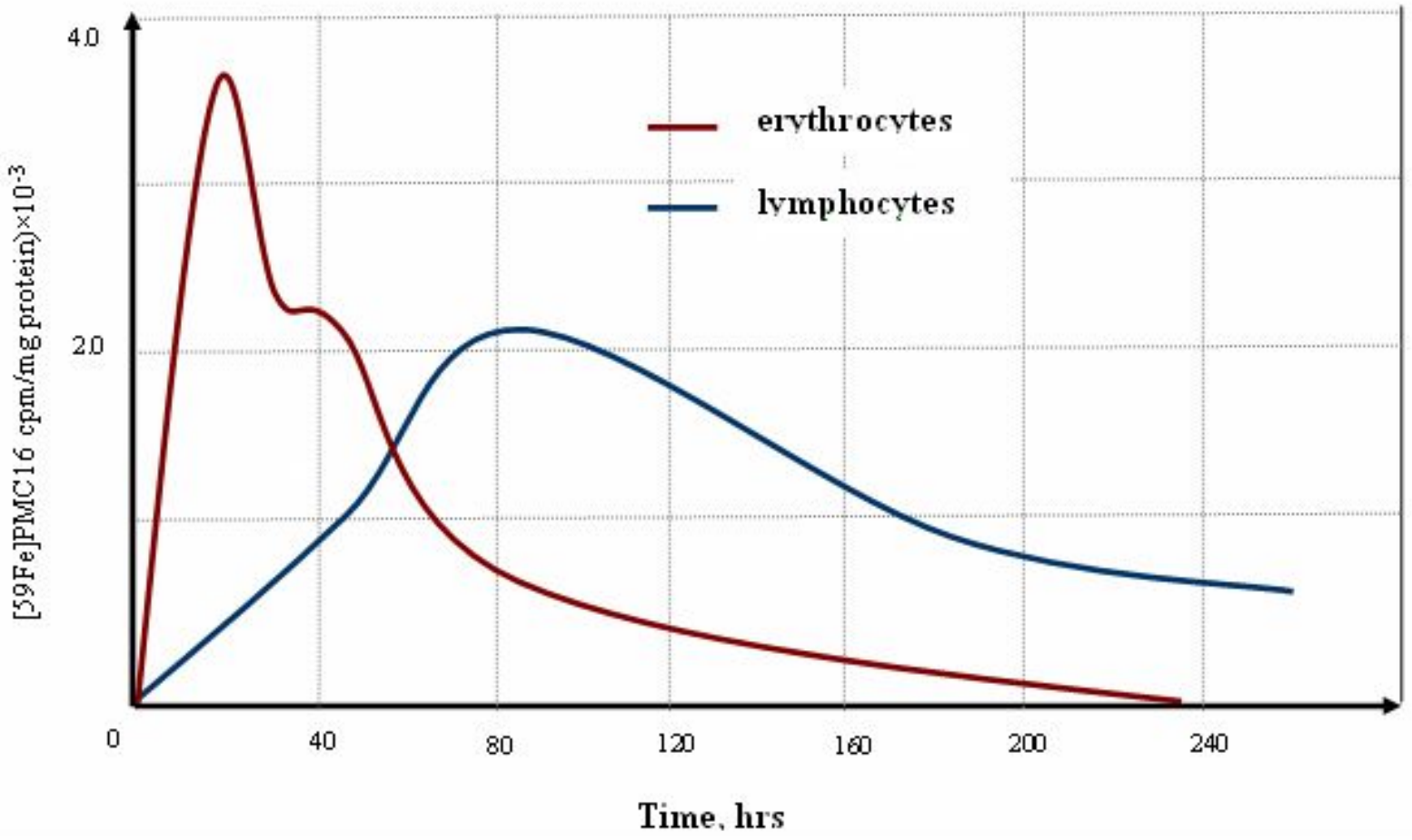

THE PMC16-RELATED ^{59}Fe TURNOVER IN RAT

(20 mg/kg, 380-420 Ci/kg [^{59}Fe]PMC16, single i.v. injection)

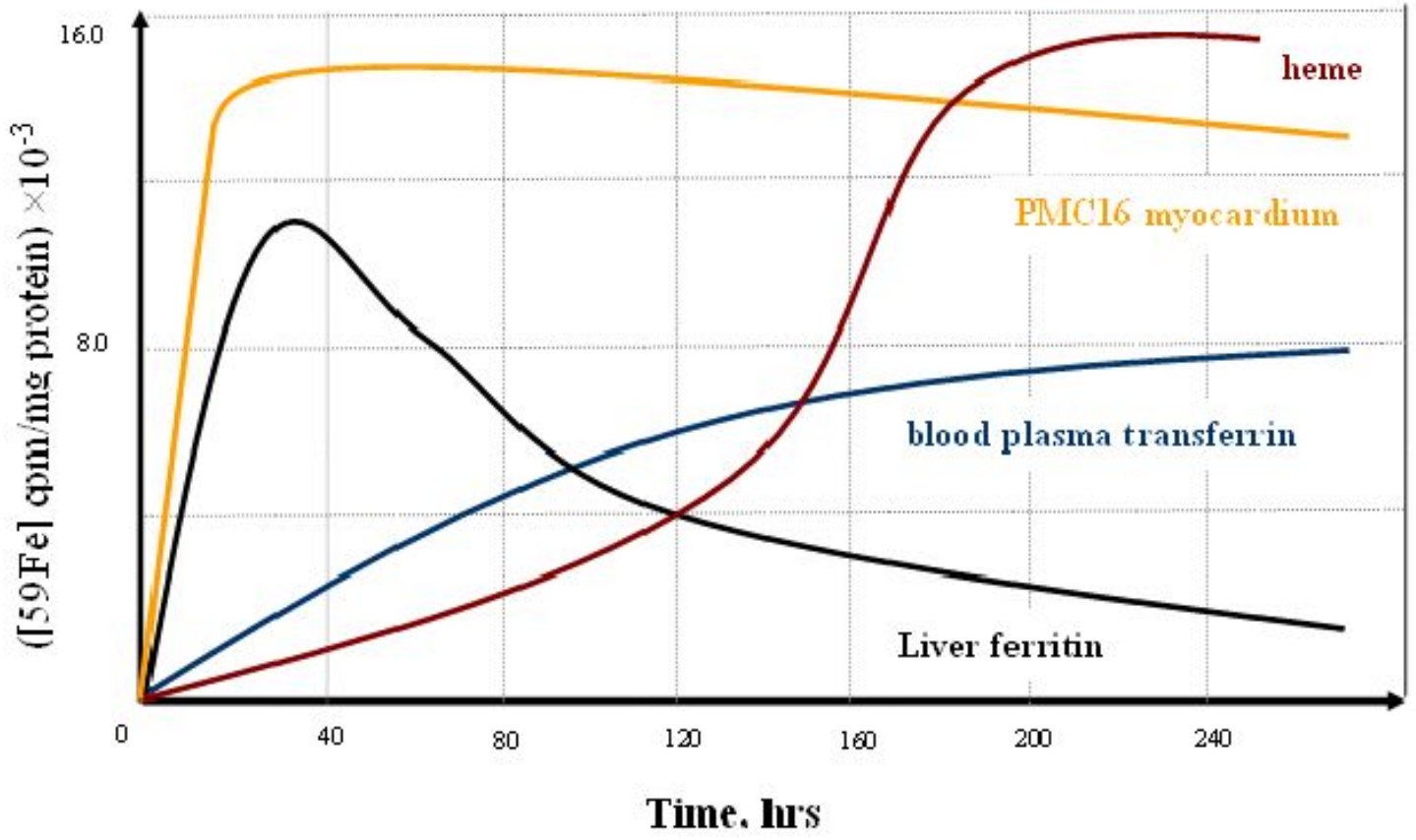

THE RAT HEART MUSCLE ATP PRODUCTION
AS A FUNCTION OF Mg ISOTOPES TISSUE CONTENT IN *in vivo* EXPERIMENTS
WITH [^{25}Mg]PMC16 (A) AND [^{26}Mg]PMC16 (B) SPECIES.

(i.v. 25 mg/kg 1-methylnicotine amide, 6 hours after → i.v. 30 mg/kg [Mg]PMC16)

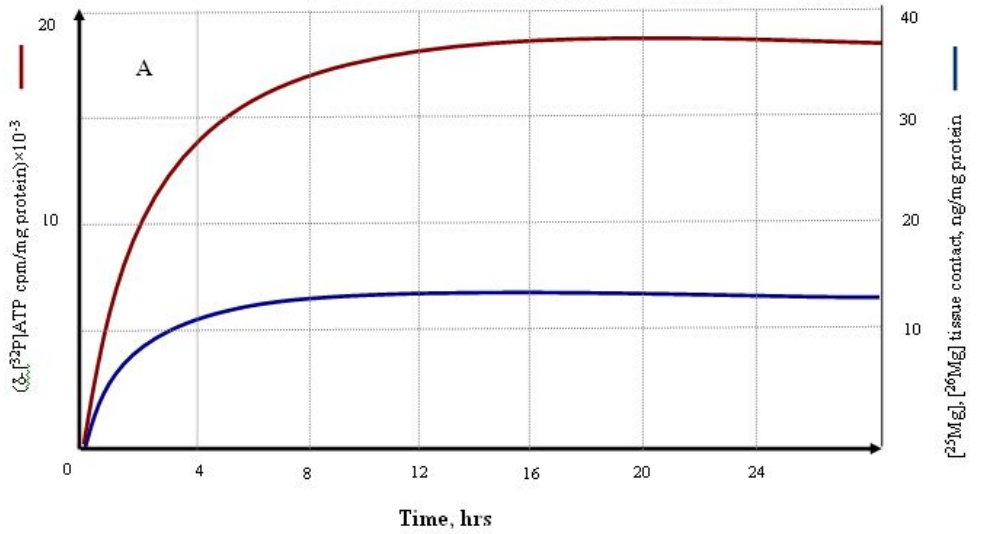

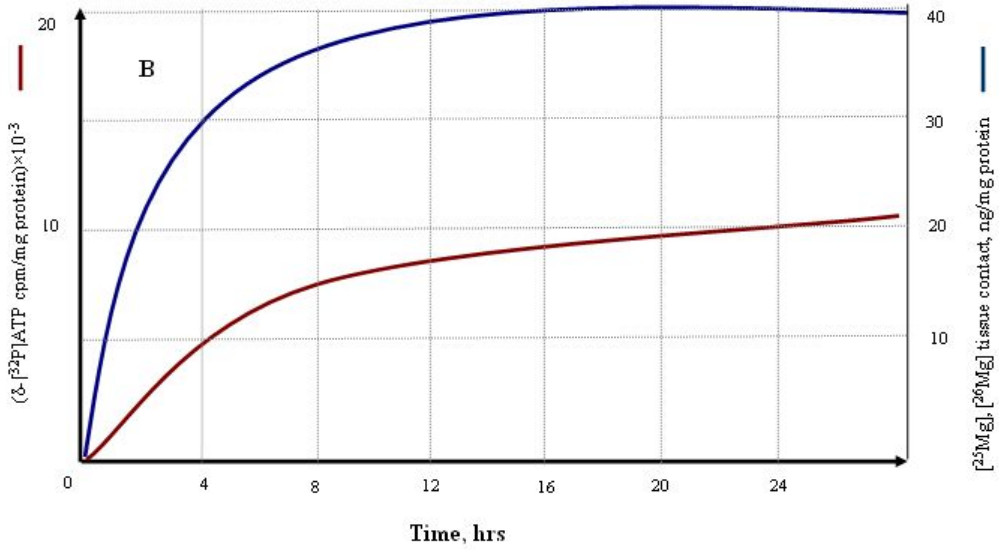

THE HYPOXIA-AFFECTED PMC16 METABOLIC DECAY IN RAT

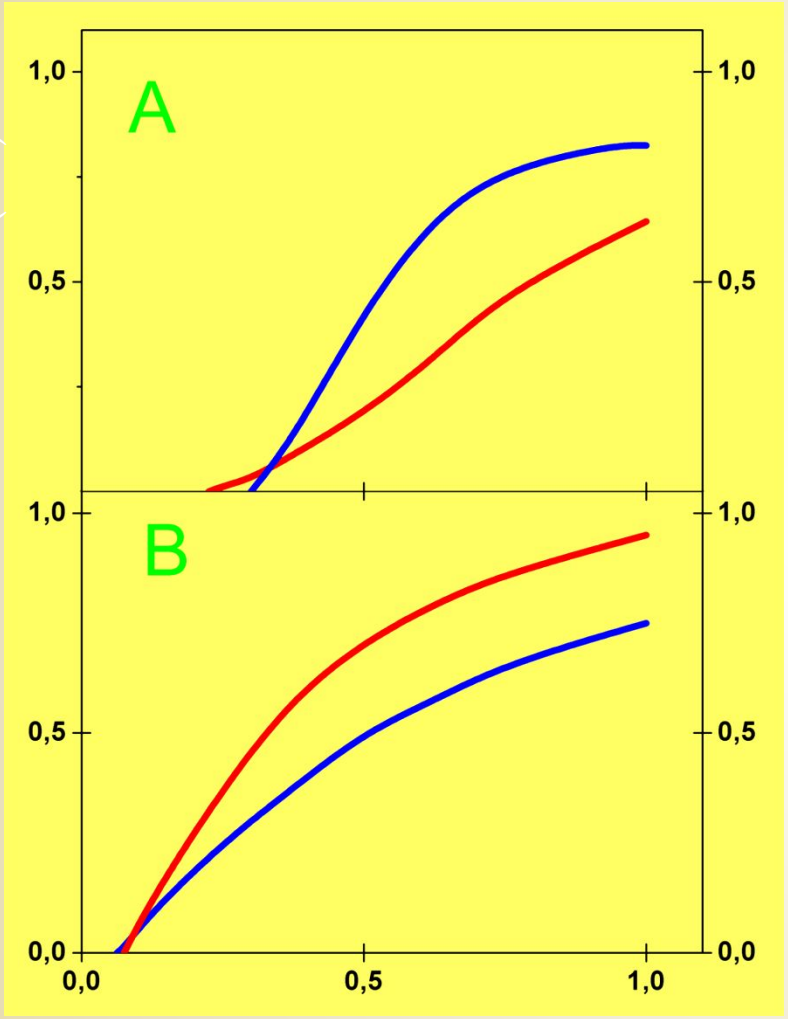

A – Chemically Induced Hypoxia (0.005-0.5 DL_{50} MNA, 12 hrs);

B – Oxygen Depleted Inhalation Hypoxia (15%, O_2, 1-10 days)

A HIGHLY SELECTIVE TRAGETING OF PMC16 NANOPARTICELS TOWARDS THE RAT HEART MUSCLE IN A COURSE OF THE LONG – TERM ADMINISTRATION OF AN EXTRA LOW DRUG DOSAGE

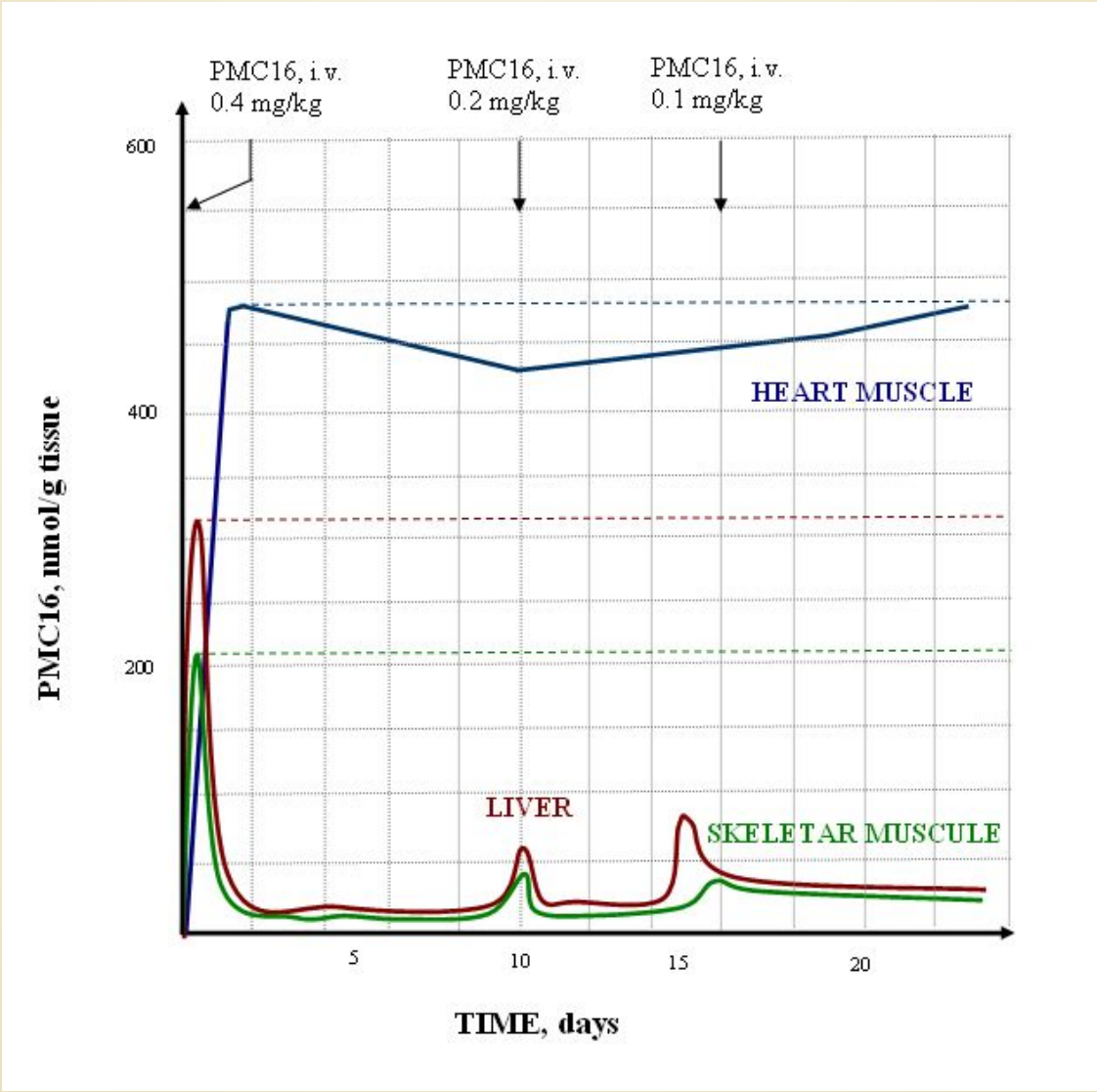

THE RAT MYOCARDIUM TISSUE RESPIRATION AFFECTED BY DOXORUBICIN (DXR) AND 1-METHYLNICOTINE AMIDE (MNA) IN A COURSE OF [^{25}Mg]PMC16 ADMINISTRATION (0.4→0.2→0.1 mg/kg, i.v.)

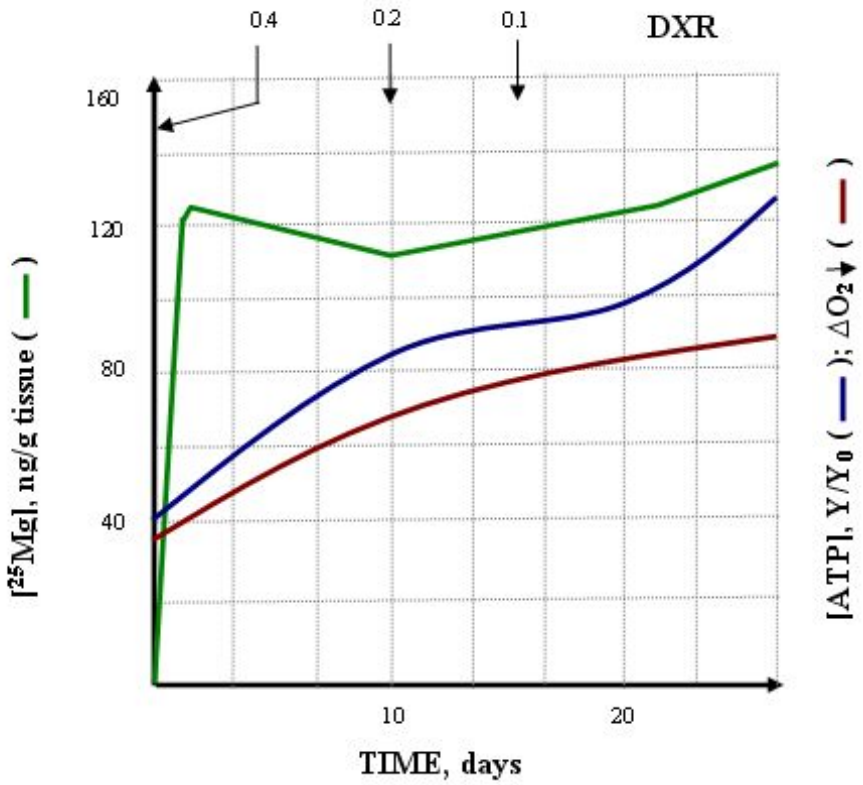

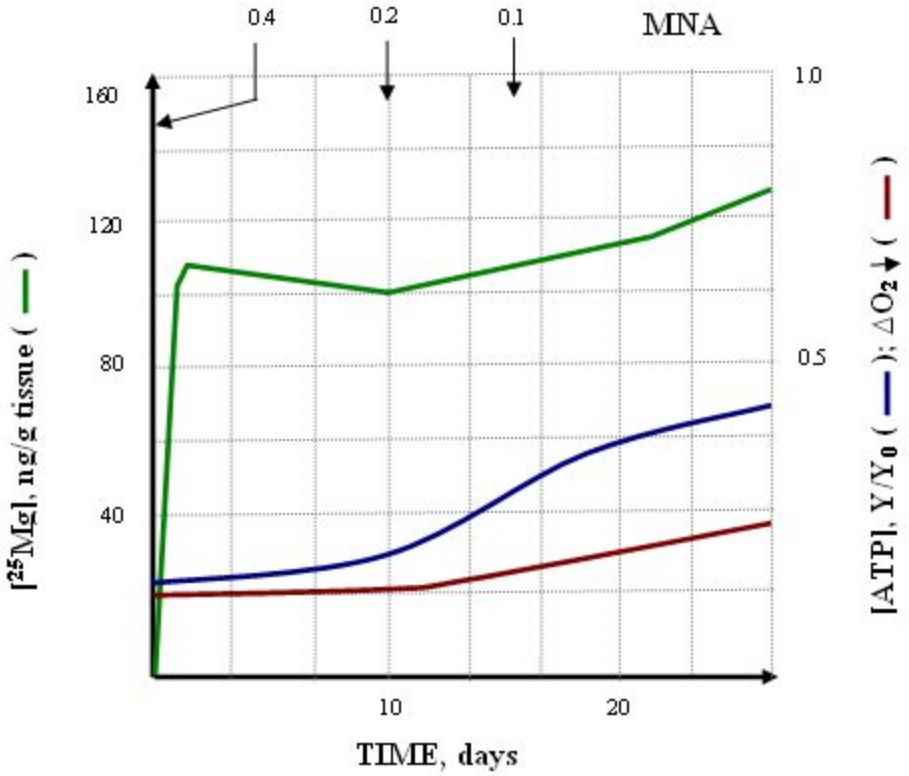

NOTE: *DXR, 20 mg/kg/24 hrs, i.v.:*

MNA, 10 mg/kg/24 hrs, i.v.:

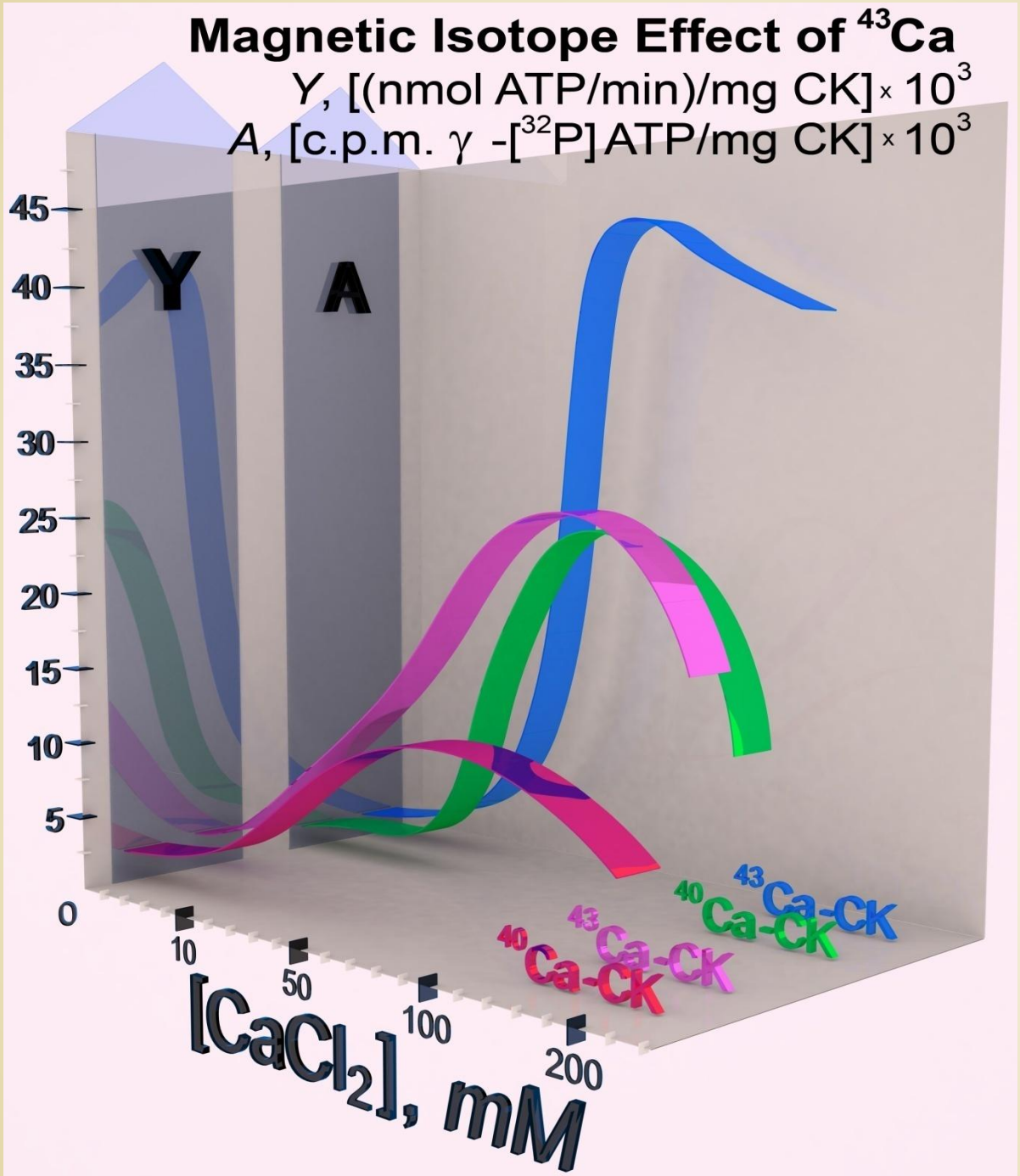
Magnetic Isotope Effect of ^{43}Ca
Y, [(nmol ATP/min)/mg CK] × 10^3
A, [c.p.m. γ -[^{32}P]ATP/mg CK] × 10^3
Y
A
45
40
35
30
25
20
15
10
5
0
10
50
100
200
[CaCl2], mM
40Ca-Ck
43Ca-Ck
40Ca-Ck
43Ca-Ck


دانشگاه علوم پزشکی تهران
مرکز قلب تهران
TEHRAN HEART CENTER

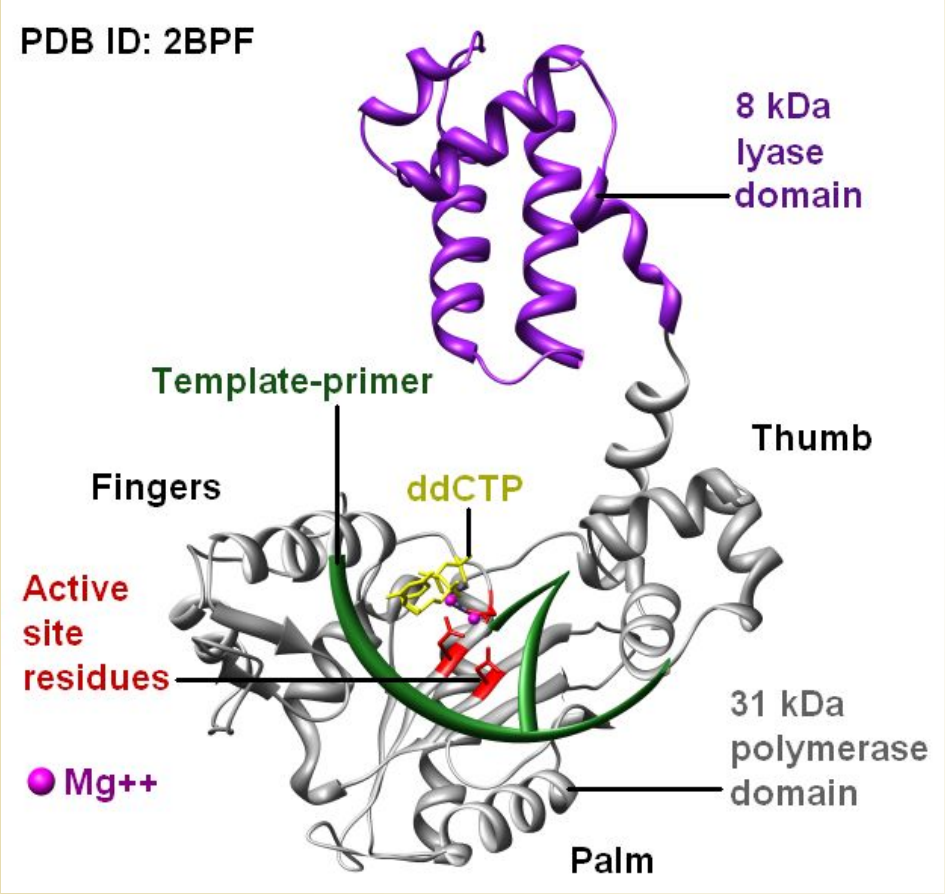
PDB ID: 2BPF
8 kDa
lyase
domain
Template-primer
Thumb
Fingers
ddCTP
Active
site
residues
Mg++
31 kDa
polymerase
domain
Palm

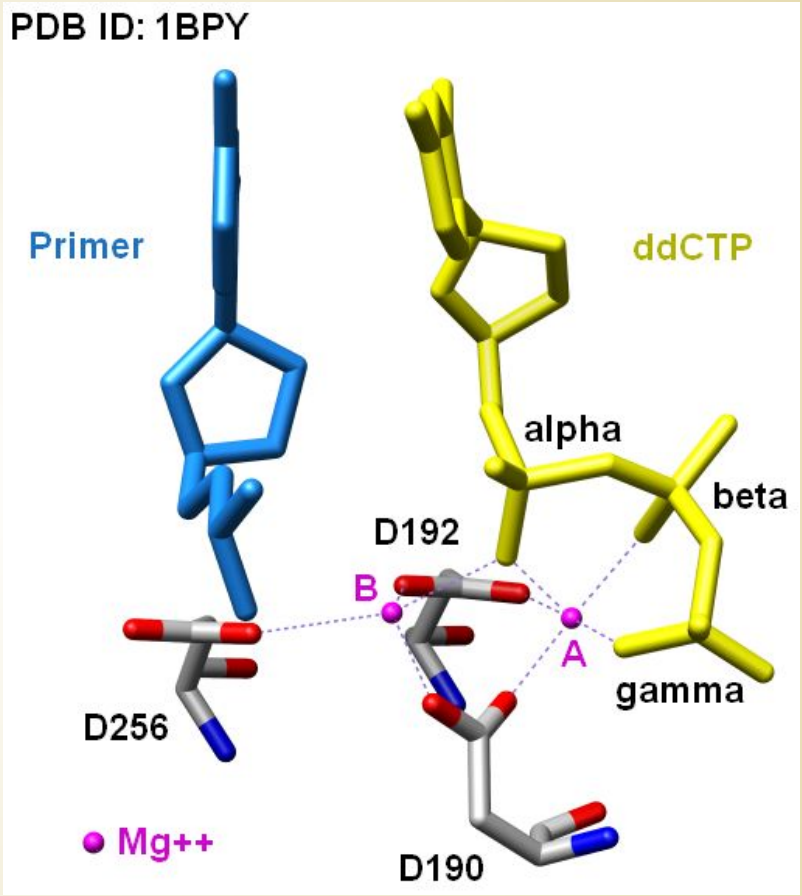
PDB ID: 1BPY
Primer
ddCTP
alpha
beta
D192
B
A
gamma
D256
Mg++
D190

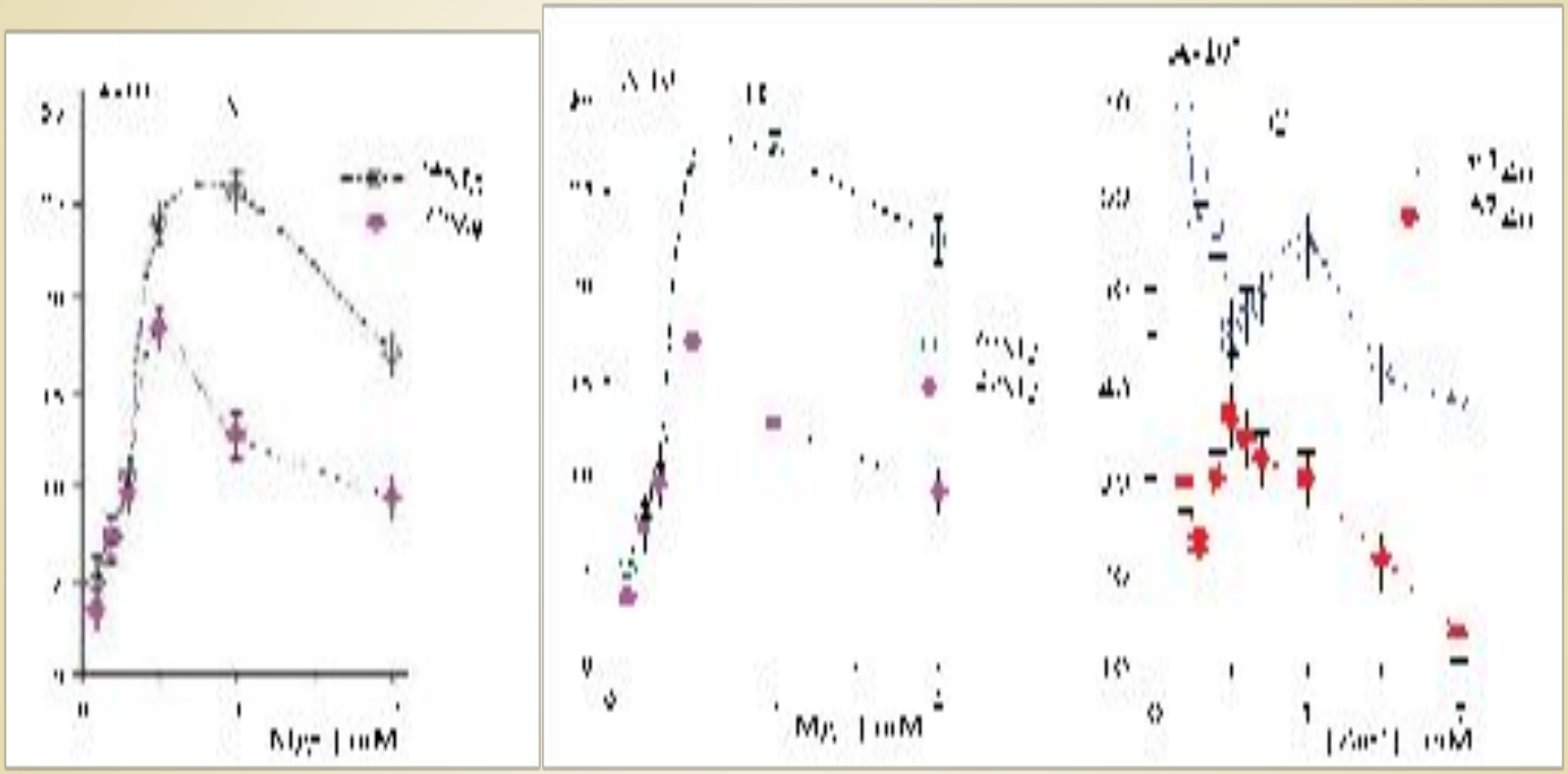

Figure 10: The rate of the DNA synthesis by polymerase β as a function of the magnesium and zinc ion concentration in pairs $^{24}Mg^{2+}/^{24}Mg^{2+}$ (A), $^{26}Mg^{2+}/^{26}Mg^{2+}$ (B), and $^{64}Zn^{2+}/^{64}Zn^{2+}$ (C).

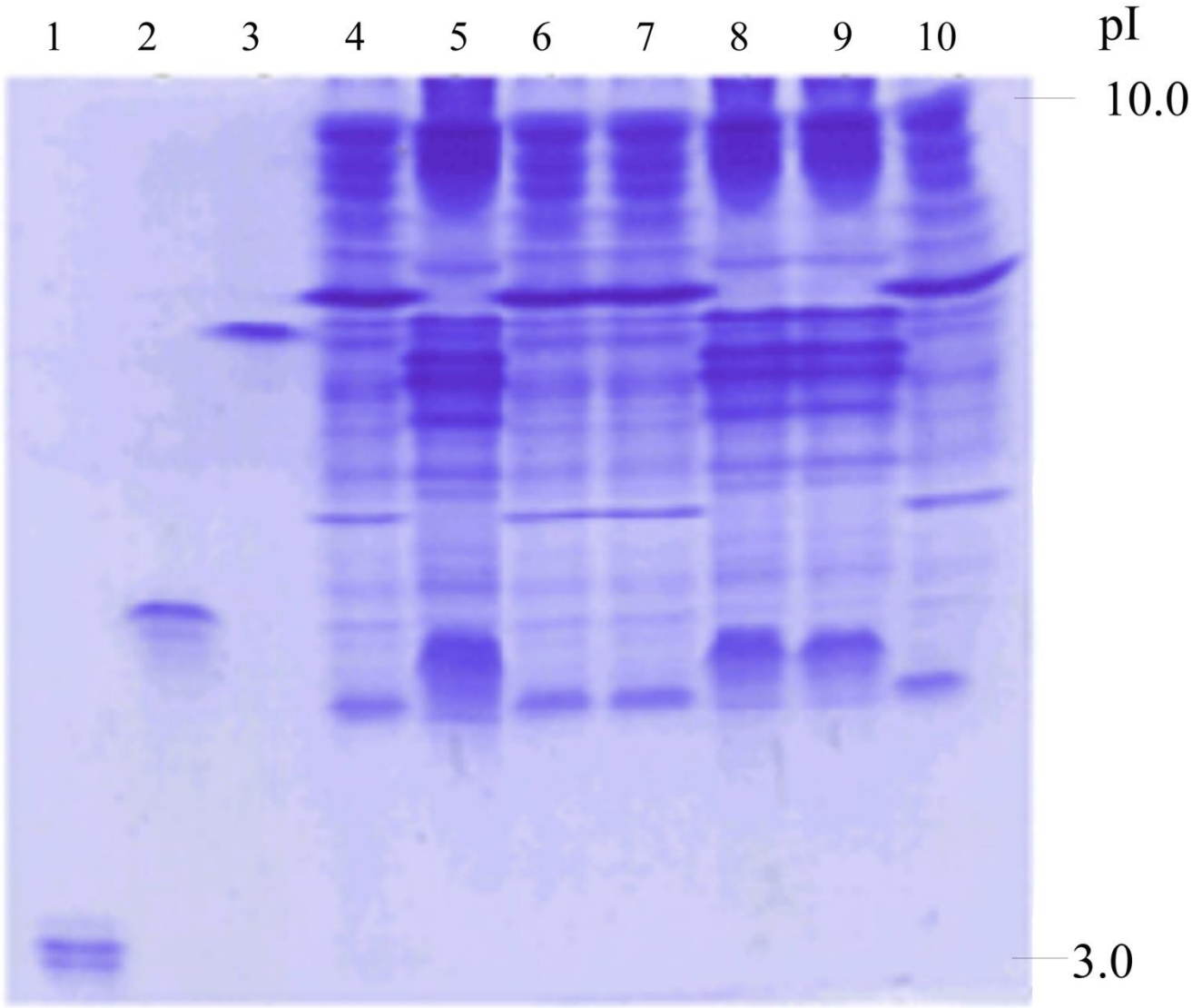
1
2
3
4
5
6
7
8
9
10
pI
10.0
3.0

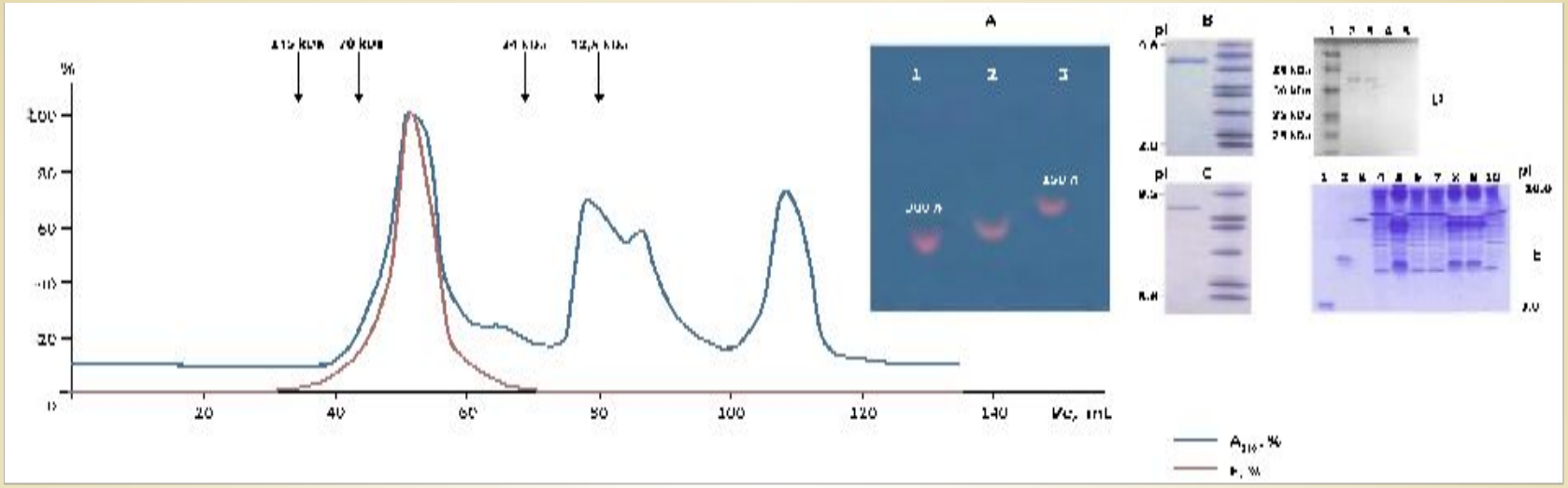

For technical details, see Materials and Methods

Tandem elution profile: UV-280 absorbance (A280, blue line) and DNApolβ specific catalytic activity (Г, red line) were monitored

1A: Agarose gel DNA electrophoresis:

1, 3 – single strand DNA fragments (markers);

2 –DNA sequences pool processed in vitro by the β-like DNA polymerase purified from the HL-60 cell chromatin

1B, 1C: Isoelectric focusing of the β like DNA polymerase purified from the HL60 cell chromatin performed along with the commercial markers sets.

1D: SDS PAGE analysis of the purified HL60 chromatin associated β like polymerase.

1 – Markers set,

2 – 5, 5.0, 1.0, 0.5 μg pure enzyme per a slab gel.

1E: Isoelectric focusing of the cell nuclei subtraction proteins:

1 –acidic glycoprotein of the HeLa cell plasmatic membrane

(Courtesy, RAMS Institute for Carcinogenesis Research, Moscow, Russia);

2, HeLa cell histone H1A

(Courtesy, RAMS Institute for Carcinogenesis Research, Moscow, Russia);

3, β–like DNA polymerase purified from chromatin of HL60 cells;

4 – 10, cell nuclei subtractions total protein;

4, 6, 7, chromatin from the healthy donor myelocytes, three individuals.

5 – HL-60 cell nuclei total protein;

8, 9, HL60 chromatin proteins;

10, HL-60 nucleoplasm proteins.

Figure 1: Fractionation of HL-60 cell chromatin proteins on hydroxyl HW55F column and a subsequent evaluation of physico–chemical properties and catalytic function of the resulted purified β –like DNA polymerase.

CATALYTIC ACTIVITY OF THE BETA-LIKE DNA POLYMERASE FROM HL60 CELLS CHROMATIN AFFECTED BY INHIBITORS AND BY HIGH CONCENTRATION OF POTASSIUM CHLORIDE

Effector tested	DNA pol activity, [^{3}H]DNA cpm/mg protein *n*=6 (M± SEM)
Aphidicolin, 5.0 µg/mL	30,789 ± 398
N-ethyl-melamide, 0.5 mM	27,632 ± 437
ddTTP, 2.5 µM	1,370 ± 186
Trypsin, 20 µg/mL	207 ± 16
KCl, 200 mM	74,613 ± 441
No effectors added *(optimized incubation mixture)*	29,838 ± 322

SDS-PAGE:
HL-60 Cell DNA Polymerase β

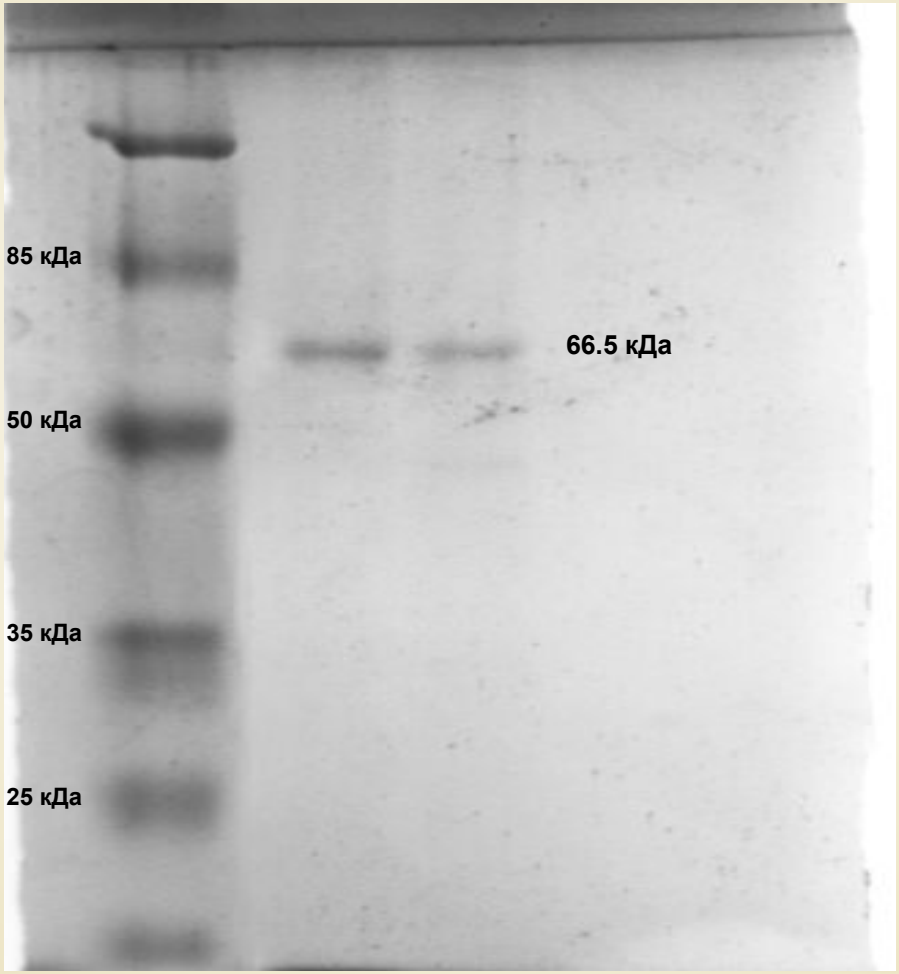

AN IMPACT OF ISOTOPY OF THE DNApolβ INCUBATION MIXTURE ON A LENGTH OF THE DNA FRAGMENTS PROCESSED. AGAROSE GEL ELECTROPHORESIS.

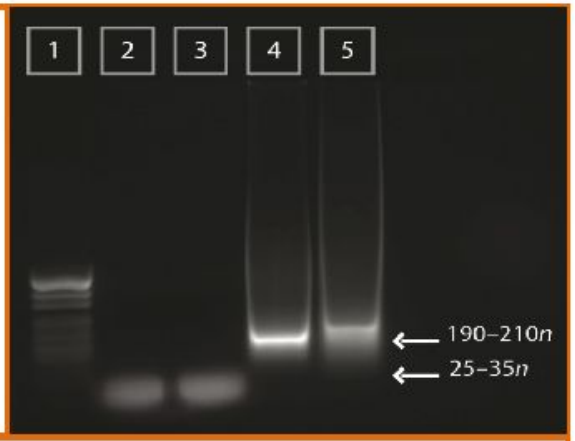

1 – DNA markers kit, 110 – 489 *n*;

2 – 20 mM $^{43}CaCl_2$, Mg – free;

3 - 20 mM $^{25}MgCl_2$, Ca – free;

4 – 20 mM $^{40}CaCl_2$, Mg – free;

5 – 20 mM $^{24}MgCl_2$, Ca – free;

All the enzyme incubation conditions were kept at the optimum level (pH 8.0; +37°C, 60 min).

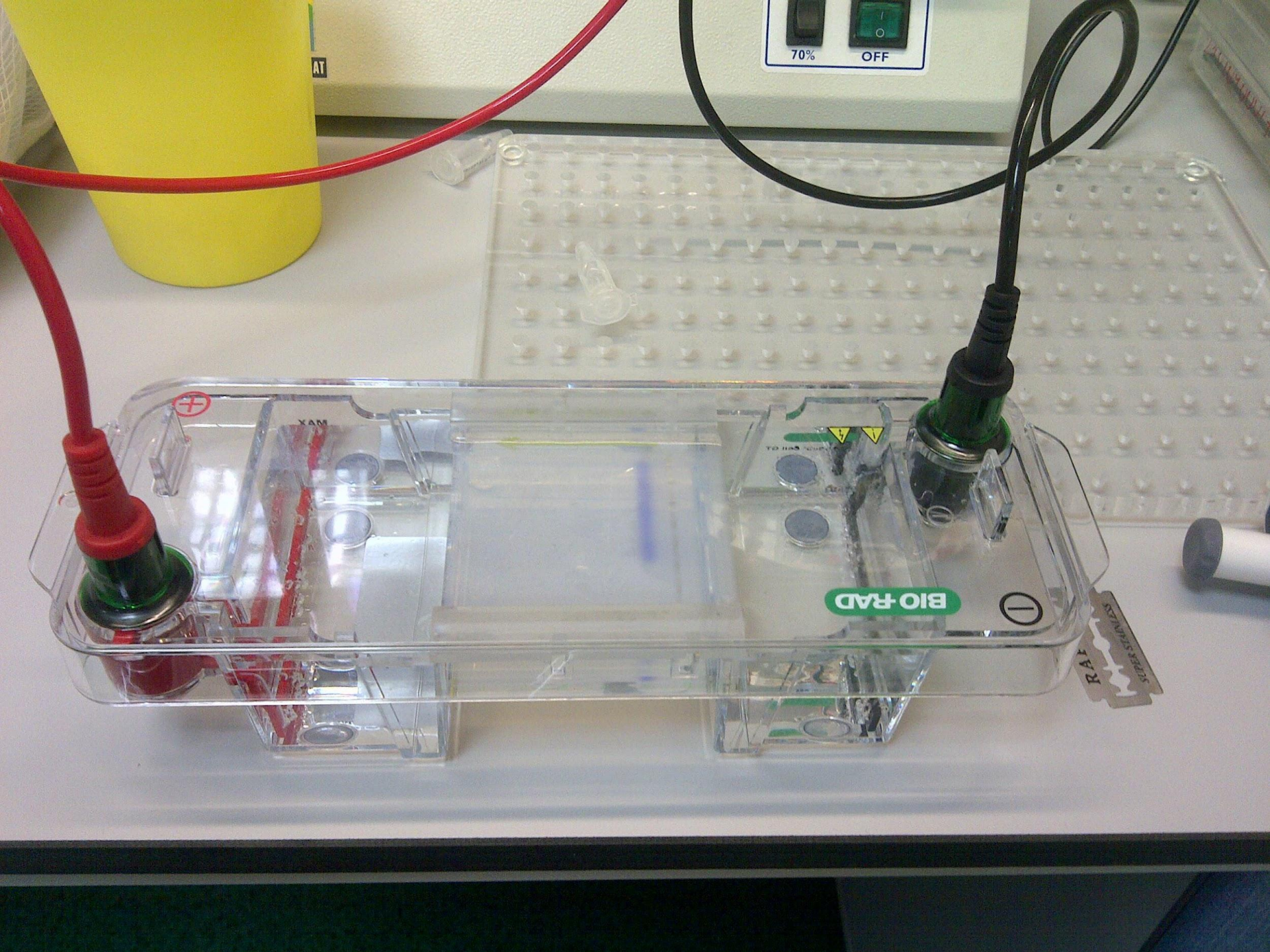
70%
OFF
BIO-RAD

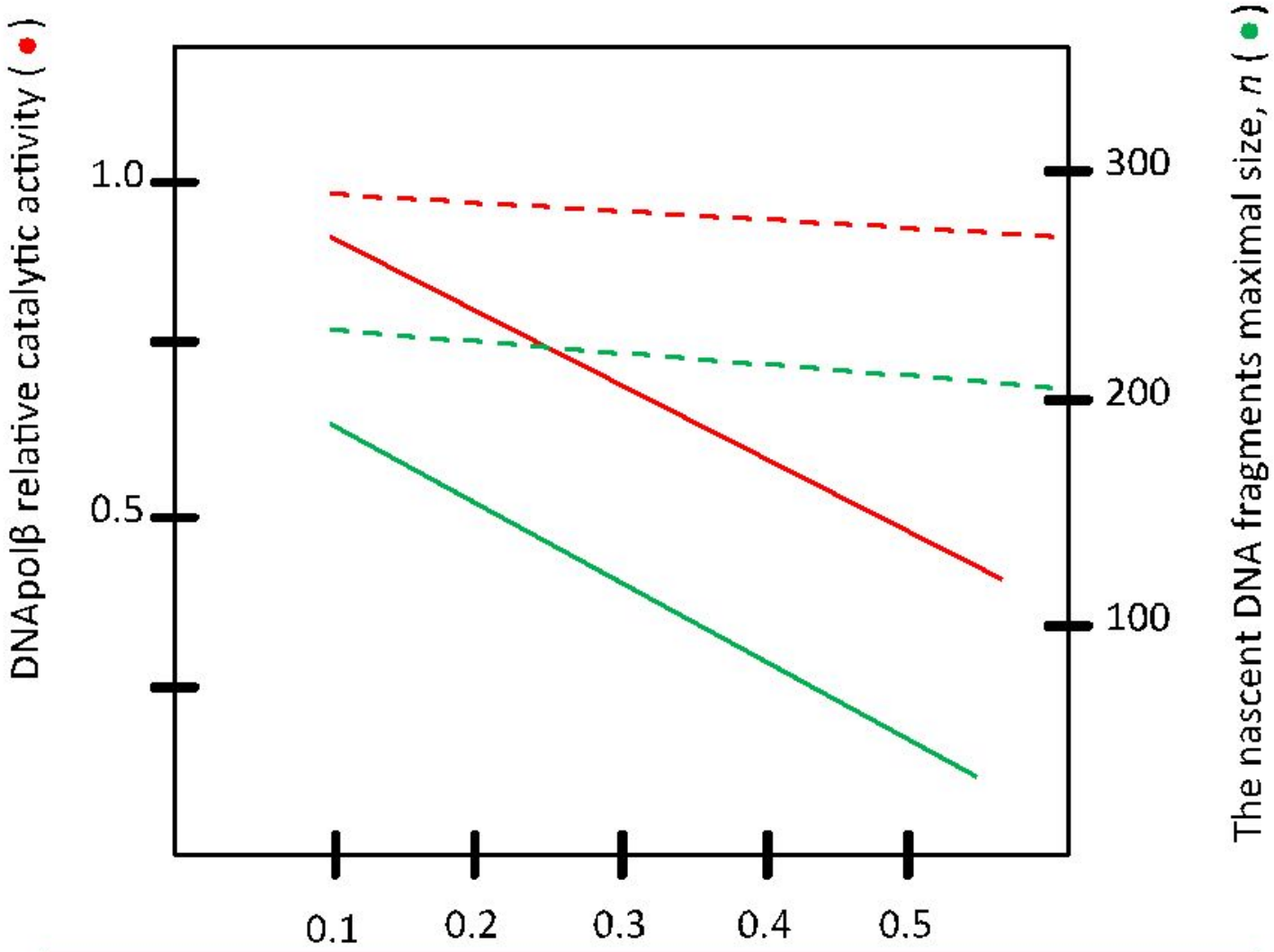

^{43}Ca-MIE in DNApolβ FUNCTION

Controls: ^{40}Ca/Mg substitution (---/---);

Experiment: ^{43}Ca/Mg substitutio (/).

Структура диссертационного исследования

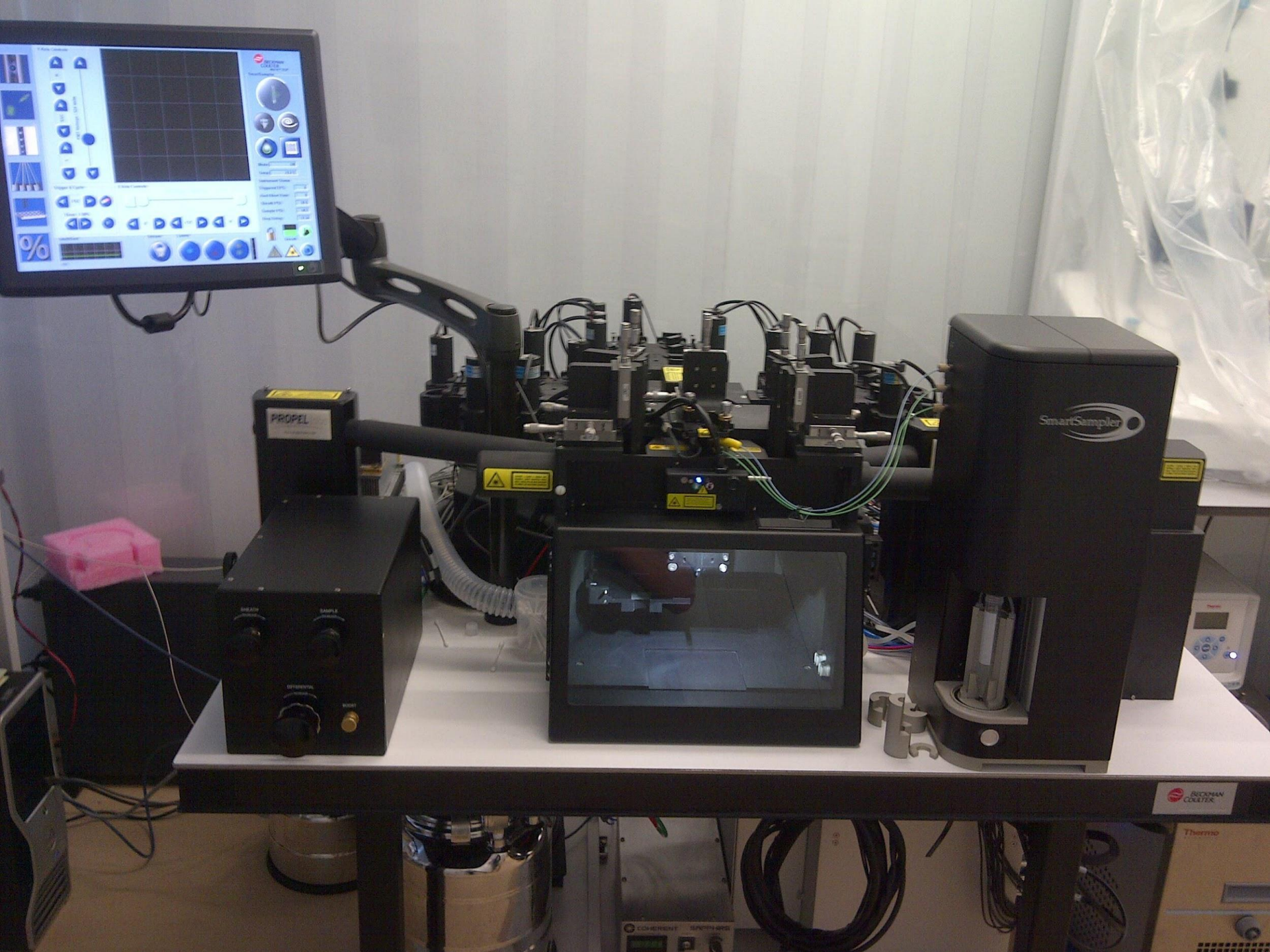
PROPEL
SmartSampler
BECKMAN COULTER
Thermo

MIE Impact on the HL-60 cell DNApolβ catalytic activity

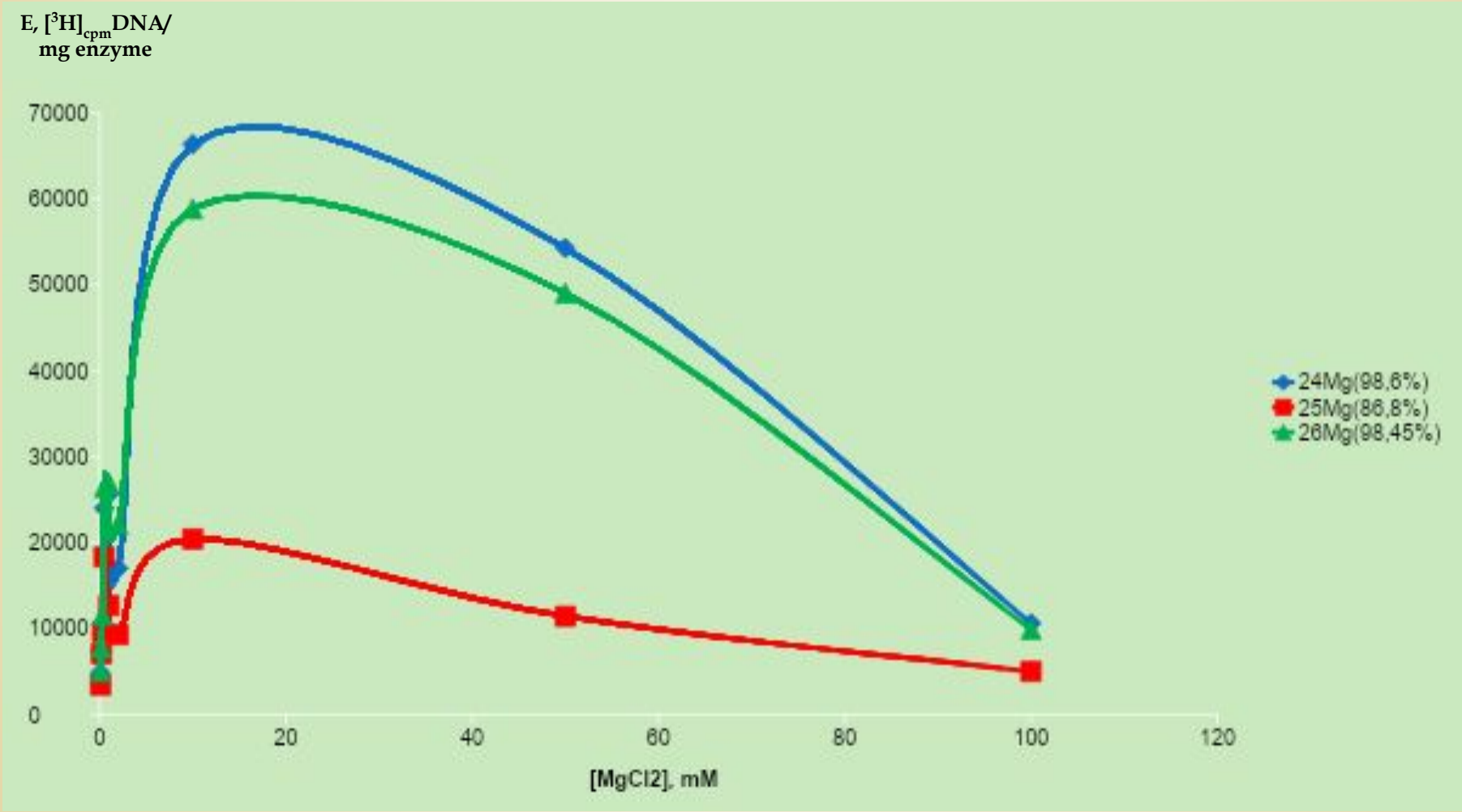

MIE Impact on the HL-60 cell DNApolβ catalytic activity

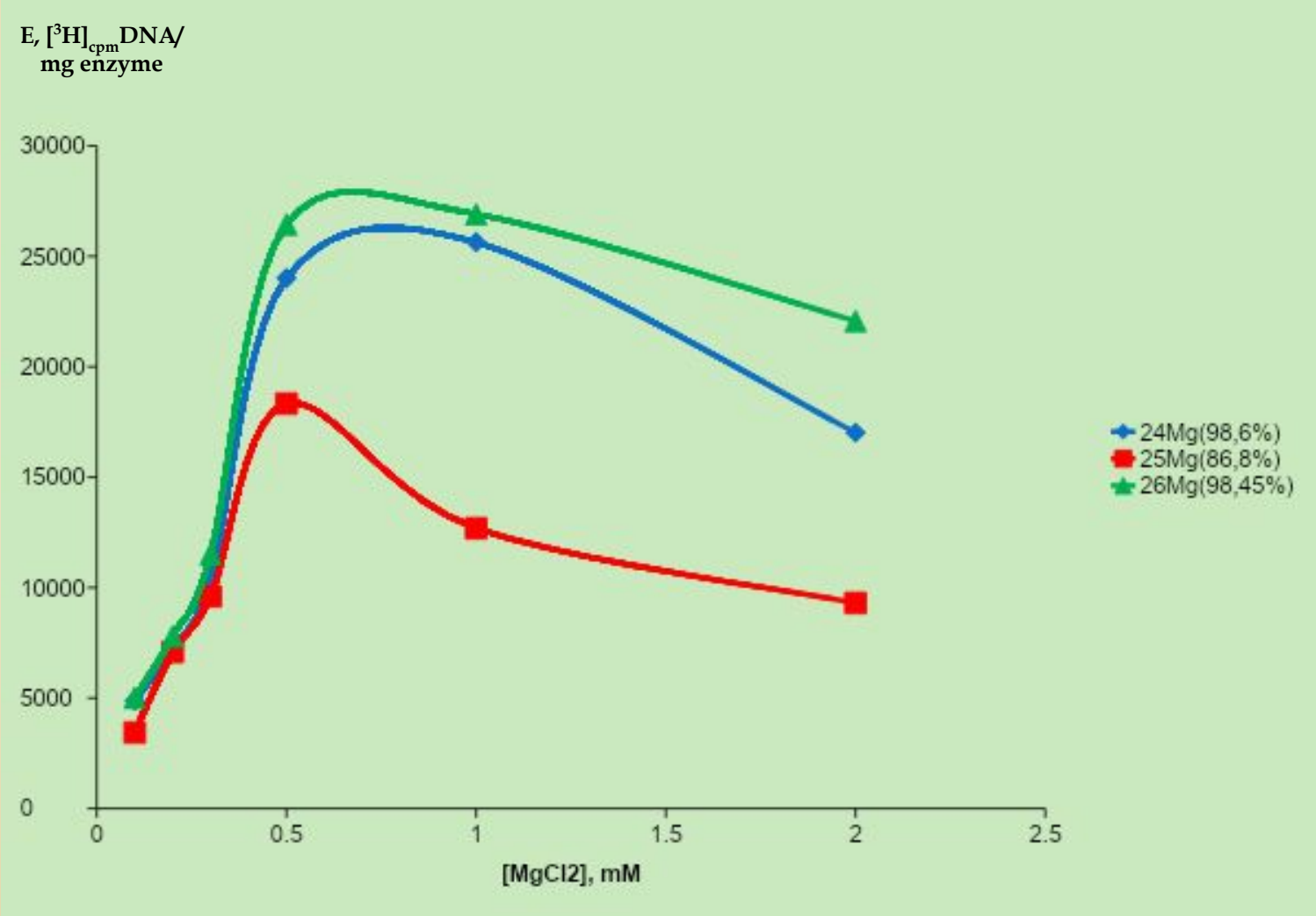

MIE Impact on the HL-60 cell DNApolβ catalytic activity

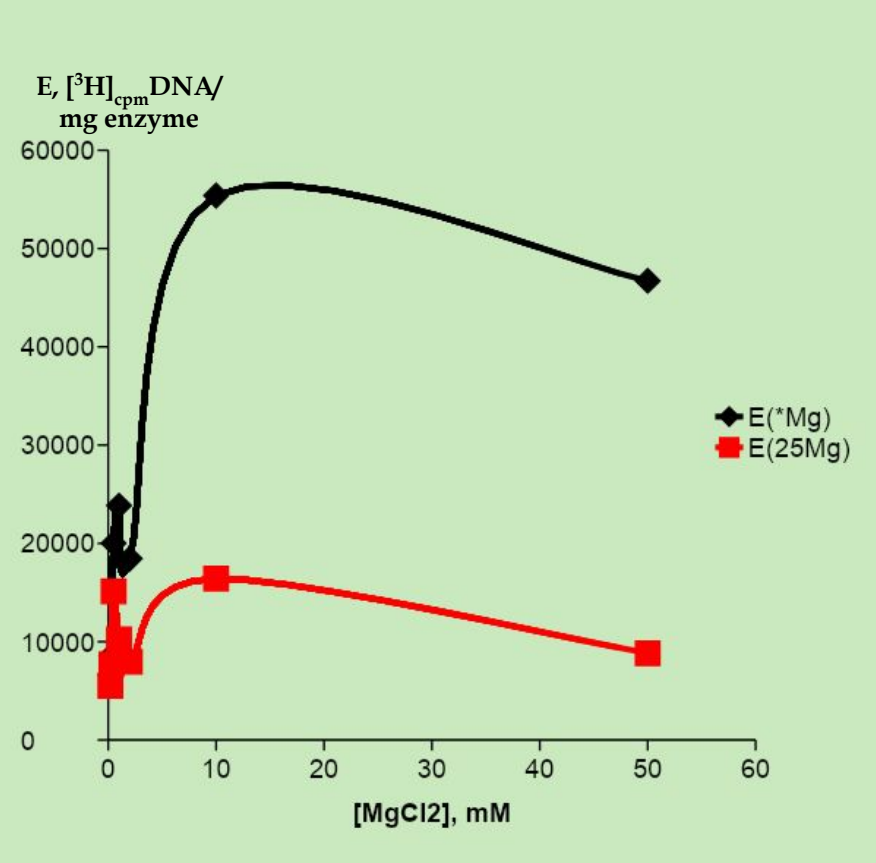

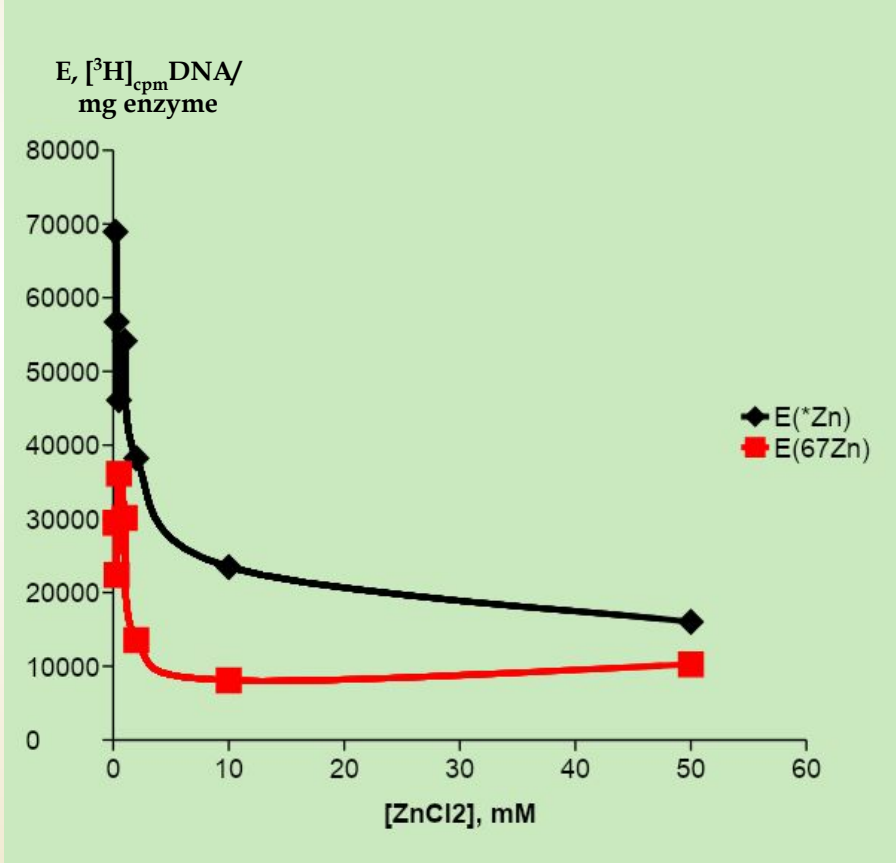

The rate of DNA replication as a function of Mg^{2+} ion concentration. Tritium radioactivity A is measured as the number of counts/min/mg of DNA. The contents of ^{25}Mg and ^{24}Mg in Mg^{2+} ions are 86.8 and 98.6% respectively.

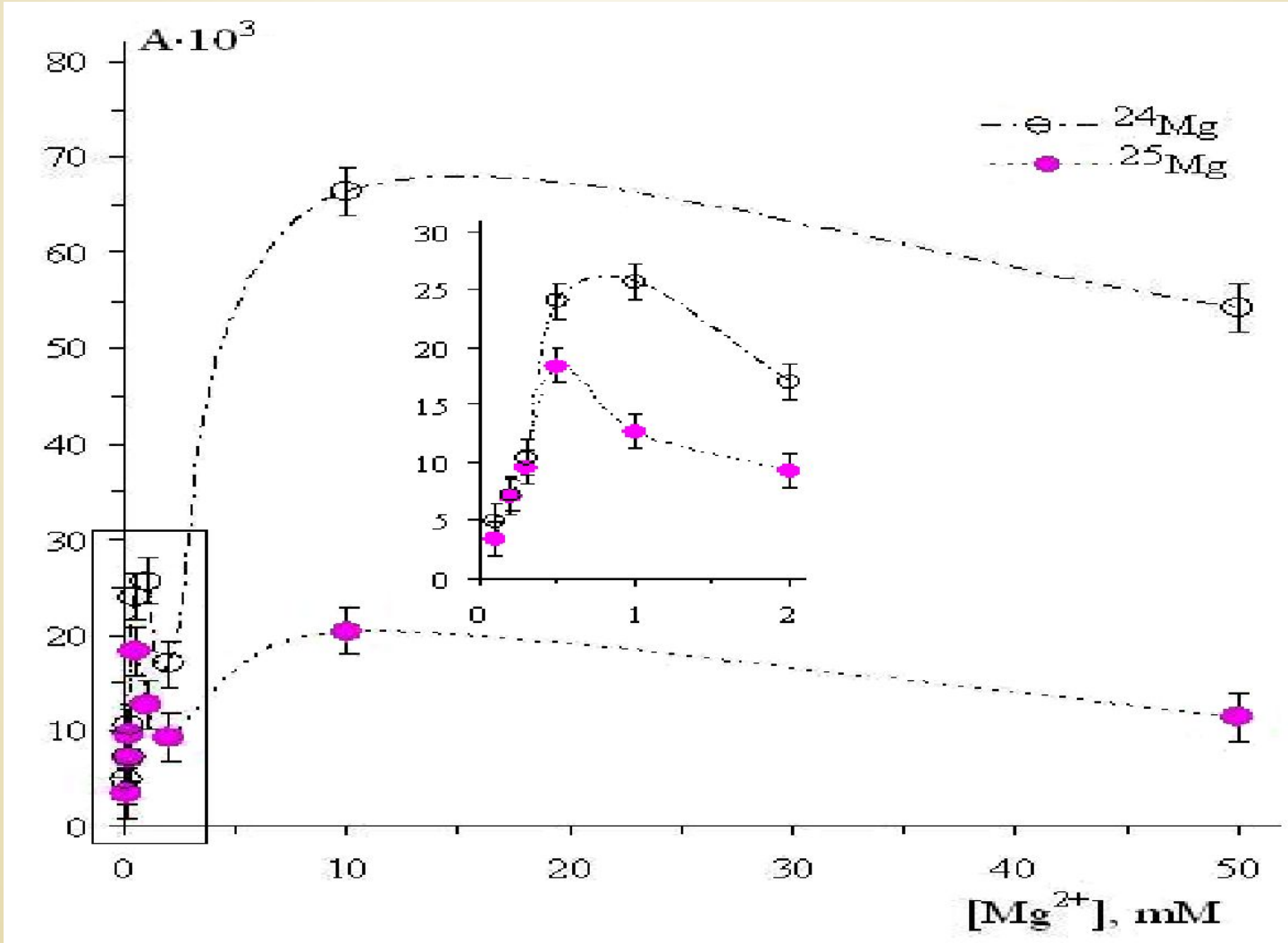

The rate of DNA replication as a function of Mg^{2+} ion concentration. Tritium radioactivity A is measured as the number of counts/min/mg of DNA. The contents of ^{25}Mg and ^{26}Mg in Mg^{2+} ions are 86.8 and 98.6% respectively.

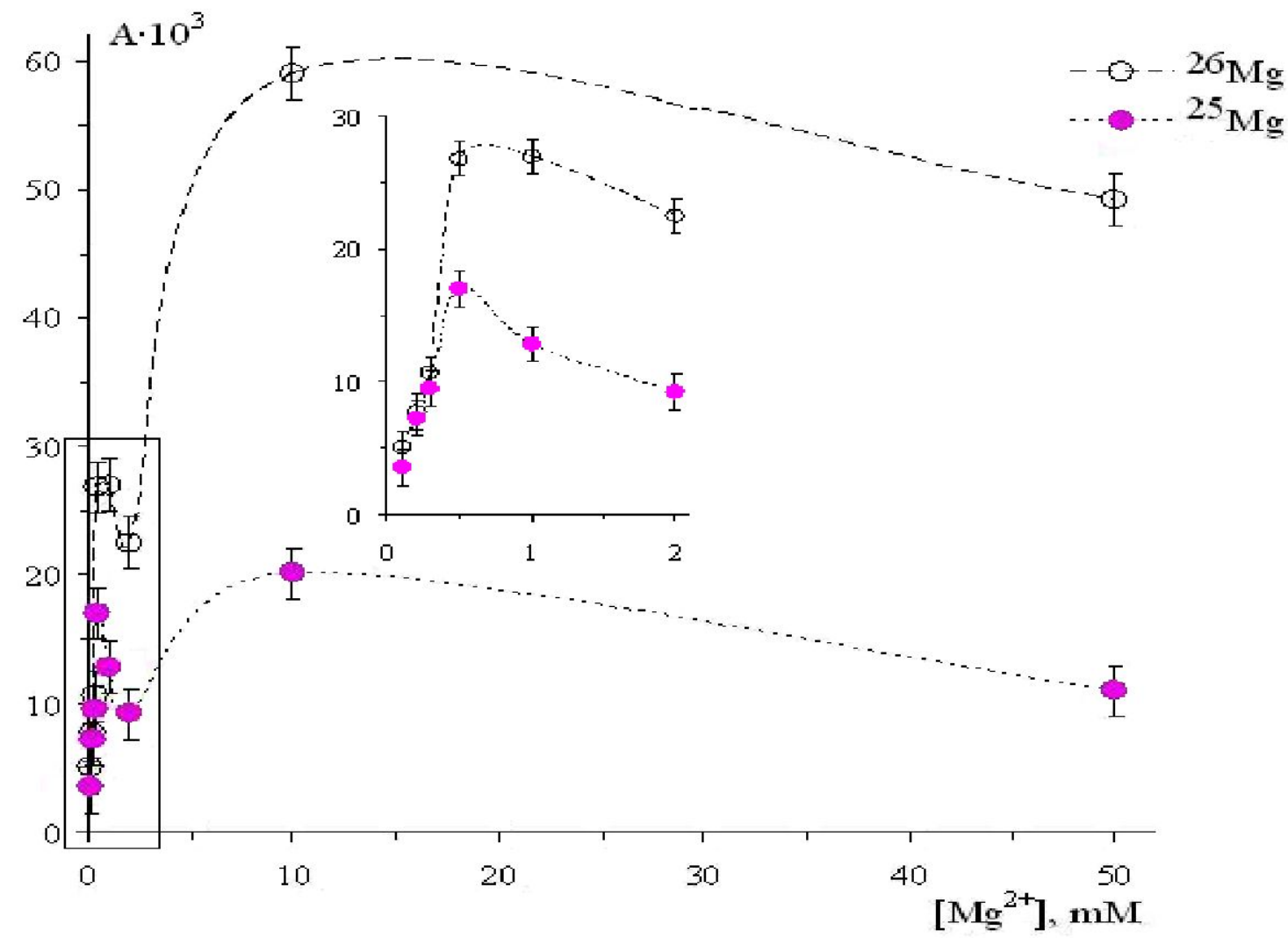

The rate of DNA replication as a function of Zn^{2+} ion concentration. Tritium radioactivity A is measured as the number of counts/min/mg of DNA. The content of ^{67}Zn in Zn^{2+} ions is 00%.

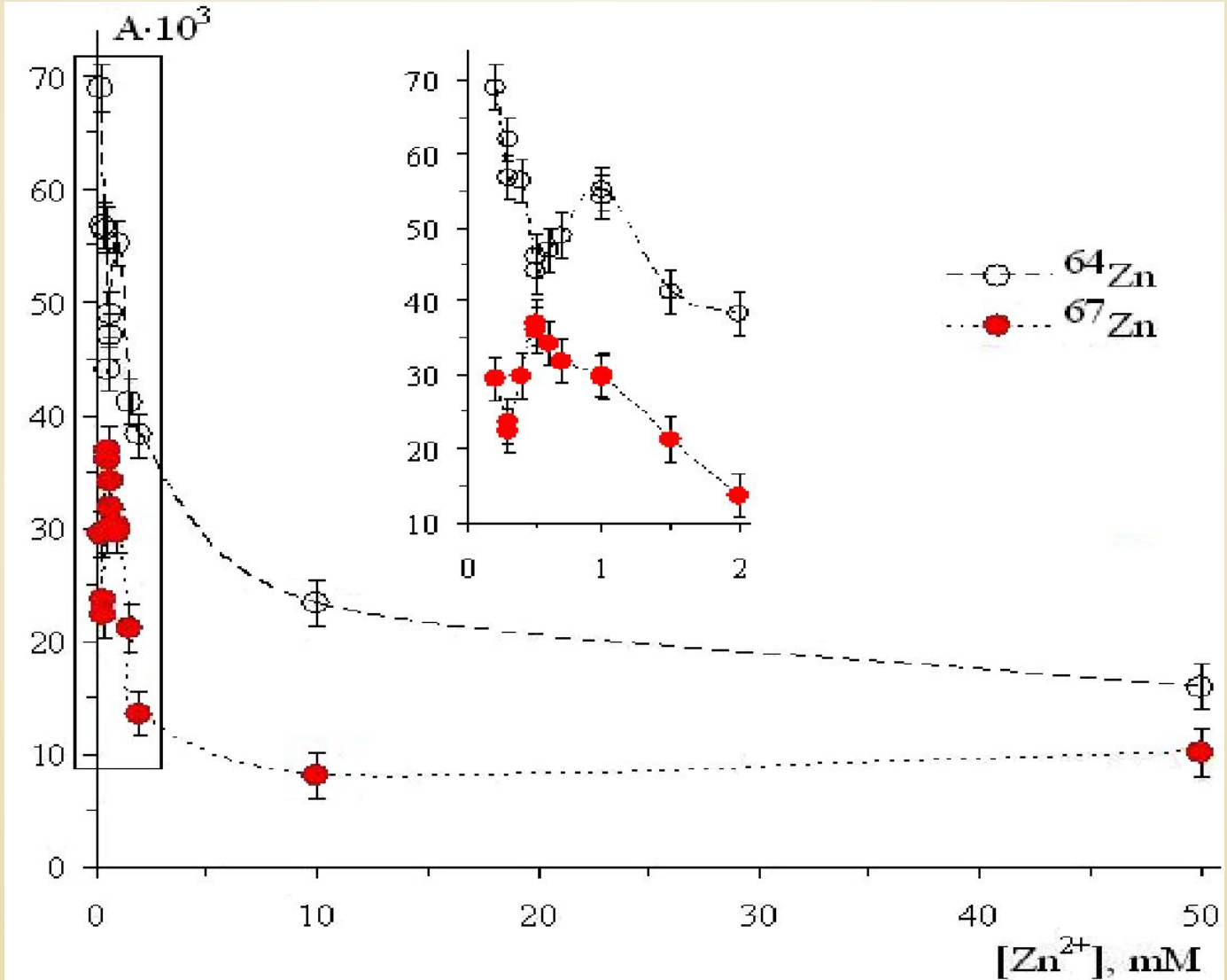

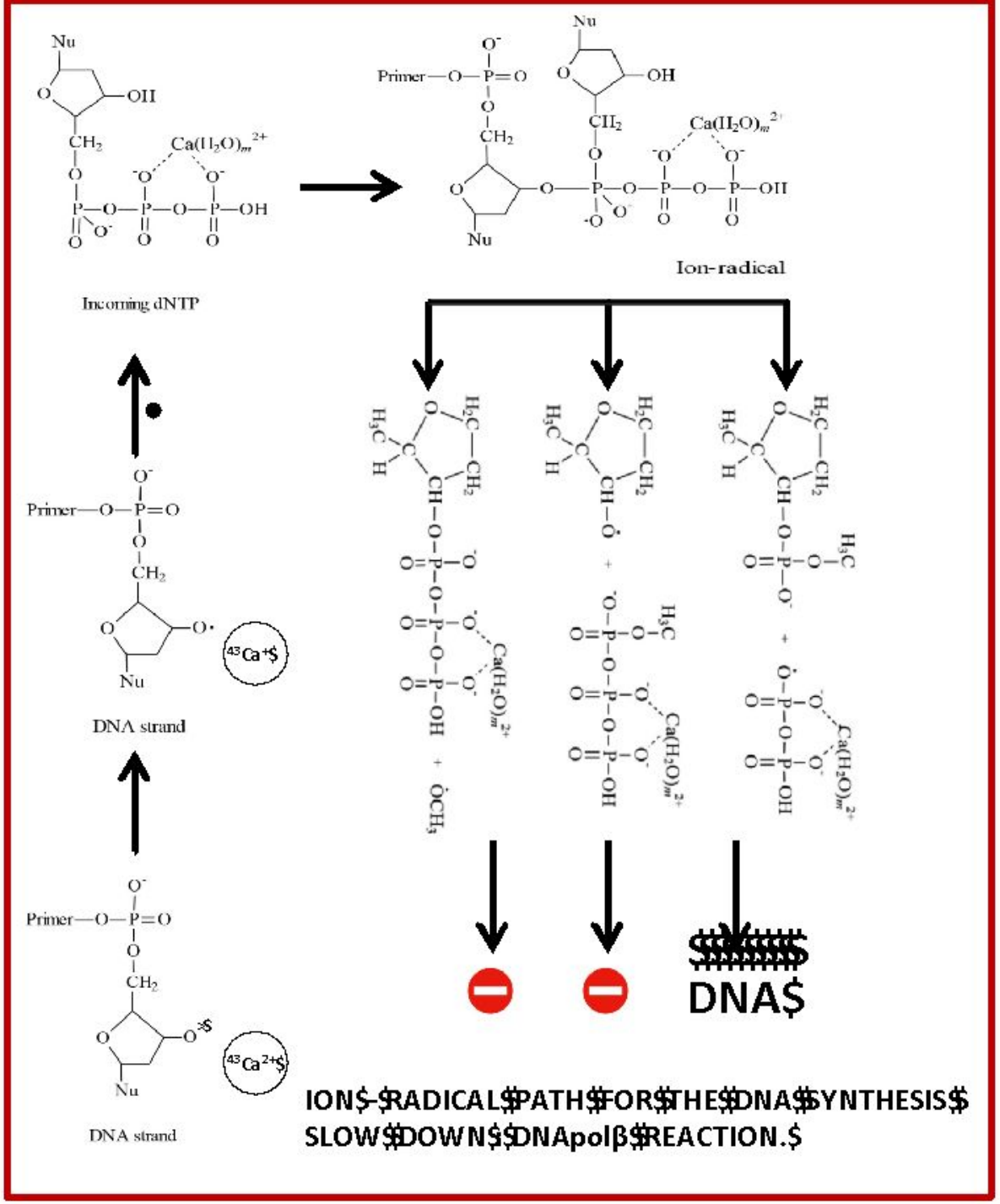
Incoming dNTP
Ion-radical
DNA strand
DNA strand
DNA$
ION$-$RADICAL$PATH$FORTHEDNA$$YNTHESIS$
SLOW$DOWN$$DNApolβ$REACTION.$

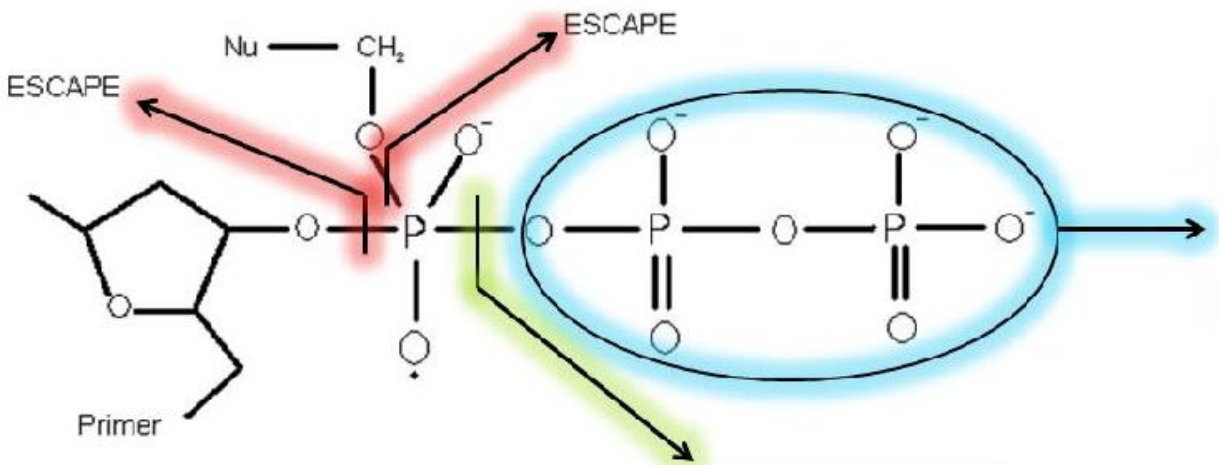

Diphosphate#to#
#emove#by#the#
#2nd#enzyme's#
#Mg2+#on,unless#
#eplaced#

INSERTION#
to#the#nascent#
DNA#chain#
#

THE##dNTP#-#DXYRADICAL#THREE#CHANNEL#SPREADING##
DECAY.#DNApolβ#REACTION.#

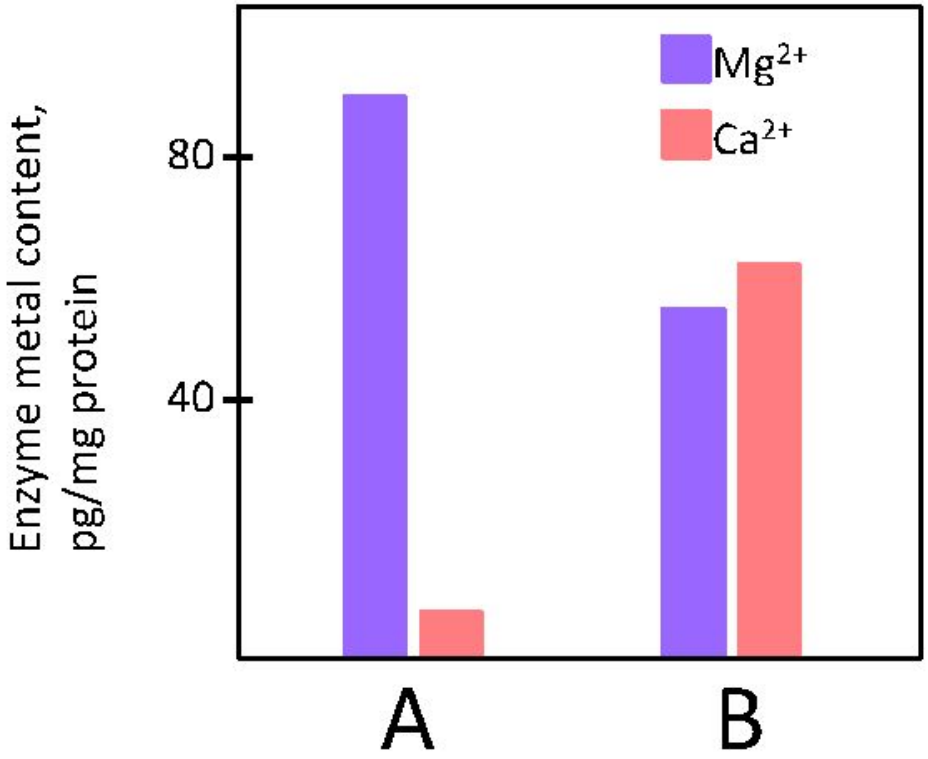

THE HIGHEST – REACHABLE LEVELS OF SUBSTITUTION OF ENDOGENOUS Mg^{2+} WITH CALCIUM IN PURIFIED HL60 DNApolβ (20 mM$CaCL_2$/15 mM Tris-HCl (pH 8.0)/1.5 mM EDTA/ +37°C/2hrs).

A – Control (intact enzyme);
B – Experiment (Mg – Ca substitution).

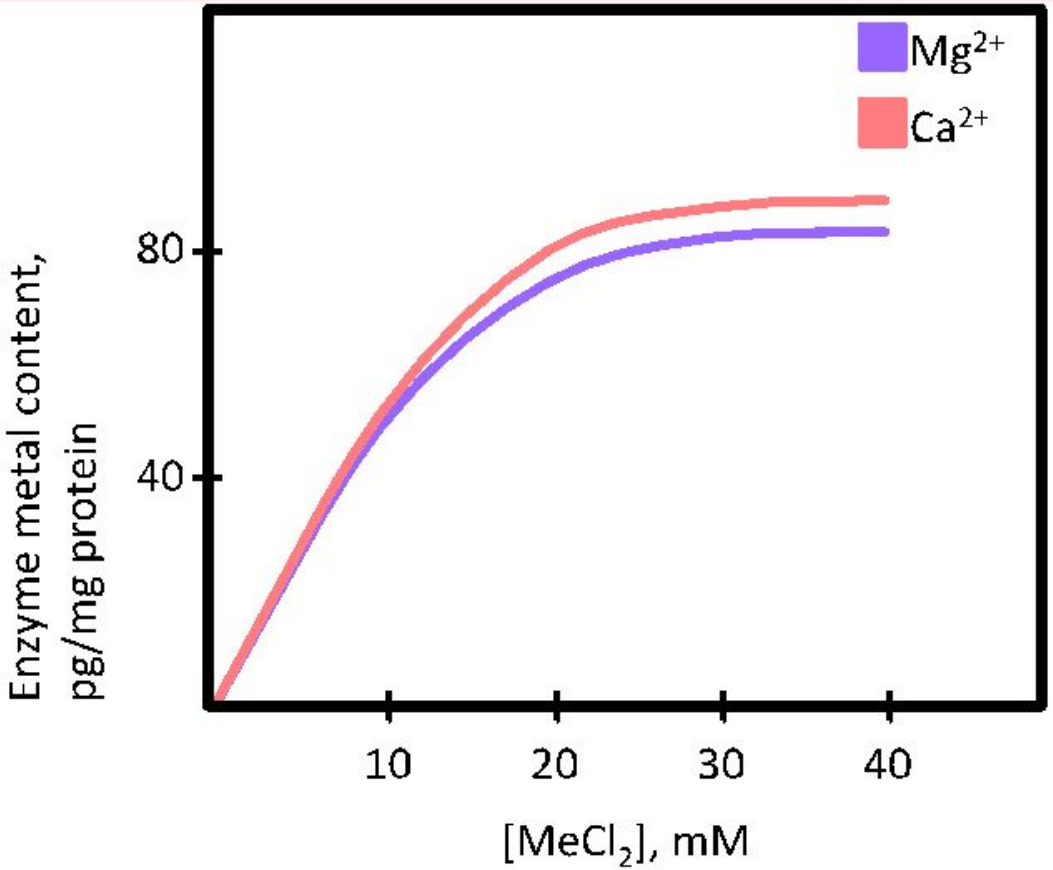

AN IMPACT OF THE METAL INCUBATION MIXTURE CONCENTRATION ON EXOGENOUS IONS INCORPORATION INTO THE DNApolβ STRUCTURE (20 mM $MeCl_2$/15 mM Tris-HCl (pH 8.0)/ /1.5 mM EDTA/+37°C).

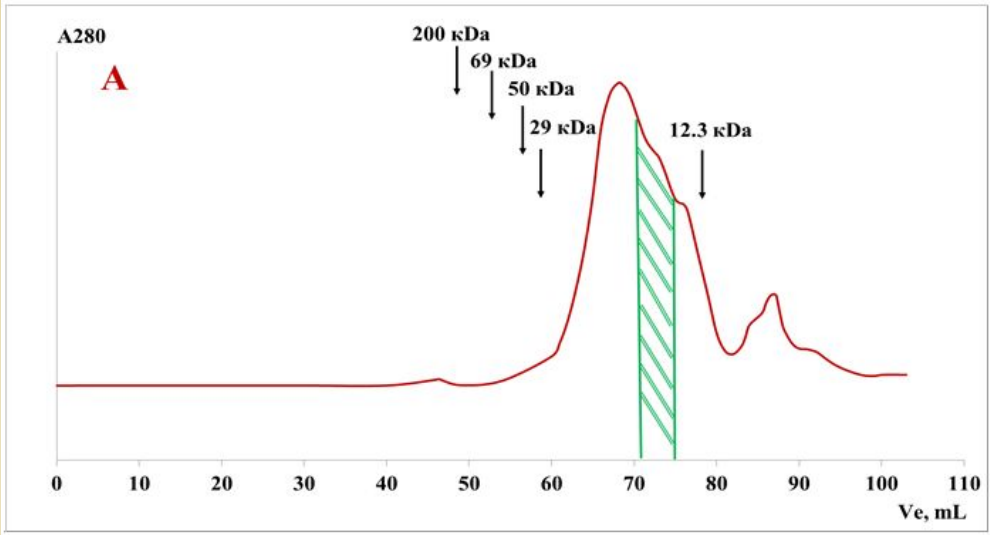

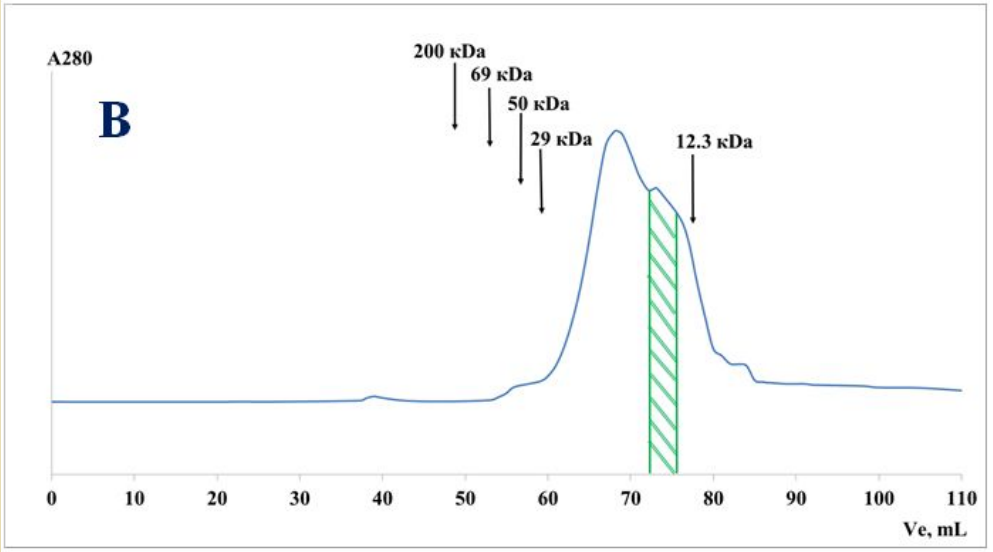

Fractionation of the human retinoblastoma (Y79 and WERI-RB) cell chromatin proteins on TOYPEARL HW 55F column and subsequent evaluation of structural and catalytic properties of the purified DNA Polymerases β by SDS-PAGE

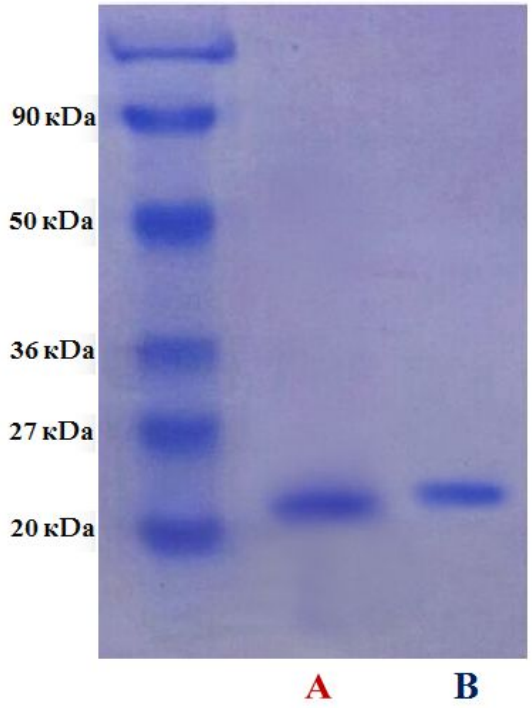

— DNA Polymerase activity, [^{3}H]DNA cpm/mg protein.

A — Y79

B — WERI-RB


eppendorf

DNA Polymerase ß Properties

Enzyme Pattern	*Cell Type*		
	HL-60	**Y79**	**WERI-RB**
Quaternary structure	–	–	–
Monomer	+	+	+
MW, kDa	**66.5**	**23.5**	**23.5**
pI	**8.45**	**8.20**	**8.50**
K*M*, µM (dTTP pool)	**0.016**	**0.013**	**0.010**
K*cat*, µM ([dTTP /min]mg protein)	**0.622**	**0.394**	**0.418**
3',5'-exonuclease activity	–	–	–
KCl effect (200 mM)	**↑ 2.1**	**↑ 2.2**	**↑ 1.8**
ddTTP effect (2.5µM)	**↓ 30.2**	**↓ 28.0**	**↓ 33.8**
Aphidicolin effect (5.0 µg/mL)	–	–	–
N-ethyl-melamide effect (0.5 mM)	–	–	–

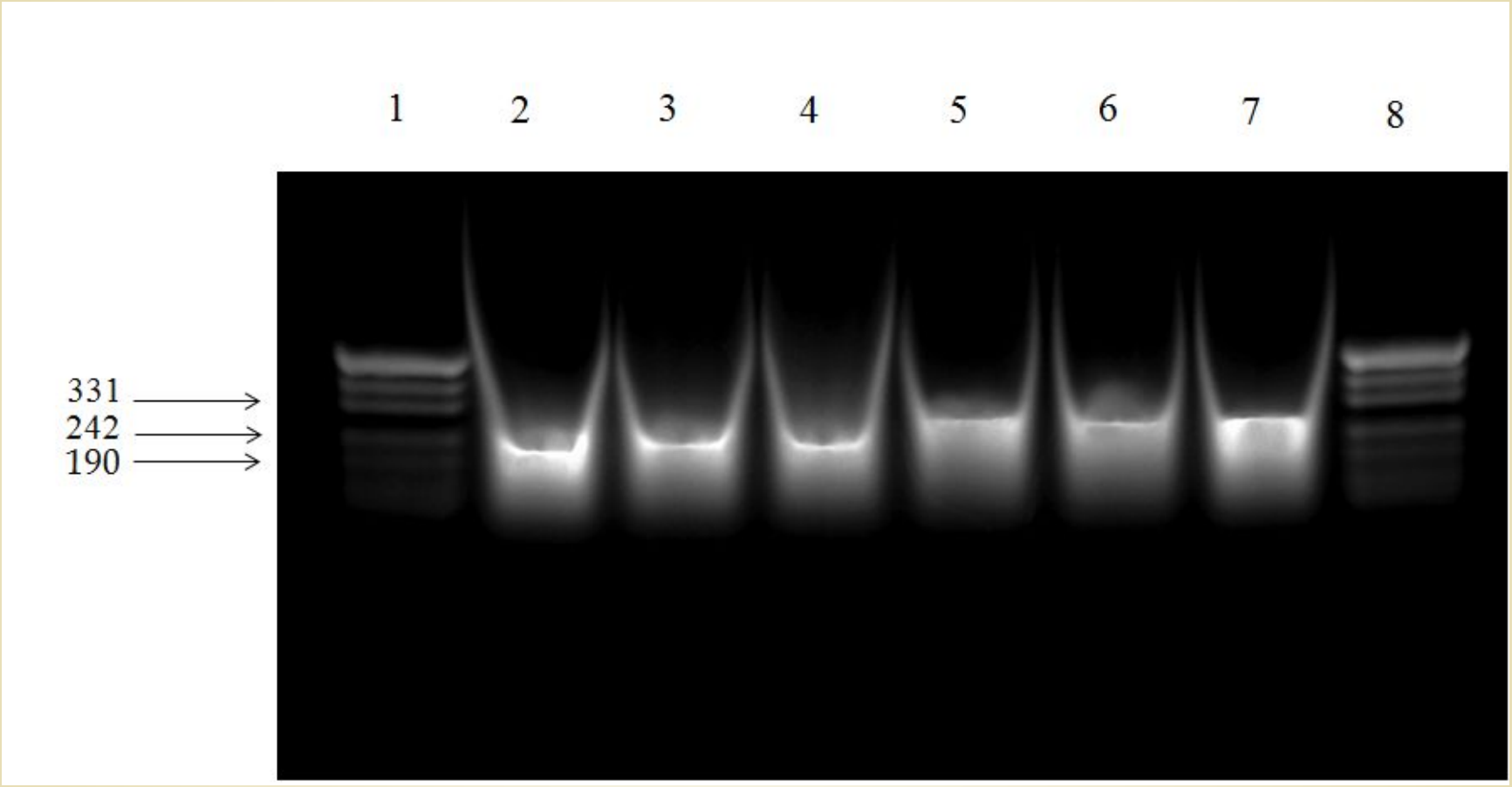
1
2
3
4
5
6
7
8
331
242
190


21010400049639
LUMINESCENT IMAGE ANALYZER
POWER
BUSY
ERROR
ImageQuant
LAS 4000
PHILIPS

[^{3}H] Autoradiography/agarose gel electrophoresis of the retinoblastoma DNA Polymerase β reaction products

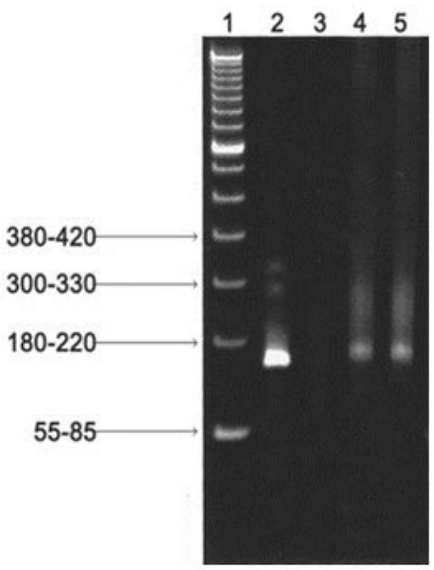

1- Markers
2- Y79, *Mg, 37 ºC
3- Y79, *Mg, 0 ºC
4- Y79, *Ca, 37 ºC
5-Y79, *Zn, 37 ºC

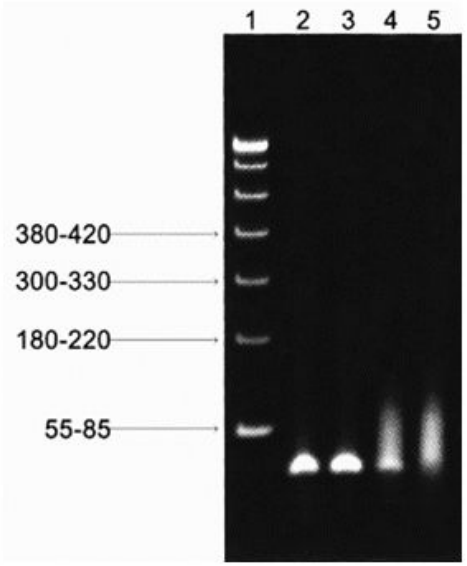

1- Markers
2- Y79, 43Ca
3- WERI-RB, 43Ca
4- Y79, 67Zn
5- WERI-RB, 67Zn

КОНЦЕПЦИЯ БУЧАЧЕНКО – КУЗНЕЦОВА :

Синергизм цитоплазматических и внутриядерных событий, конвертирующих МИЭ ^{25}Mg в цитостатическое воздействие на клетку опухоли

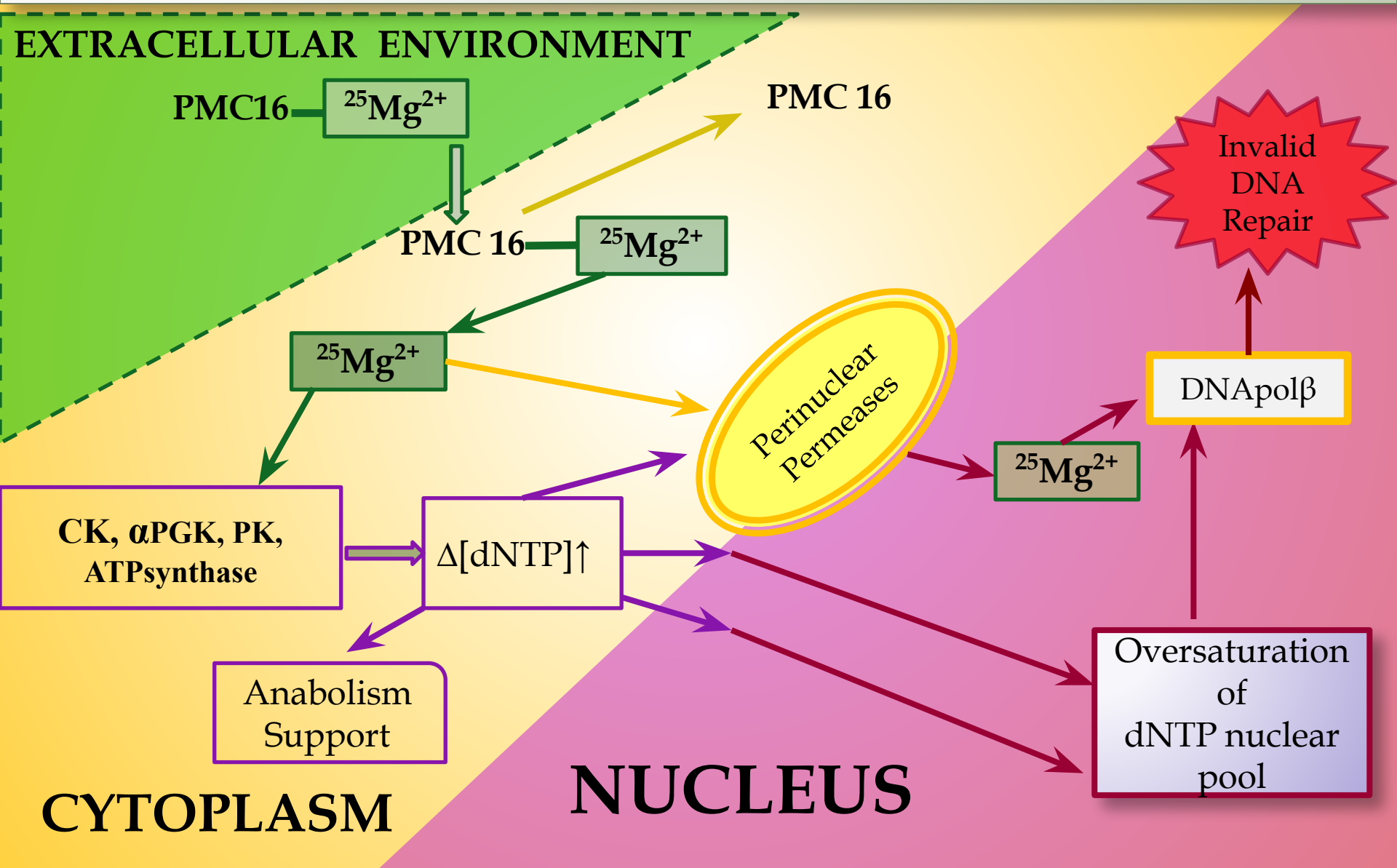

1. Jorg Pedersen, South Denmark University, Biophisical enzymology department, Denmark, Odense
2. Nikita Lukzen, Duke University, laboratory of magnetic biology, USA
3. William Robinson, Nantes University, Isotopic research center, France
4. Nicolas Turro (+), Ron Barthels, Columbia University, USA
5. Nima Amirshahi, Teheran Medical University, Iran
6. Xeng Wu, Nankin State University, China
7. S.A. Roumyantsev, M.A. Orlova, State Research center of gematology, oncology and immunology, Russia
8. Wolfgang Maret, King's college of London, UK

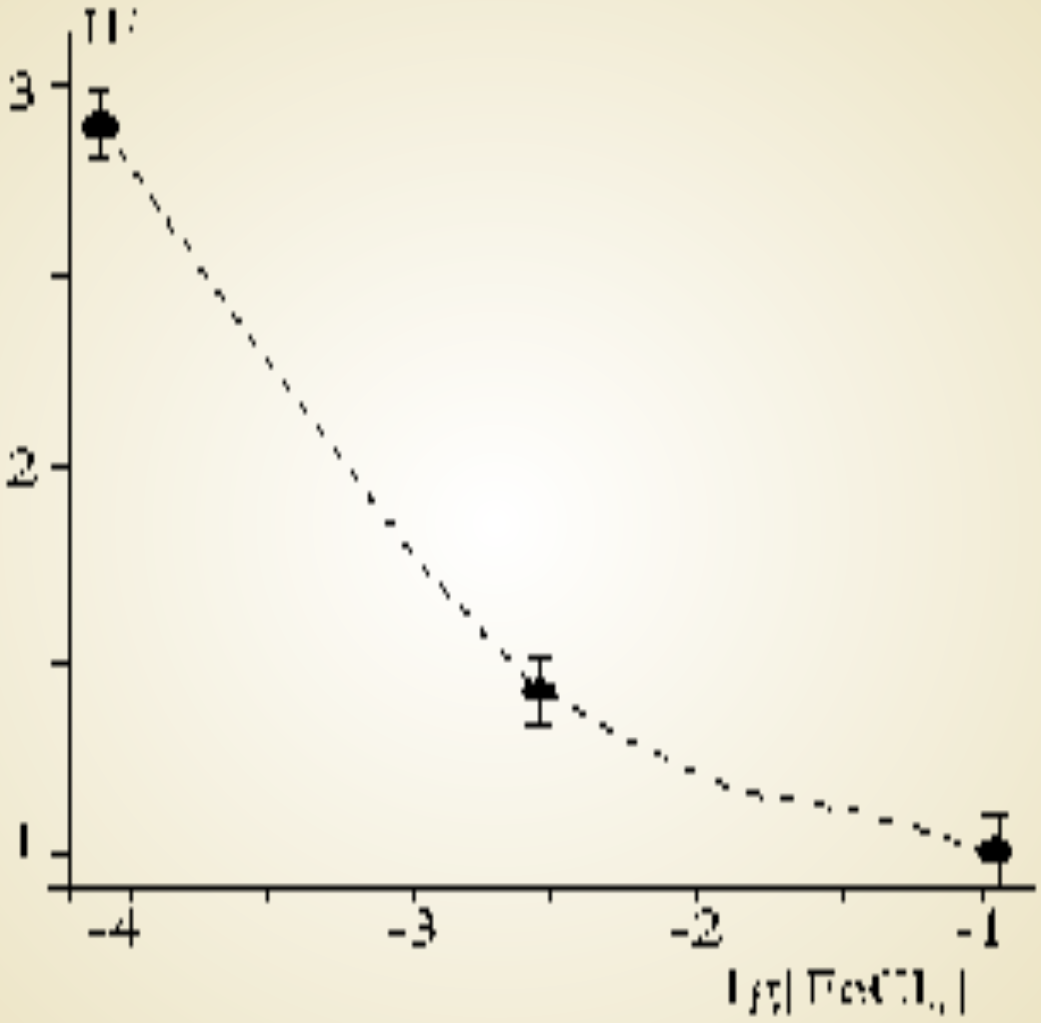

Figure 14: Isotope effect IE as a function of $FeCl_3$ concentration (in mM; pay attention to the log scale for the latter)

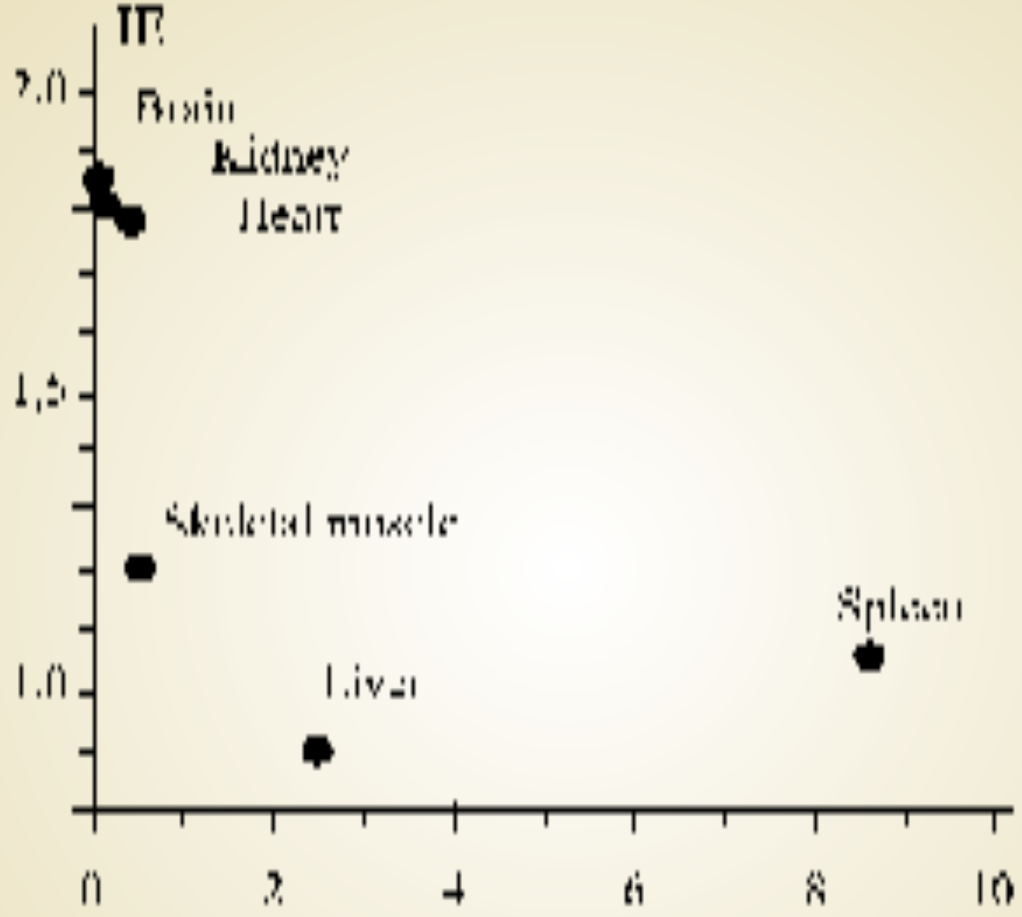

Figure 15: Isotope effect IE in the ATP production by mitochondria from different tissues as a function of iron contents in these mitochondria [Fe^{3+}] is expressed in µg per g of mitochondria.

Grazie per l'attenzione!